OAK RIDGE
NATIONAL LABORATORY
MANAGED BY UT-BATTELLE
FOR THE DEPARTMENT OF ENERGY

ORNL/SUB/99-B99398V-5

Neutronics Experimental Benchmarks for the Utilization of Mixed-Oxide Fuel—Verification of the Reference Monte Carlo Codes Applied to Water-Moderated Reactors with MOX Fuel

M. S. Yudkevich

Fissile Materials Disposition Program

UT-BATTELLE
ORNL-27 (4-00)

DOCUMENT AVAILABILITY

Reports produced after January 1, 1996, are generally available free via the U.S. Department of Energy (DOE) Information Bridge.

Web site http://www.osti.gov/bridge

Reports produced before January 1, 1996, may be purchased by members of the public from the following source.

National Technical Information Service
5285 Port Royal Road
Springfield, VA 22161
Telephone 703-605-6000 (1-800-553-6847)
TDD 703-487-4639
Fax 703-605-6900
E-mail info@ntis.fedworld.gov
Web site http://www.ntis.gov/support/ordernowabout.htm

Reports are available to DOE employees, DOE contractors, Energy Technology Data Exchange (ETDE) representatives, and International Nuclear Information System (INIS) representatives from the following source.

Office of Scientific and Technical Information
P.O. Box 62
Oak Ridge, TN 37831
Telephone 865-576-8401
Fax 865-576-5728
E-mail reports@adonis.osti.gov
Web site http://www.osti.gov/contact.html

This report was prepared as an account of work sponsored by an agency of the United States Government. Neither the United States Government nor any agency thereof, nor any of their employees, makes any warranty, express or implied, or assumes any legal liability or responsibility for the accuracy, completeness, or usefulness of any information, apparatus, product, or process disclosed, or represents that its use would not infringe privately owned rights. Reference herein to any specific commercial product, process, or service by trade name, trademark, manufacturer, or otherwise, does not necessarily constitute or imply its endorsement, recommendation, or favoring by the United States Government or any agency thereof. The views and opinions of authors expressed herein do not necessarily state or reflect those of the United States Government or any agency thereof.

ORNL/SUB/99-B99398V-5

NEUTRONICS EXPERIMENTAL BENCHMARKS FOR THE UTILIZATION OF MIXED-OXIDE FUEL—VERIFICATION OF THE REFERENCE MONTE CARLO CODES APPLIED TO WATER-MODERATED REACTORS WITH MOX FUEL

M. S. Yudkevich

Date Published: February 2001

Prepared by
Russian Research Center "Kurchatov Institute"
Institute of Nuclear Reactors
under subcontract 85B-99398V

Funded by
Office of Fissile Materials Disposition
U.S. Department of Energy

Prepared by
Computational Physics and Engineering Division
OAK RIDGE NATIONAL LABORATORY
Oak Ridge, Tennessee 37831
managed by
UT-BATTELLE, LLC
for the
U.S. DEPARTMENT OF ENERGY
under contract DE-AC05-00OR22725

RRC
"Kurchatov
Institute"

Neutronics Experimental Benchmarks for the Utilization of Mixed Oxide Fuel

Final Report

June, 1999

Water Reactor -1
Joint U.S./Russian Project to Update, Verify and Validate
Reactor Design/Safety Computer Codes
Associated with MOX Fuel Usage in Water Reactors.

P. 99-9

Prepared by the

Russian Research Center "Kurchatov Institute"

Verification
of the Reference Monte Carlo Codes
Applied to Water Moderated Reactors with MOX Fuel

Mark S. Yudkevich

Russian Research Centrum "Kurchatov Institute

Moscow. June, 1999

CONTENTS

ACKNOWLEDGMENTS .....
ABSTRACT .....
INTRODUCTION 1
1. PLUTONIUM NITRATE SOLUTION 3
1.1. Weapons-grade plutonium 3
1.2. Burn-up plutonium. 13
1.3. Mixed plutonium and uranium nitrate solution 20
1.4. Solutions of plutonium nitrate poisoned with gadolinium 24
2. CRITICAL ASSEMBLIES WITH POLYSTYRENE AS THE MODERATOR 27
2.1. Homogenous PuO_2–polystyrene at low hydrogen content 27
2.2. Low-moderated mixtures of plutonium and uranium oxides with polystyrene 29
2.3. Homogeneous mixtures of polystyrene moderated plutonium and uranium oxides. 32
2.4. Neutron poison plates in PuO_2 – UO_2 – polystyrene mixtures. 36
2.5. Discussion 40
3. CLEAR LATTICES OF MOX RODS IN WATER. 42
3.1. MOX fuel with 20 wt.% Pu 42
3.2. MOX fuel with 2 wt.% Pu 44
4. Saxton critical experiments. 46
4.1. Multiplication factors calculation results 47
5. ESADA critical experiments. 91
5.1. Description of Experimental Configuration and multiplication factors calculation results. 91
5.2. Pin Power Distribution 100
CONCLUSION 115
REFERENCE 116

ACKNOWLEDGMENTS

The results reported herein were obtained by:
V.A. Barshevtsev, T.T. Ivanova, G.N. Manturov, Y.V. Rozhikhin, M. Yu. Semenov, A.A. Tsiboulia (SSC RF IPPE, Russia);
J.J. Lichtenwalter (ORNL, U.S.)
N.I. Mexeyev, V.I. Brisgalov, S.V. Marin, M.S. Yudkevich (RRC “KI”, RUSSIA)
G. Radulescu and H. Akkurt (University of Texas, U.S.)

Recommendations and discussions of Mr. R.T. Primm, III were extremely useful for author.

ABSTRACT

This document provides results of criticality benchmark calculation conducted during years 1997 – 1999. The list of tasks mutually agreed by United States and Russia specialists in November 1996 meeting. It is applicable to mixed oxide fuel cycles for light water reactors. The calculation results obtained with Russian and U.S. codes of Monte Carlo method are compared. The comparison with the experimental results is also provided. Brief descriptions of all investigated critical assemblies are presented and references for detailed descriptions are indicated.

INTRODUCTION

In the current report computer investigation results of the experimental critical assemblies are collected and analyzed. Earlier this information has been published as Progress Reports of the Joint U.S./Russian Project, presented and discussed at the specialist meetings.

The objective of this work is the validation of the reference Monte Carlo codes and the neutron data in application to MOX fuel usage in water moderated reactors and to criticality safety in a operation of MOX fuel fabrication.

The calculation results were obtained by the staff of following science nuclear centers:

State Scientific Centre of the Russian Federation Institute for Physics and Power Engineering (IPPE), Russia;
Oak Ridge National Laboratory (ORNL), U.S.
Russian Research Center "Kurchatov Institute" (RRC "KI"), Russia
University of Texas, U.S.

Descriptions of the critical assemblies were either taken from International Handbook Ref. [1] or were provided by U.S. part of the Joint Project. Ref [2 - 7]

Several codes and different neutron databases were used:

MCNP. This widely known code described everywhere. In this work MCNP was used with ENDF/B-V and ENDF/B-VI evaluated data libraries. The calculations have been carried out in U.S. In a text below the code and the data are referred as "MCNP (ENDF/B-V)" or "MCNP (ENDF/B-VI)"

MCU. This code, likewise MCNP, model a continuous energy neutron history in a neutron multiplied system of an arbitrary geometry. The version MCU/RFFI/A, Ref [8, p.3-i] was used in the current work. MCU code have her own neutron database DLC/MCUDAT. In the current work the version DLCIMCUDAT-1 .0 was used. The calculations have been carried out in RRC "KI". In a text below the code and the data are refer as "MCU".

KENO-V.a.

This code, Ref [9] models a neutron history in a group approach. In the current report calculation results with 238 group which were generated from ENDF/B-V are presented. The calculations have been carried out in U.S. In a text below the code and the data are referred as "KENO-V (ENDF/B-V)"

ABBN-93.

The calculations have been carried out in IPPE using the Monte-Carlo code KENO-V.a and ABBN-93 constants set Ref [10]. The CONSYST/ABBN system with ABBN-93 constants set Ref [11] was used for calculation the mixed material cross-sections and for converting data to the CCC-254/ANISN formats. The IPPE calculations were performed in the P_5 order of anisotropy approximation with the 299-group ABBN-93 cross-sections data set. In the text below the code and the data are referred as "KENO-V (ABBN-93)"

In current report the brief description of all considered critical assemblies is given. It was done to give the reader the general picture on the subject. Therefore the inessential details were omitted, the geometry parameters were rounded, and the material content is not mentioned. The source of detailed description is indicated, the variant names in the report coincide with names in original description.

The parameter uncertainty calculated by the Monte Carlo codes (one standard deviation) is identified in parenthesis. That is a reported value of X.XXXX(YY) should be interpreted as X.XXXX±0.00YY.

In the number of cases the averaging of the calculation results was carried out. At that the statistical dispersion of the particular variant wasn't taken into account. It's valid as the scattering of values to be averaged is much greater than the statistical dispersion. Results are written in a form $A \pm \delta A$, where A is the average value, δA is the mean-square error.

1. PLUTONIUM NITRATE SOLUTION

1.1. Weapons-grade plutonium

1.1.1. Water-reflected cylinders of 9-, 11- and 12-inch diameter

These critical experiments are described in Ref. [1, v. I.b, PU-SOL-THERM-010].

The reactor core is a cylindrical, thin-walled, stainless steel vessel filled with $Pu(NO_3)_2$ solution. Cylinder's inner diameter is equal to 9, 10 or 11 inch (about 23, 28, 30 cm). The solution heights depend on the plutonium concentration and were adjusted to critical. Critical heights lie between 22 cm and 44 cm, critical volumes lie between 12 liter and 18 liter.

A cylindrical vessel is inserted in a large water-filled tank. Above the level of fissionable solution each cylinder is fitted with a water-filled piston 'tamper' 30 cm thick. So reactor cores were surrounded with effectively infinite water reflector.

Benchmark specification includes geometry dimensions and isotopes' nuclear density. The plutonium composition includes only ^{239}Pu and ^{240}Pu with ^{240}Pu content of 2.9 wt.%.

Uncertainty in K_{eff} of the benchmark models is, at most, ± 0.0048.

Calculation results of K_{eff} are presented in Table 1. 1 and Figure 1. 1. The results do not reveal the correlation between the K_{eff} and the diameter of a core or value of $H/^{239}Pu$ relation, so it is possible to average the values of K_{eff}. Averaged K_{eff} are also given in Table 1.1. For each code a dispersion of results corresponds to the K_{eff} experimental uncertainty.

MCU and KENO-V (ABBN93) codes predict value approximately 0.005 grater then experimental K_{eff} = 1. It doesn't exceed an experimental error.

ENDF/B-V data overestimate K_{eff} value by 0.017. Comparison of MCNP and KENO-V results shows that the group approach gives roughly 0.0005 error of K_{eff}. It slightly offsets imperfection of neutron data.

Table 1. 1. Multiplication factors for reflected cylinders.

D (inch) – Case Number	Plutonium		K_{eff}			
	g/l	H / ^{239}Pu	MCU	MCNP (ENDF/B-V)	KENO-V (ABBN-93)	KENO-V (ENDF/B-V)
9-1	99.09	266.9	1.0131(9)	1.0238(10)	1.0127(9)	1.0184(22)
9-2	73.92	356.9	1.0082(10)	1.0226(10)	1.0068(9)	1.0152(25)
9-3	54.53	484.2	1.0033(10)	1.0142(10)	1.0026(9)	1.0104(23)
11-1	54.43	485.0	1.0067(10)	1.0196(10)	1.0074(9)	1.0166(23)
11-2	47.21	558.1	1.0062(9)	1.0167(9)	1.0065(9)	1.0116(20)
11-3	47.21	558.1	1.0045(9)	1.0168(10)	1.0048(9)	1.0126(19)
11-4	41.73	605.9	0.9983(9)	1.0092(10)	0.9975(9)	1.0061(18)
11-5	36.90	665.4	0.9985(9)	1.0102(9)	1.0000(9)	1.0059(19)
11-6	63.99	414.3	1.0095(9)	1.0223(10)	1.0098(9)	1.0200(21)
11-7	48.98	535.2	0.9994(9)	1.0089(10)	0.9989(9)	1.0065(21)
12-1	48.75	543.4	1.0069(9)	1.0176(10)	1.0056(9)	1.0160(19)
12-2	42.29	618.3	1.0069(9)	1.0179(10)	1.0052(9)	1.0102(20)
12-3	36.52	728.1	1.0121(9)	1.0211(9)	1.0110(9)	1.0215(22)
12-4	31.14	849.7	1.0048(9)	1.0168(9)	1.0073(9)	1.0160(22)
Averaged			1.0056 ± 0.0046	1.0170 ± 0.0047	1.0054 ± 0.0043	1.0133 ± 0.0049

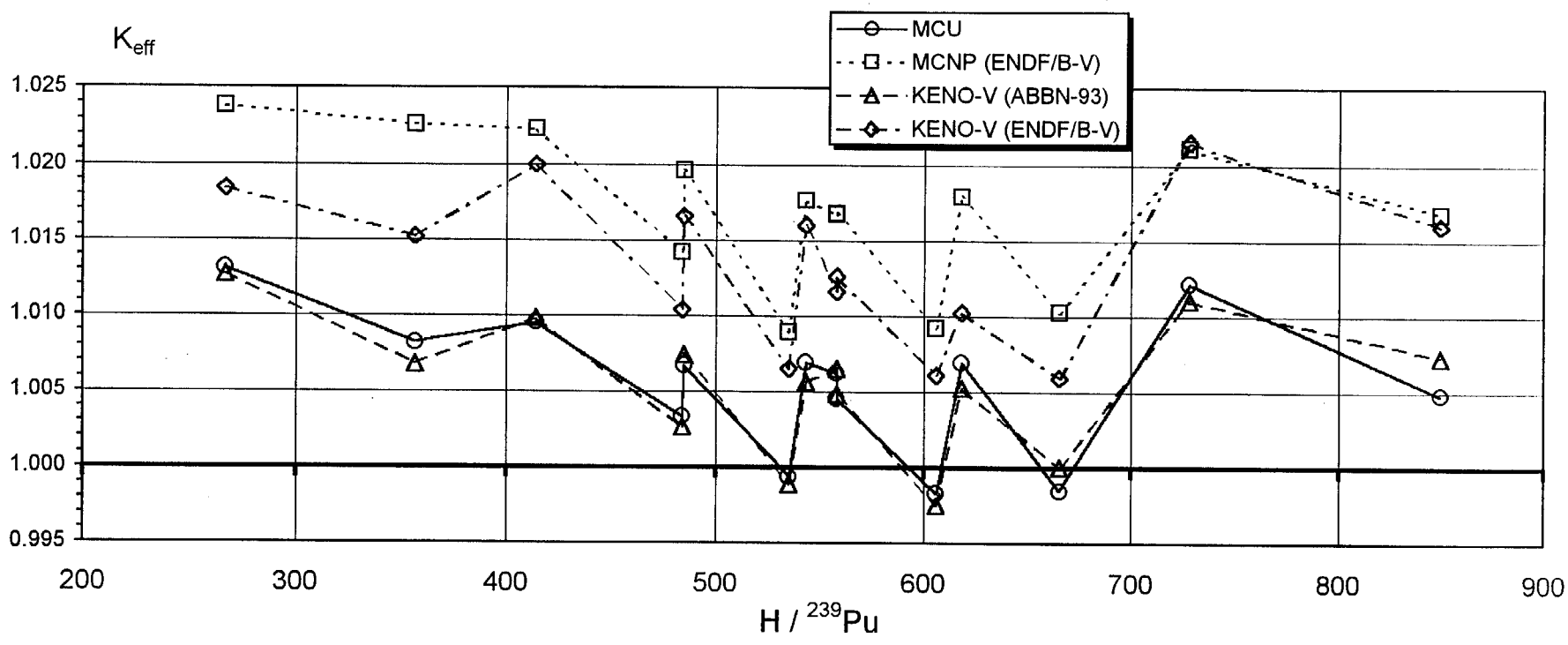

Figure 1. 1. Multiplication factors for reflected cylinders

1.1.2. Water-reflected spheres of 11.5-, 12,- 13 and 14-inch diameter.

These critical experiments are described in Handbook [1, v. I.b, PU-SOL-THERM-001 through –005].

Benchmark reactor model is thin-walled, stainless steel sphere (core) surrounded with effectively infinite water (reflector). Sphere fully filled with $Pu(NO_3)_2$ solution.

Benchmark specification includes geometry dimensions and isotopes' nuclear density.

Particular attributes of each series are indicated bellow.

- PU-SOL-THERM-001

Evaluated volumes differ within the limits of 0.6% in different cases, diameter lies between 12.80 cm and 12.87 cm.

The plutonium composition includes all isotopes from ^{238}Pu to ^{242}Pu, ^{240}Pu content is equal to 4.6 wt.%.

K_{eff} uncertainty was evaluated to be ± 0.0050.

- PU-SOL-THERM-002

Adjusted volume of the fissionable solution is equal to 15.12 liters. It corresponds to 30.68 cm sphere diameter.

The plutonium composition includes only ^{239}Pu and ^{240}Pu, ^{240}Pu content is equal to 3.12 wt.%.

K_{eff} uncertainty was evaluated to be ± 0.0047.

- PU-SOL-THERM-003

In seven cases the core vessels have steel shell. Adjusted volume of the fissionable solution is equal to 17.97 liters. It corresponds to 33.03 cm sphere diameter.

In one case the core vessel has aluminum shell. Adjusted volume of the fissionable solution is equal to 18.87 liters. It corresponds to 32.50 cm sphere diameter.

The plutonium composition includes only ^{239}Pu and ^{240}Pu, ^{240}Pu content is equal to 1.76 or 3.12 wt.%.

K_{eff} uncertainty is at most ± 0.004.

- PU-SOL-THERM-004

Adjusted volume of the fissionable solution is equal to 23.57 liters. It corresponds to 35.57 cm sphere diameter.

The plutonium composition includeds only ^{239}Pu and ^{240}Pu, ^{240}Pu content is equal to 0.54, 1.76, 3.12 or 3.43 wt.%.

K_{eff} uncertainty is ± 0.004, at the most.

- PU-SOL-THERM-005

Adjusted volume of the fissionable solution is equal to 23.57 liters. It corresponds to 35.57 cm sphere diameter.

The plutonium composition includes only ^{239}Pu and ^{240}Pu, ^{240}Pu content is equal to 4.05 or 4.40 wt.%.

K_{eff} uncertainty is at most ± 0.004.

Calculation results are presented in Table 1. 2 and shown at.Figure 1. 2

An overall picture is similar with previous one: MCU and ABBN-93 predicts K_{eff} to be close to the experimental value, K_{eff} obtained by ENDF/B-V exceed 1 of ~ 0.01

Table 1. 2. Multiplication factors for reflected spheres.

D (inch) – Case Number	Plutonium		K_{eff}		
	g/l	H / ^{239}Pu	MCU	KENO-V (ABBN-93)	MCNP (ENDF/B-V)
11.5 – 1	73.0	354.0	1.0013(9)	0.9984(9)	1.0110(10)
11.5 – 2	96.0	258.3	1.0047(9)		1.0132(10)
11.5 – 3	119.0	206.6	1.0050(9)		1.0153(10)
11.5 – 4	132.0	180.1	0.9976(10)		1.0088(10)
11.5 – 5	140.0	171.0	1.0026(10)	1.0008(9)	1.0111(10)
11.5 – 6	268.7	87.0	1.0018(10)	0.9941(9)	1.0078(10)
12 – 1	49.84	524	0.9998(10)	0.9992(9)	1.0126(10)
12 – 2	51.42	504	1.0000(9)		1.0095(10)
12 – 3	56.09	451	0.9976(9)		1.0105(10)
12 – 4	59.64	421	1.0022(10)		1.0117(10)
12 – 5	63.33	393	1.0057(9)		1.0119(10)
12 – 6	70.11	344	1.0001(10)		1.0108(10)
12 – 7	77.09	309	1.0037(10)		1.0128(10)
13 – 1	33.32	788	0.9989(9)	0.9976(9)	1.0077(9)
13 – 2	34.32	755	1.0004(9)		1.0102(9)
13 – 3	37.43	699	1.0025(9)		1.0102(9)
13 – 4	38.12	682	0.9992(9)		1.0106(9)
13 – 5	40.65	627	1.0030(9)		1.0122(9)
13 – 6	44.09	563	1.0030(9)		1.0126(9)
13 – 7	35.98	738	1.0038(9)		1.0139(9)
13 – 8	36.81	715	1.0024(9)		1.0141(9)
14 – 1	26.27	987	0.9984(9)		1.0101(9)
14 – 2	26.31	977	0.9911(9)		1.0069(9)
14 – 3	27.20	935	0.9967(9)		1.0072(9)
14 – 4	28.09	889	0.9947(9)		1.0046(9)
14 – 5	27.58	943	0.9939(9)		1.0077(9)
14 – 6	28.60	927	0.9988(9)		1.0074(9)
14 – 7	29.57	891	1.0019(9)		1.0140(9)
14 – 8	29.95	870	0.9962(9)		1.0086(9)
14 – 9	31.60	805	0.9973(9)		1.0083(9)
14– 10	35.36	689	0.9983(9)		1.0076(9)
14 – 11	39.38	598	0.9966(9)		1.0082(9)
14 – 12	29.44	893	0.9977(9)		1.0105(9)
14 – 13	29.27	903	0.9963(9)		1.0070(9)
14 – 1	29.65	902	0.9977(9)		1.0094(9)
14 – 2	30.54	868	0.9986(9)		1.0093(9)
14 – 3	31.43	834	0.9991(9)		1.0097(9)
14 – 4	33.54	766	1.0015(9)		1.0119(9)
14 – 5	36.04	695	1.0020(9)		1.0116(9)
14 – 6	38.49	634	1.0034(9)		1.0108(9)
14 – 7	40.91	580	1.0022(9)		1.0110(9)
14 – 8	30.58	869	0.9949(10)		1.0077(9)
14 – 9	31.85	825	0.9969(10)		1.0087(9)
Averaged			0.9998±0.0032	0.9980±0.0022	1.0102±0.0023

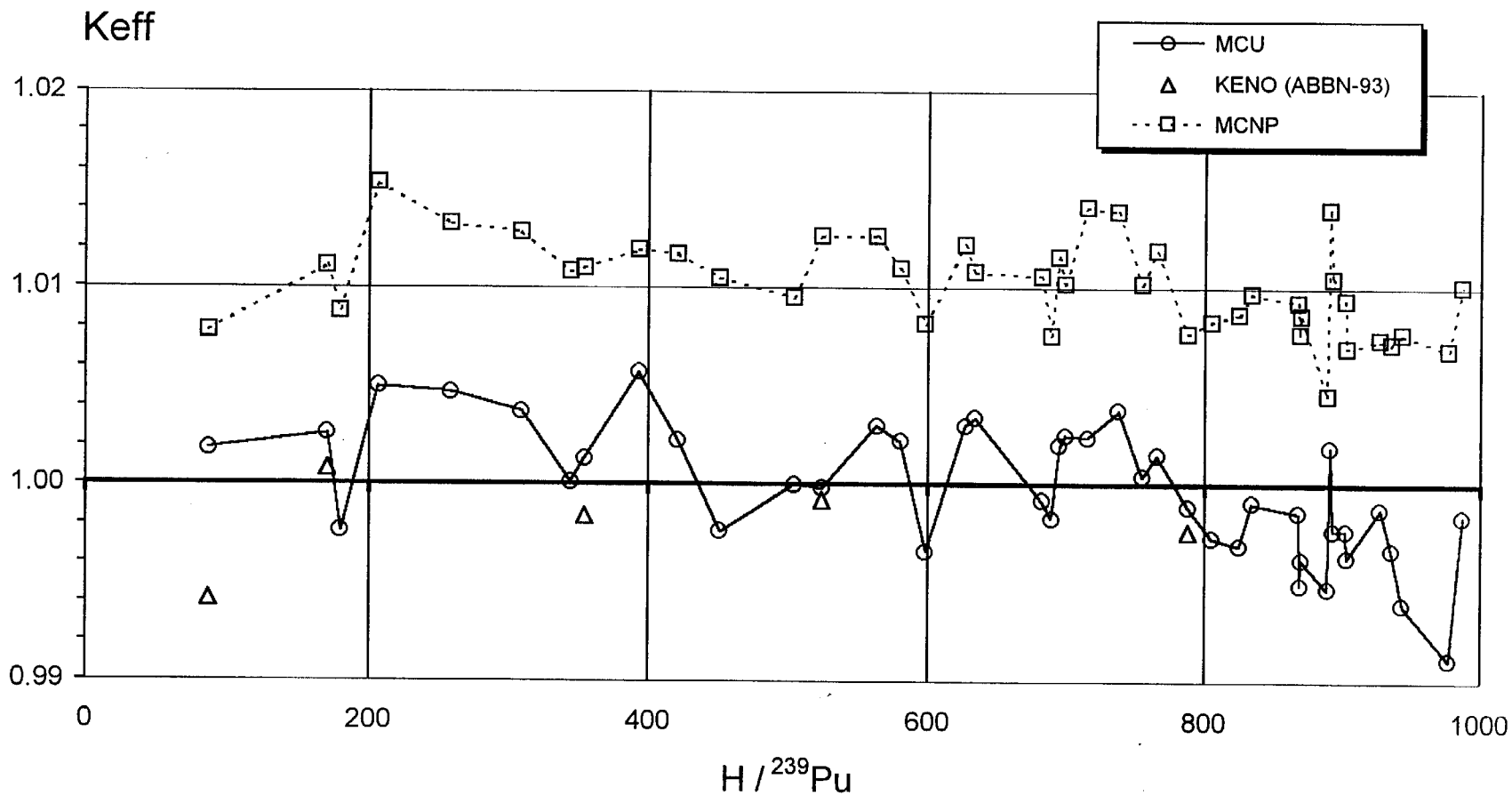

Figure 1. 2. Multiplication factors for reflected spheres.

1.1.3. Unreflected cylinders of 13.4- and 17.9-inch diameter.

These critical experiments are described in Ref. [2, p. 58].

Benchmark reactor model is thin-walled, stainless steel vessel partly filled with $Pu(NO_3)_2$ solution. ^{240}Pu content is equal to 4.88 wt.%..

The vessel was modeled as a cylinder with 34 cm diameter and 51 cm height or cylinder with 45 cm diameter and 61 cm height.

The solution height depends on the plutonium concentration. For 13.4-inch cylinder critical heights lie between 28 cm and 34.9 cm. Only one case of 17.9-inch cylinder was investigated, the critical height is equal to 21.95 cm.

Benchmark specification includes critical height of fissionable solution and isotopes' nuclear density. The plutonium composition includes only ^{239}Pu and ^{240}Pu.

Uncertainty in K_{eff} of the benchmark models is not indicated.

Calculation results by KENO-V code with different databases are presented in Table 1. 3 and Table 1. 4 and shown at Figure 1. 3. A calculation by MCU code wasn't carried out. Calculation results by MCNP code are not known for us.

It seems that big difference in the K_{eff} calculation results for 13.4-inch and 17.9-inch-diam cases indicates an error of evaluated experimental parameters.

In the overview of the experiment is written: " ... experiments are judged to be unacceptable as criticality safety benchmark experiments until additional experimental data can be obtained".

Table 1. 3. Multiplication factors for unreflected 13.4-in-diam. cylinder.

Case Number	Plutonium		K_{eff}	
	g/l	H / ^{239}Pu	KENO (ABBN-93)	KENO (ENDF/B-V)
5-13 1	226	106	0.9994(9)	1.0088(24)
5-13 2	165	151	1.0000(9)	1.0030(23)
5-13 3	133	189	0.9956(9)	1.0033(23)
5-13 4	91.4	280	0.9992(9)	1.0058(21)
5-13 5	73.5	351	1.0006(9)	1.0028(24)
5-13 6	60.4	429	1.0033(9)	1.0100(23)
5-13 7	43.3	602	1.0038(9)	1.0043(25)
Averaged			1.0003 ± 0.0025	1.0054 ± 0.0028

Table 1. 4. Multiplication factors for unreflected 17.9-inch diameter cylinder.

Case Number	Plutonium		K_{eff}	
	g/l	H / ^{239}Pu	KENO-V (ABBN-93)	KENO-V (ENDF/B-V)
5-18 1	50.7	509	0.9915(9)	0.996

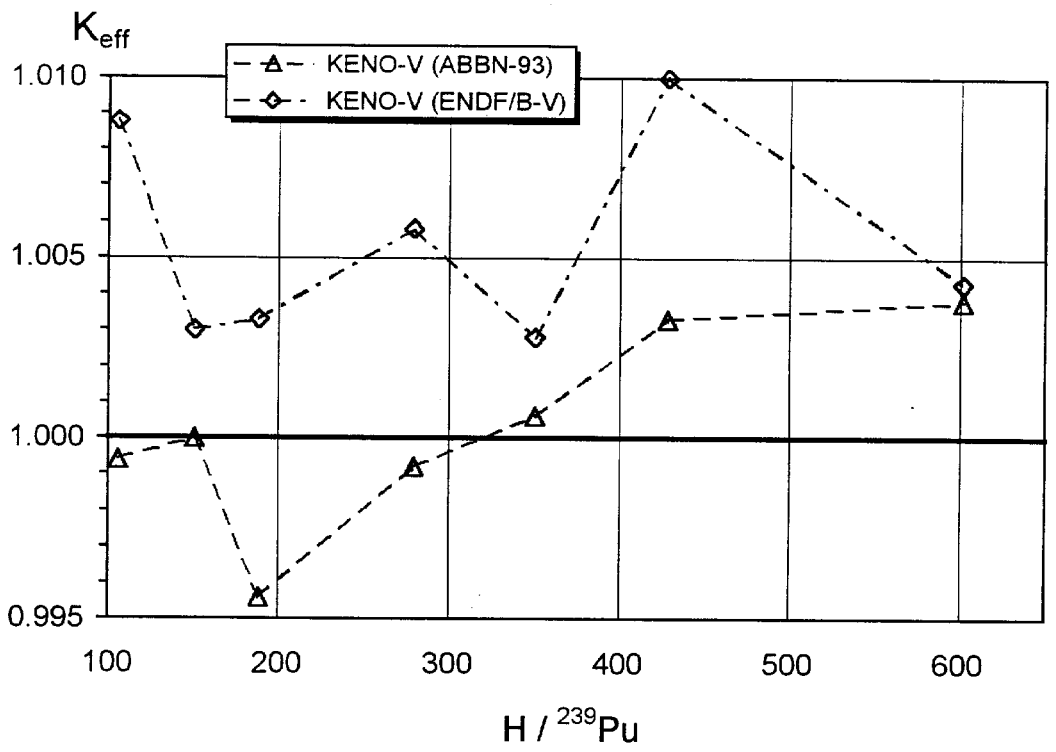

Figure 1. 3. Multiplication factors for unreflected 13.4-in-diam. cylinder.

1.1.4. Summary

The main calculation results of critical assemblies with weapons-grade plutonium nitrate solution are collected inTable 1. 5. and are presented at Figure 1. 4. Relative to neutron data, these results may be of interest because of the deviation of a calculation K_{eff} from the experimental $K_{eff} = 1$ is connected with only isotope ^{239}Pu.

The results for unreflected 17.9-inch-diam. cylinders (only one $H/^{239}Pu$ value) differ heavily from other assemblies. Below this case is not considered.

Table 1. 5. Summary results of weapons-grade plutonium nitrate solution.

Assembly	K_{eff}			
	MCU	MCNP (ENDF/B-V)	KENO-V (ABBN-93)	KENO-V (ENDF/B-V)
Ref. cylinders	1.006 ± 0.005	1.017 ± 0.005	1.005 ± 0.004	1.013 ± 0.005
Refl. spheres	1.000 ± 0.003	1.010 ± 0.002	0.998 ± 0.002	
Unrefl. cylinders			1.000 ± 0.003	1.005 ± 0.003

Several comments on the results obtained are given below.

- Errors of K_{eff} calculation, namely difference between calculated and and experimental values, $\Delta K_{eff} = -1$, do not depended on $H/^{239}Pu$ rathio. It depends on a geometry of the assemblies but a difference is not exceed K_{eff} experimental uncertainties.
- MCU and KENO-V (ABBN-93) results coincide in limits of statistical dispersion. The same is true for MCNP and KENO-V (ENDF/B-V) codes.
- For MCU code ΔK_{eff} intervening between 0.997 and 1.01.
- For MCNP code ΔK_{eff} intervening between 1.007 and 1.022.
- On average over all cases, neutron data used provided a precision of multiplication factors calculation as follows:

Continueus energy approach:

MCU: $\Delta K_{eff} = 0.000 \pm 0.003$

ENDF/B-V: $\Delta K_{eff} = 0.010 \pm 0.002$

Group approach:

ABBN-93: $\Delta K_{eff} = 0.000 \pm 0.003$

ENDF/B-V: $\Delta K_{eff} = 0.005 \pm 0.003$

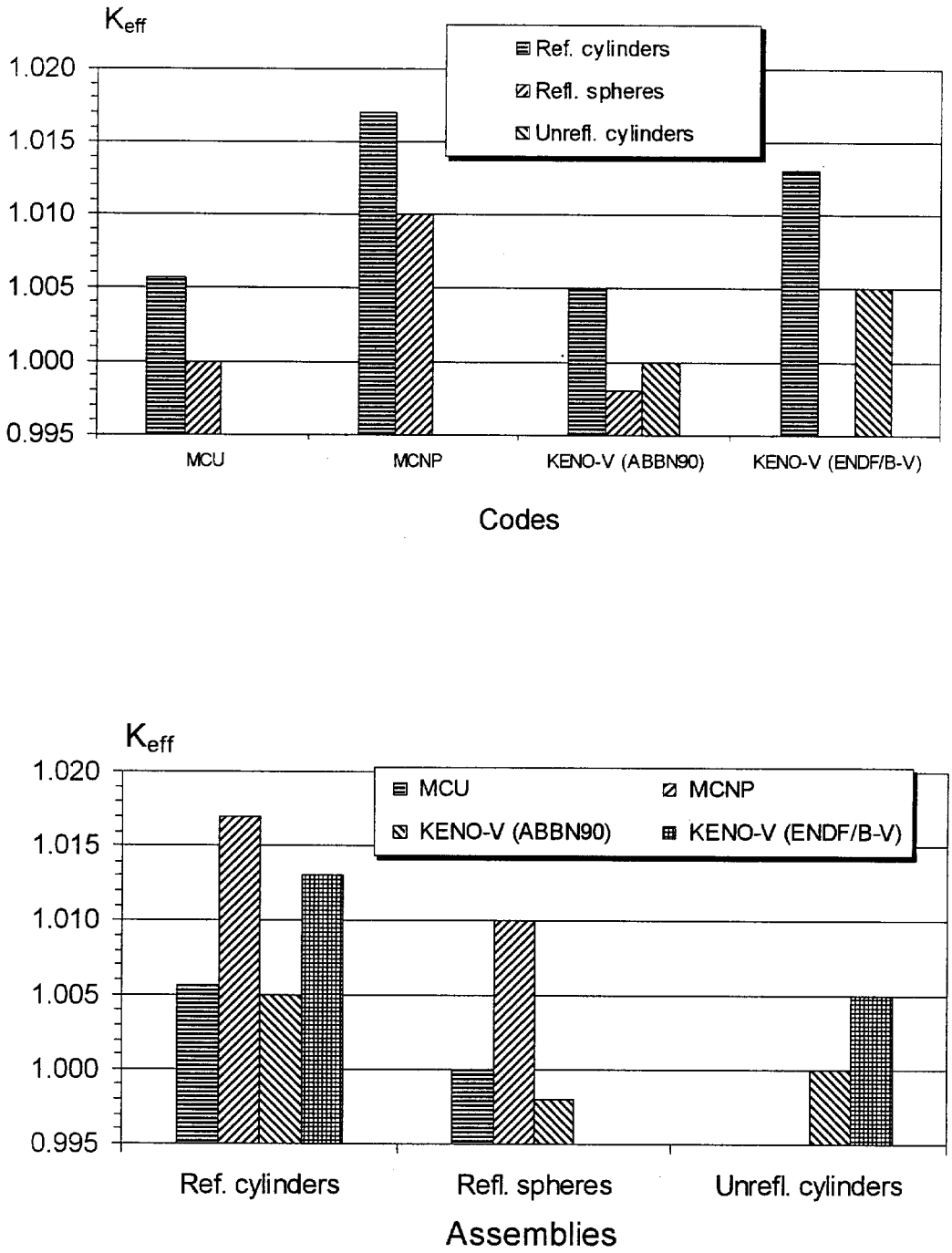

Figure 1. 4. Averaged multiplication factors of the different assemblies.

1.2. Burn-up plutonium.

1.2.1. Different plutonium isotope compositions.

In this PNL critical experiments plutonium of different isotope compositions was used. The assemblies are described in Ref. [5].

Reactor core is thin-walled sphere or cylinder filled with $Pu(NO_3)_2$ solution. Water reflectors are of practically infinite thickness or do not exist.

Uncertainty in K_{eff} of the benchmark models is not indicated in Ref. [5]. Main parameters of each series are indicated bellow.

- PNL-6

Unreflected sphere with D = 38.63 cm.
Plutonium concentration is equal to 172.3 g/l.
^{239}Pu content is equal to 95 wt.%.

- PNL-7

Reflected sphere with D = 35.56 cm
Plutonium concentration is equal to 26.3 g/l.
^{239}Pu content is equal to 99.5 wt.%.

- PNL-9

Unreflected cylinder with D = 45.47 cm, H = 36.40 cm.
Plutonium concentration is equal to 28.5 g/l.
^{239}Pu content is equal to 86.2 wt.%.

- PNL-10

Side and bottom reflected cylinder with D = 61.03 cm, H = 15.44 cm.
Plutonium concentration is equal to 116 g/l.
^{239}Pu content is equal to 90.7 wt.%.

- PNL-11

Side and bottom reflected cylinder with D = 61.03 cm, H = 80.92 cm.
Plutonium concentration is equal to 40.6 g/l.
^{239}Pu content is equal to 41.4 wt.%.

Calculation results by MCU and KENO-V (ABBN-93) codes are provided in Table 1. 6. Calculation results with ENDF/B data are not known for us.

Dependence of K_{eff} on ^{240}Pu content is not revealed.

K_{eff} value for ^{240}Pu content 13.8 wt.% is too small. Most likely, it is connected with rough description of plutonium composition (^{241}Pu is not taken in account). For other cases dependence of K_{eff} on ^{240}Pu content is not revealed

Table 1. 6. Multiplication factors for PNL assemblies.

Case Number	H / ^{239}Pu	^{240}Pu wt.%	^{241}Pu wt.%	K_{eff}	
				MCU	KENO-V (ABBN-93)
PNL-7	980	0.54		0.9991(20)	
PNL-6	125	4.6	0.31	0.9975(19)	
PNL-10	210	8.4	0.85	0.9963(15)	0.9940(18)
PNL-9	910	13.8		0.9932(11)	0.9964(7)
PNL-11	1106	42.9	10.8	0.9993(17)	0.9975(6)

1.2.2. Plutonium of 13.74 wt.% ^{240}Pu content.

The experiment is described in Ref. [2, p. 58].

Critical heights of the unreflected cylinders of 13.4- and 17.9-inch diameter were measured. The design of assemblies is completely the same as it was described in paragraph 1.1.3. The only difference is that ^{240}Pu content is equal to 13.74 wt.% instead of 4.88 wt.%.

Calculation results by KENO-V codes with ABBN-93 and ENDF/B-V neutron data are presented in Table 1. 7 and Figure 1. 5. A calculation by MCU code wasn't carried out. Calculation results with ENDF/B data are not known for us.

Analyzing results, one should have in mind that ^{241}Pu content is not indicated in the benchmark specification. So calculation might have to predict rather low K_{eff} values.

K_{eff} dependence on H/^{239}Pu is not revealed. It allows to average results.

As one can see K_{eff} values differ nearly in 0.01 for cylinders of 13.4-inch and 17.9-inch diameter. The same situation takes place for case of 4.88 wt.% ^{240}Pu content.

Table 1. 7. Multiplication factors for ^{239}Pu = 86 wt.%. unreflected cylinders

Case Number	Plutonium		K_{eff}	
	g/l	H / ^{239}Pu	KENO (ABBN-93)	KENO (ENDF/B-V)
13.4 inch diameter				
14-13-1	163	129	0.9978(9)	1.0050(25)
14-13-2	114	190	0.9959(9)	0.9998(21)
14-13-3	80.2	275	0.9988(9)	1.0039(23)
14-13-4	65.6	339	0.9998(9)	1.0104(22)
14-13-5	58.6	380	0.9995(9)	1.0106(22)
Averaged			0.9984 ± 0.0014	1.0059 ± 0.0041
17.9 inch diameter				
14-18-1	215.5	93	0.9927(8)	0.9965(22)
14-18-2	174.5	118	0.9920(9)	0.9974(20)
14-18-3	135.0	156	0.9878(9)	0.9987(24)
14-18-4	102.5	210	0.9876(9)	0.9977(25)
14-18-5	73.0	299	0.9902(9)	0.9938(22)
14-18-6	53.5	410	0.9844(9)	0.9885(22)
14-18-7	43.6	511	0.9906(9)	0.9965(28)
14-18-8	28.5	786	0.9964(9)	1.0071(24)
14-18-9	22.0	1023	0.9953(9)	1.0055(17)
Averaged			0.9908 ± 0.0053	0.9908 ± 0.0036

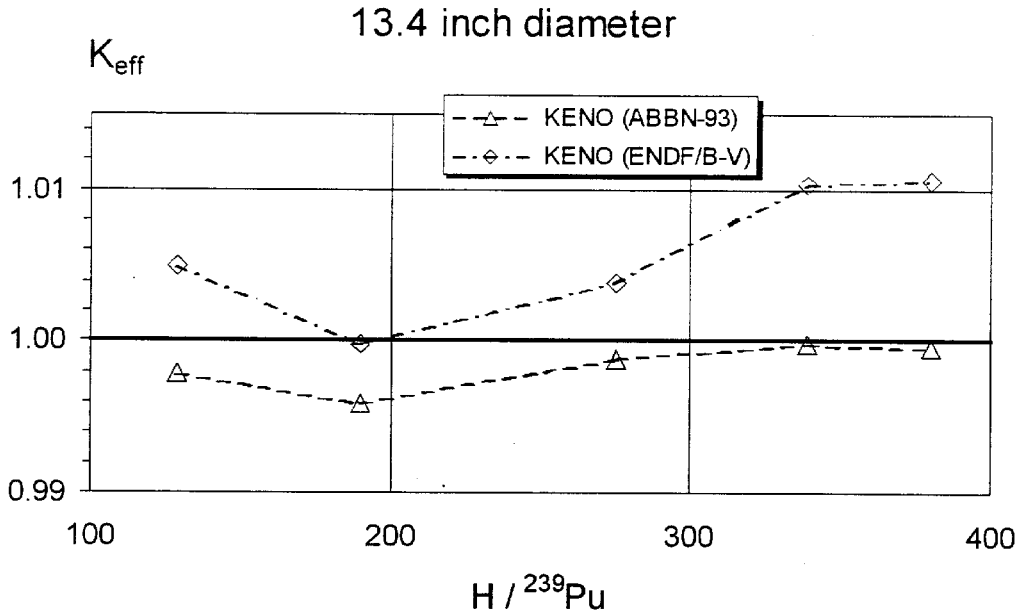

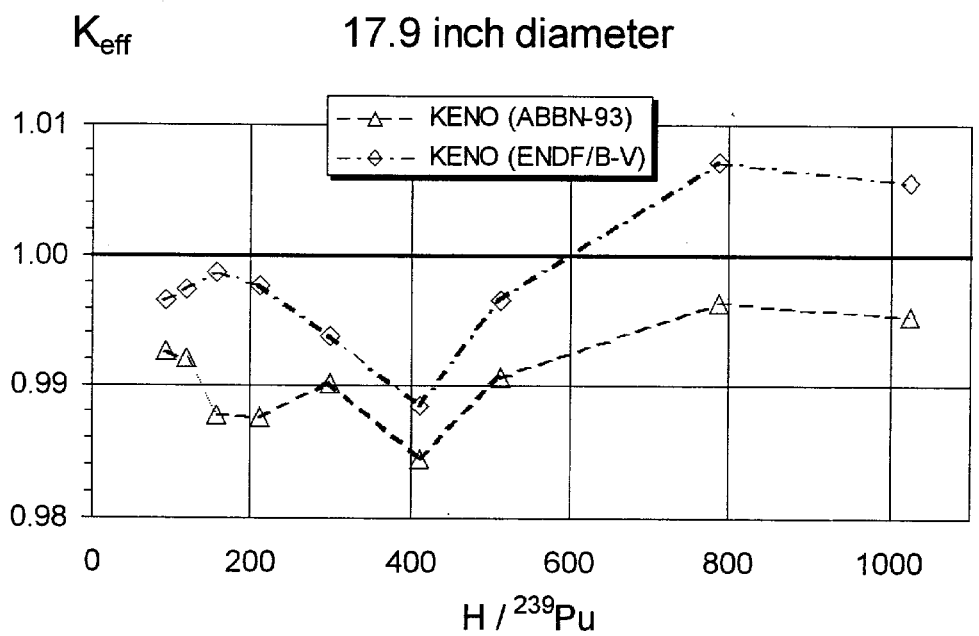

Figure 1. 5. Multiplication factors for ^{239}Pu = 86 wt.%. unreflected cylinders

1.2.3. Critical assembly with extremely high burnup plutonium.

In this experiment the isotopic compositions (wt.%) of plutonium were as follows: 0.2% ^{238}Pu, 41.4% ^{239}Pu, 42.9% ^{240}Pu, 10.8% ^{241}Pu, 4.7% ^{242}Pu.

The benchmark description was taken from Ref. [2, p. 67]

The plutonium nitrate solution was contained within a 24-inch diameter (61 cm), 105-cm-height stainless steel vessel. A reflector tank enclosed the vessel and provided at least 20 cm of water on the sides and bottom of the vessel.

The solutions were contaminated by trace amounts of gadolinium. ^{241}Am were present in the solutions in the amount of 1.08 wt.% Pu.

Among the experiments, the plutonium concentration and nitric acid molarity were increased and the critical solution height was measured.

No uncertainties were provided for measured values of the critical height, plutonium concentration and nitric acid molarity. So K_{eff} experimental error is not known.

K_{eff} calculation results are presented in Table 1. 8

If the concentration of plutonium is minimal, a precision of K_{eff} calculation is the same as for the assemblies with weapon grade plutonium: K_{eff} are about 1.0 for MCU and KENO (ABBN-93) codes and equal to ~1.01 for KENO (ENDF/B-V) code.

With the increase of plutonium's concentration the K_{eff} values grow and come to 0.025 for all codes.

In the Table 1. 9 and Figure 1. 6 the distribution of neutron absorption according to the isotope's list is given. The calculation is fulfilled by the MCU code, all values are normalized to one fission neutron.

It's likely that the source of a K_{eff} error of calculations could be found in a ^{241}Pu neutron data. At the same time it's the only experiment with so high ^{241}Pu content and it's desirable to confirm its results before making the final conclusion.

Table 1. 8. Multiplication factors for plutonium of extremely high burnup.

Case	Plutonium		K_{eff}		
	g/l	H / ^{239}Pu	MCU	KENO-V (ABBN-93)	KENO (ENDF/B-V)
1	40.6	1106	1.0008(9)	0.998	1.009
2	46.8	954	1.0016(10)	1.000	1.012
3	56.3	780	1.0054(12)	1.002	1.016
4	65.1	671	1.0066(14)	1.006	1.018
5	75.6	572	1.0108(15)	1.008	1.017
6	85.5	500	1.0122(15)	1.012	1.020
7	99.3	425	1.0233(15)	1.016	1.022
8	116.0	360	1.0242(15)	1.022	1.023
9	140.0	290	1.0253(15)	1.022	1.025

Table 1. 9. Neutron balance.

Case	H/^{239}Pu	K_{eff}	Absorption				Leakage
			^{239}Pu	^{240}Pu	^{241}Pu	Rest	
1	1106	1.0008	0.378	0.185	0.116	0.303	0.019
2	954	1.0016	0.380	0.190	0.115	0.293	0.022
3	780	1.0054	0.383	0.197	0.115	0.282	0.024
4	671	1.0066	0.386	0.203	0.115	0.272	0.026
5	572	1.0108	0.391	0.209	0.115	0.261	0.026
6	500	1.0122	0.392	0.214	0.114	0.255	0.025
7	425	1.0233	0.399	0.222	0.115	0.239	0.026
8	360	1.0242	0.401	0.229	0.114	0.231	0.025
9	290	1.0253	0.406	0.241	0.114	0.220	0.023

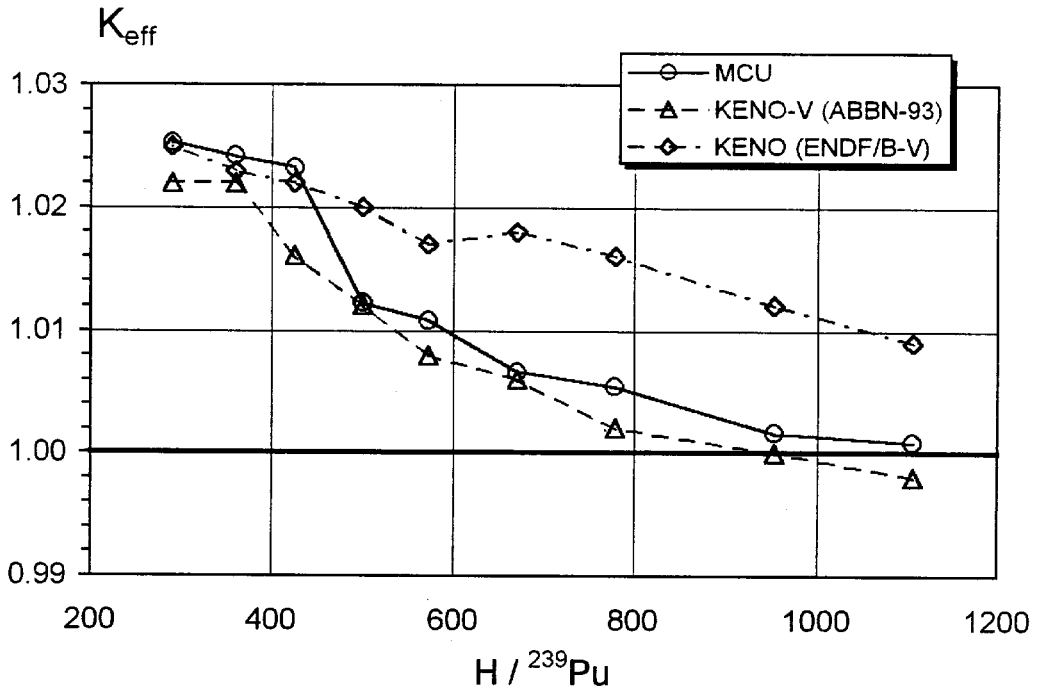

Figure 1. 6. Multiplication factors for plutonium of extremely high burnup.

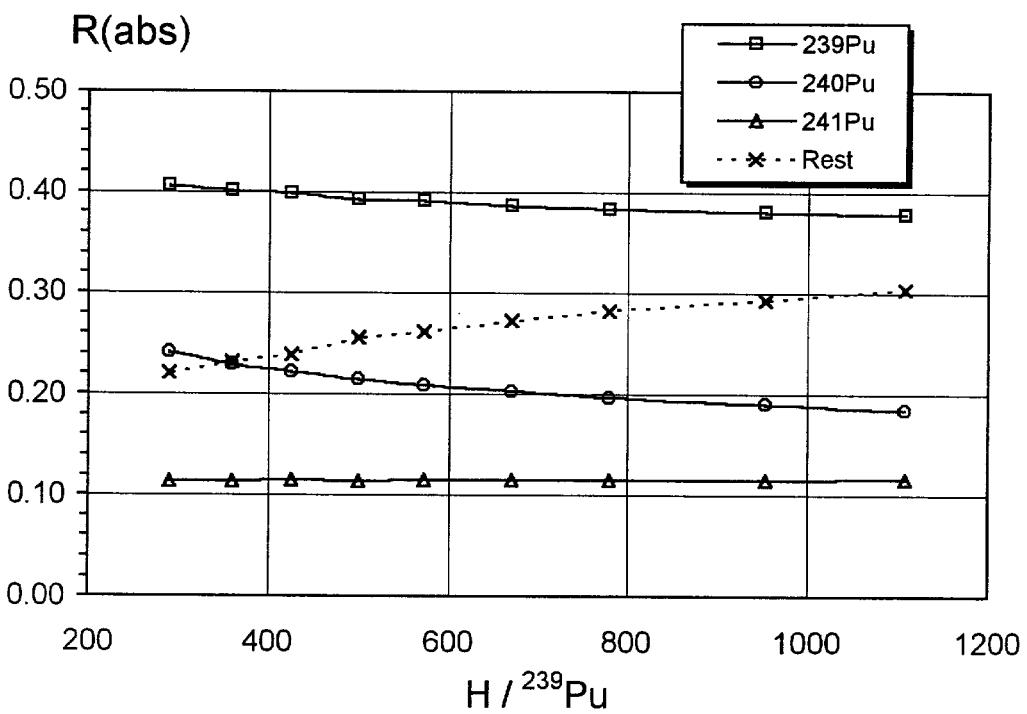

Figure 1. 7. Absorption rate of different isotopes.

1.3. Mixed plutonium and uranium nitrate solution

1.3.1. Water reflected cylinder.

These critical experiments are described in Handbook [1, v. I.b, MIX-SOL-THERM-002].

Mixed plutonium-uranium nitrate solution was contained in thin-walled, stainless steel cylindrical vessel. Cylinder has an inside diameter of 69 cm and height of 109 cm. Critical heights of a fissionable solution were equal to 76.80 cm, 83.14 cm and 81.72 cm.

The tank was centered in the cuboid water reflector, which is about 100 cm by 100 cm and 123 cm high. A distance between bottoms of the inner and outer vessels was equal to 16 cm.

Rations of plutonium to plutonium plus uranium were equal to 0.52 and 0.23. Plutonium contained 8 wt.% ^{240}Pu. ^{235}U isotope content in uranium was equal to 0.702 wt.% in experiments number 058 and 059 and equal to 0.438 in experiment number 061.

An uncertainty of K_{eff} benchmark models was evaluated as 0.0024.

Calculation K_{eff} results are presented in Table 1. 10. and . Figure 1. 8

Results obtained are similar to ones of pure plutonium nitrate solution.

Table 1. 10. Multiplication factors for mixed plutonium and uranium solution of cylindrical geometry

Case Number	Plutonium		Uranium	K_{eff}		
	g/l	H / ^{239}Pu	g/l	MCU	KENO-V (ABBN-93)	MCNP (ENDF/B-V)
058	11.88	240	11.05	1.0005(10)	0.9945(5)	1.0082(2)
059	11.73	243	10.78	1.0012(11)	0.9963(5)	1.0074(5)
061	12.19	231	41.04	1.0013(12)	0.9963(5)	1.0079(4)
Averaged				1.0010 ± 0.0004	0.9957 ± 0.0008	1.0078 ± 0.0003

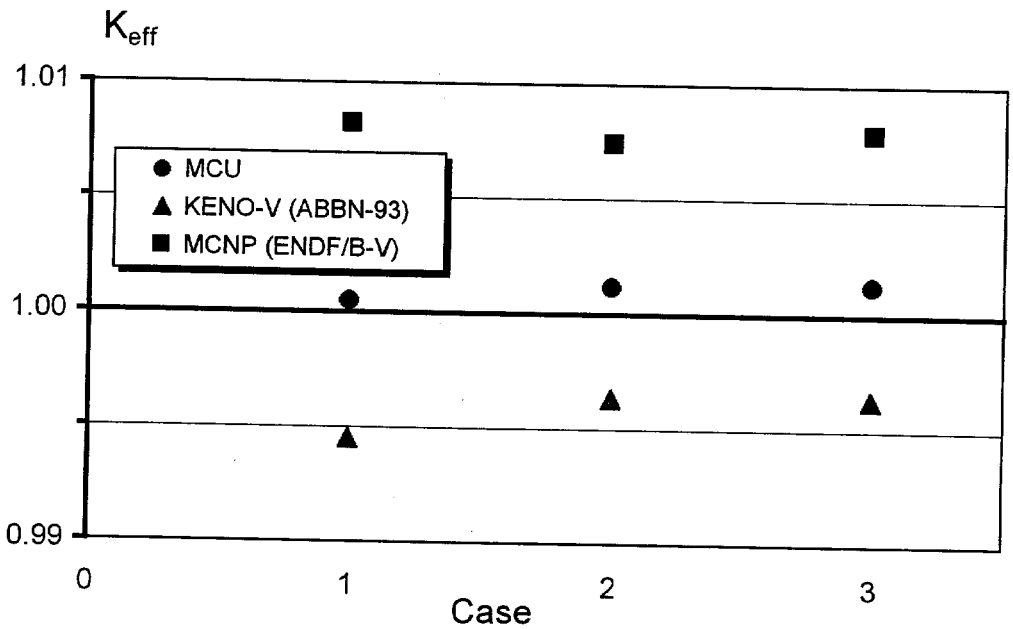

Figure 1. 8. Multiplication factors for mixed plutonium and uranium solution of cylindrical geometry.

1.3.2. Annular cylindrical geometry.

These critical experiments are described in Handbook [1, v. I.b, MIX-SOL-THERM-001].

This assembly is typical of a storage configuration for fissile materials. A mix of plutonium (8 wt % ^{240}Pu) and uranium (nature condition) nitrate solution filled the annular cylindrical vessel and was surrounded with a water reflector. The annular cylindrical inset was placed in the central region of the annular tank. In most of the experiments, the inset was fabricated from borate concrete. An interior to the inserts was a stainless steel bottle containing an additional plutonium-uranium nitrate solution. In Case 99 cadmium-covered polyethylene inserts were used. In cases considered here, the critical height changed from 27.5 to 79.2 cm.

An uncertainty of K_{eff} benchmark models was evaluated as 0.0052 of 99 experiment and as 0.0016 of all other cases.

Calculation K_{eff} results are reported in Table 1. 11 and shown in Figure 1. 9.

For MCU codes results are similar to ones of pure plutonium solution.

For KENO-V with ABBN-93 data and for MCNP (ENDF/B-V) code calculation value of K_{eff} fall approximately in 0.01. It is surprising because that uranium absorbs no more then 5% fission neutrons.

Table 1. 11. Multiplication factors for mixed plutonium and uranium solution of annular geometry.

Case Number	Plutonium		Uranium	K_{eff}		
	g/l	H / ^{239}Pu	g/l	MCU	KENO-V (ABBN-93)	MCNP (ENDF/B-V)
87	102.19	233	365.2	0.9931(14)	0.9842(8)	0.9981(10)
95	195.61	125	6.5	0.9998(13)	0.9878(9)	1.0030(12)
97	58.3	477	2.3	0.9988(12)	0.9888(8)	1.0051(12)
99 [a]	73.64	349	250.3	0.9968(12)	1.0003(8)	1.0098(10)
108	47.08	569	161.7	0.9977(10)	0.9866(8)	1.0028(11)
Averaged				0.9979 ± 0.0023	0.9895 ± 0.0051	1.0038 ± 0.0035

[a] with polyethylene

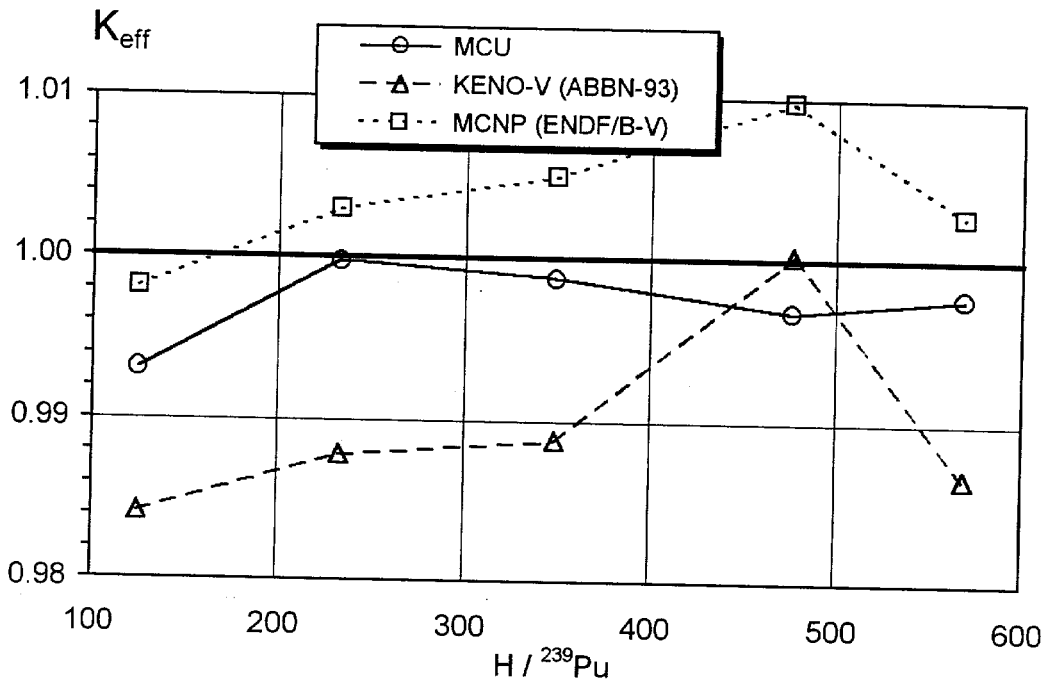

Figure 1. 9. Multiplication factors for mixed plutonium and uranium solution of annular geometry

1.4. Solutions of plutonium nitrate poisoned with gadolinium

These critical experiments are described in Ref [2, p. 48]

Critical configurations were 61-cm-diam cylinders surrounded by a thick water reflector on the bottom and at the sides. A water level height of the reflector considerably exceeded the heights of the solution in the central vessel.

Two series of experiments have been realized. In the first series, the solution contained 116 g of plutonium per liter of solution (H /^{239}Pu = 520), the critical height was varied from ~15 cm up to ~ 8 cm. In the second one, the solution contained 363 g of plutonium per liter of solution (H /^{239}Pu = 135), the critical height varied from ~ 26 cm up to ~ 59 cm.

The ^{240}Pu isotopic content in Pu was equal to 8 wt.%.

The uncertainty in K_{eff} from the uncertainty in plutonium concentration may be monotonic with increasing gadolinium concentration.

g Pu/l	g Gd/l	δK_{eff}
116	0.00	± 0.0049
116	2.38	± 0.0031
363	4.40	± 0.0020
363	12.58	± 0.0015

Calculation results are given in Table 1. 12 and Figure 1. 10. In addition to K_{eff} values, in this Table the fraction of fission neutron absorbed by gadolinium is presented.

In this section, it was not expedient to average values of calculated results, it was more important to estimate the dependence of calculation-to-experiment differences on the gadolinium concentration.

In low and high concentration of plutonium, the difference between the calculation and experimental data does not show a clearly expressed dependence on gadolinium concentration. For all codes, a scatter of calculated K_{eff} does not exceed a value of experimental errors.

Let's compare present results with the case of pure plutonium. At that, we assume that results of pure plutonium are reliable.

All codes give K_{eff} for poisoned solution less then for pure one. A difference is equal to 0.005÷0.01. It is evident that a capture cross section of gadolinium is too high in all neutron data. At the same time, this conclusion seems to be in contradiction with the fact that K_{eff} calculated is't depend on the atomic rations of gadolinium to plutonium Gd/Pu and gadolinium to hydrogen Gd/H. So it's possible that the real reason for calculation errors is some error of the benchmark model.

Table 1. 12. Multiplication factors for gadolinium-poisoned solution

Case Number	Gadolinium g Gd/l	K_{eff}			Gd R(cap) [a]
		MCU	KENO-V (ABBN-93)	KENO-V (ENDF/B-V)	
116 g Pu/l					
116-1	0.00	0.9958(12)	0.994	1.0057(12)	0.0
116-2	0.48	0.9997(11)	0.995	1.0051(20)	0.074
116-3	0.96	0.9967(11)	0.993	1.0063(17)	0.116
116-4	1.42	1.0019(10)	0.992	1.0128(16)	0.159
116-5	1.92	0.9943(10)	0.991	1.0090(13)	0.198
116-6	2.38	0.9974(16)	0.990	1.0095(15)	0.228
363 g Pu/l					
363-1	4.40	0.9979(6)	0.988	1.0033(17)	0.076
363-2	5.28	0.9965(11)	0.991	1.0020(17)	0.086
363-3	6.28	0.9943(11)	0.992	1.0002(18)	0.095
363-4	8.21	0.9940(10)	0.989	0.9985(15)	0.112
363-5	9.88	0.9950(10)	0.990	0.9994(17)	0.124
363-6	12.58	0.9950(10)	0.992	0.9997(15)	0.139
363-7	15.55	0.9944(11)	0.990	0.9980(16)	0.153
363-8	18.4	0.9906(11)	0.991	0.9986(15)	0.165
363-9	20.25	0.9911(11)	0.989	0.9984(15)	0.173

[a] calculated by MCU code

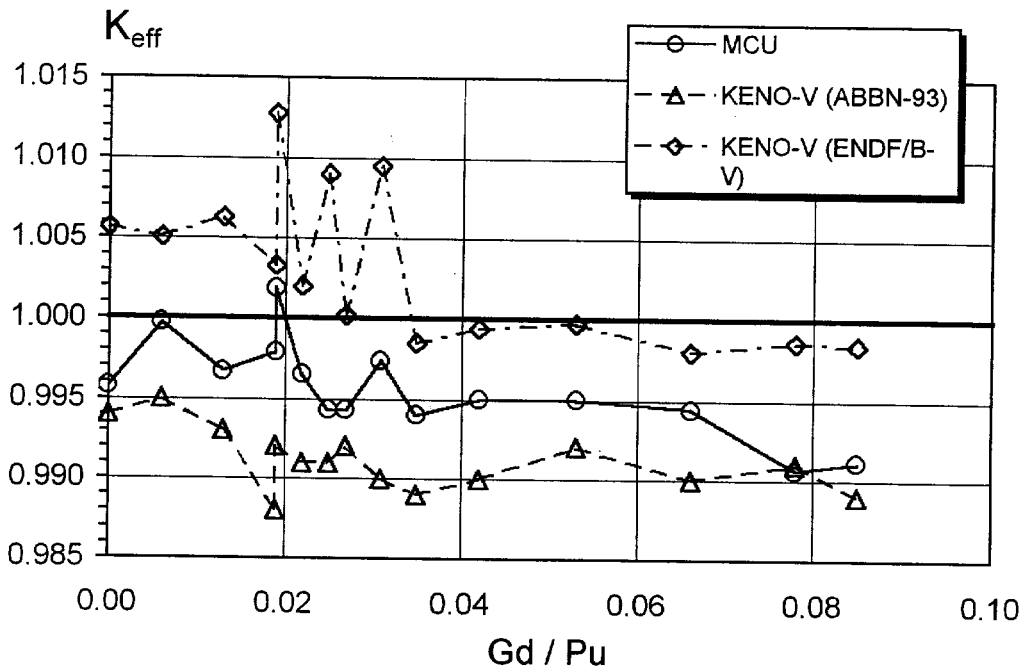

Figure 1. 10. Multiplication factors for gadolinium-poisoned solution

2. CRITICAL ASSEMBLIES WITH POLYSTYRENE AS THE MODERATOR

2.1. Homogenous PuO_2–polystyrene at low hydrogen content

The experiment is described in Ref. [2, p. 24].

The cores were rectangular parallelepipeds composed of PuO_2-polystyrene. A 15.25-cm-thick Plexiglas reflector was placed on each face of the core. Cases differ by dimensions of the core.

The hydrogen-to-plutonium (H/Pu) atomic ratio was equal to 5. The isotopic composition of plutonium was 11.5 wt % ^{240}Pu.

The benchmark model not including the rubberized plastic coating of each fuel compact. The effect of plastic coating on criticality was obtained by experiment. Value of correction is not reported.

Four critical configurations were investigated. Main parameters of the assemblies are indicated in Table 2. 1 together with uncertainty of K_{eff} benchmark models.

Calculated multiplication factors are given in Table 2. 2 and shown in Figure 2. 1. MCNP code predicts K_{eff} values over MCU code at ~ 0.02. Experimental $K_{eff} = 1$ are placed in the middle between MCNP and MCU results.

MCU results are differing from KENO-V (ABBN-93) ones in about 0.0005. At the same value of MCNP (ENDF/B-V) differ from KENO-V (ENDF/B-V), but difference has opposite sign.

Table 2. 1. Critical parameters.

Case Number	Critical Dimensions, cm			Plutonium kg	K_{eff} Uncertainty
	Length	Width	Height		
1	25.88	25.88	19.04	27.66	± 0.0006
2	31.24	30.96	14.77	30.94	± 0.0015
3	41.66	41.28	11.03	41.20	± 0.0009
4	52.07	51.60	9.38	54.78	± 0.0008

Table 2. 2. Multiplication factors of PuO_2-polystyrene at low hydrogen content.

Case Number	K_{eff}			
	MCU	MCNP (ENDF/B-V)	KENO-V (ABBN-90)	KENO-V (ENDF/B-V))
1	0.9917(15)	1.0092(12)	0.9971(8)	1.0041(25)
2	0.9905(10)	1.0108(11)	0.9948(8)	1.0070(25)
3	0.9801(10)	1.0150(9)	0.9961(8)	1.0109(24)
4	0.9901(14)	1.0139(11)	0.9966(8)	1.0086(27)
Averaged	0.9904 ± 0.0009	1.0122 ± 0.0023	0.9962 ± 0.0009	1.0077 ± 0.0025

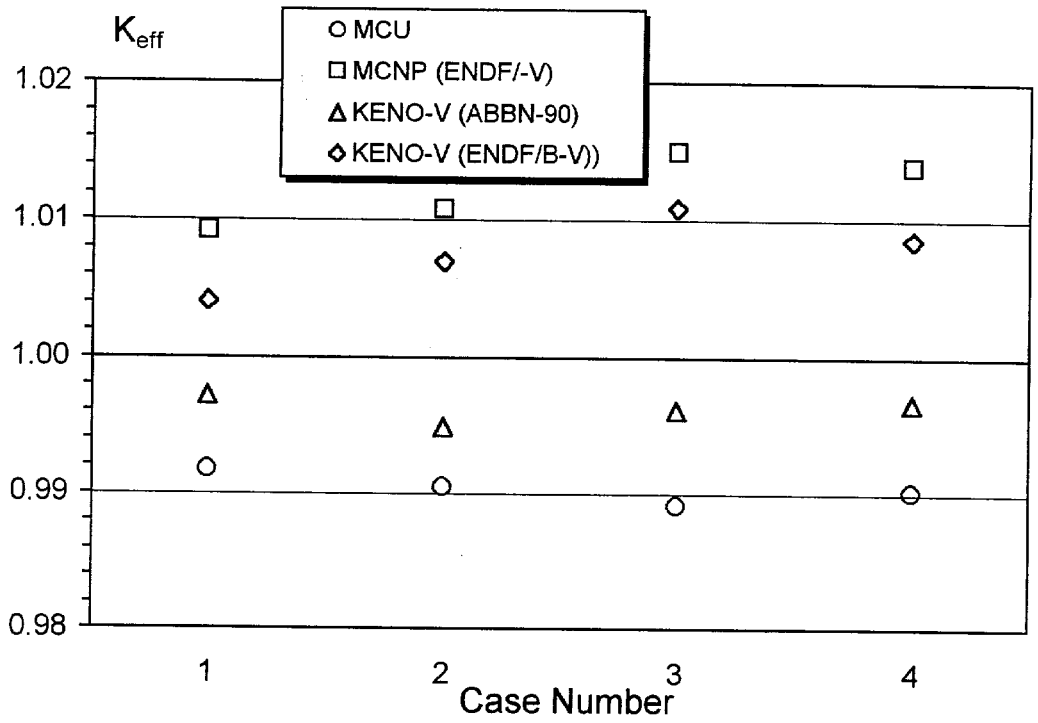

Figure 2. 1. Multiplication factors of PuO_2-polystyrene at low hydrogen content.

2.2. Low-moderated mixtures of plutonium and uranium oxides with polystyrene

The experiment is described in Ref. [1, v. VI, PU-COMP-INTER-001].

The cores were rectangular parallelepipeds composed of mixtures of PuO_2 and UO_2 with polystyrene. In all cases except two, the assemblies had thick Plexiglas reflectors.

The plutonium content was equal to 11.5 wt % ^{240}Pu. Uranium depleted to 0.2 wt.% ^{235}U was used. The fuel contained 8, 15, or 30 wt.% plutonium. The H/(U + Pu) atomic ratios were equal to 2.8, 2.86, and 7.3

The compacts were clad with thin tape. Experimentally and by calculation, was shown that this tape not affect on critical parameters. That tape was not account in the isotope density.

A K_{eff} uncertainty is not indicated in the benchmark specification.

The sizes of the core are indicated in Table 2. 3.

K_{eff} calculation results for these experiments are provided in Table 2. 4 and demonstrated at Figure 2. 2.

Table 2. 3. Critical dimensions.

Case Number	Core dimensions, cm		
	Lenght	Width	Height
Pu/(U+Pu) = 29.3 H/(U+Pu) = 2.8 H/^{239}Pu = 8			
1 [a]	50.9	50.8	45.8
2 [a]	50.9	55.9	42.7
29-1	35.6	35.6	36.5
29-2	40.7	40.7	28.9
29-3	45.8	45.7	26.0
29-4	50.9	50.8	22.1
29-5	50.9	50.8	22.1
29-6	61.1	50.8	20.4
29-7	61.1	61.0	19.0
29-8	61.1	66.1	18.5
29-9	71.3	66.1	18.0
[b]	infinite	infinite	12.9
Pu/(U+Pu) = 15.0 H/(U+Pu) = 2.86 H/^{239}Pu = 17			
15.1	50.9	50.8	54.7
Pu/(U+Pu) = 8.1 H/(U+Pu) = 7.3 H/^{239}Pu = 80			
8-1	50.9	45.7	47.2
8-2	50.9	55.9	39.7
8-3	61.1	61.0	33.7
8-4	71.3	66.1	30.2

[a] unreflected

[b] case represents a linear extrapolation of data from finite assemblies

Table 2. 4. Multiplication factors of low-moderated PuO_2-UO_2-polystyrene.

Case Number	K_{eff}		
	MCU	KENO-V (ABBN-90)	KENO-V (ENDF/B-V))
Pu/(U+Pu) = 29.3 H/(U+Pu) = 2.8 H/^{239}Pu = 8			
1 a	0.9944(10)		
2 a	0.9951(12)		
29-1	0.9886(14)	0.9887(7)	0.9997(23)
29-2	0.9917(14)	0.9874(7)	0.9943(23)
29-3	0.9974(11)	0.9966(7)	1.0077(24)
29-4	0.9875(8)	0.9874(7)	0.9865(21)
29-5	0.9912(15)	0.9861(7)	0.9930(20)
29-6	0.9870(11	0.9874(7)	0.9936(22)
29-7	0.9998(16)	0.9856(6)	0.9962(27)
29-8	0.9870(7)	0.9848(7)	0.9970(24)
29-9	0.9931(13)	0.9890(7)	0.9950(21)
b	0.9933(14)		
Averaged	0.9922 ± 0.0040	0.9881 ± 0.0031	0.9959 ± 0.0051
Pu/(U+Pu) = 15.0 H/(U+Pu) = 2.86 H/^{239}Pu = 17			
15-1	0.9925(11)	0.9848(21)	0.9828(6)
Pu/(U+Pu) = 8.1 H/(U+Pu) = 7.3 H/^{239}Pu = 80			
8-1	1.0080(12)	1.0122(27)	0.9950(7)
8-2	1.0066(9)	1.0157(27)	0.9930(7)
8-3	1.0090(11)	1.0150(27)	0.9949(7)
8-4	1.0045(12)	1.0163(27)	0.9949(7)
Averaged	1.0070 ± 0.0017	1.0148 ± 0.0016	0.9945 ± 0.0008
Averaged by all cases	0.9957 ± 0.0072	0.9955 ± 0.0125	0.9945 ± 0.0055

[a] unreflected

[b] case represents a linear extrapolation of data from finite assemblies

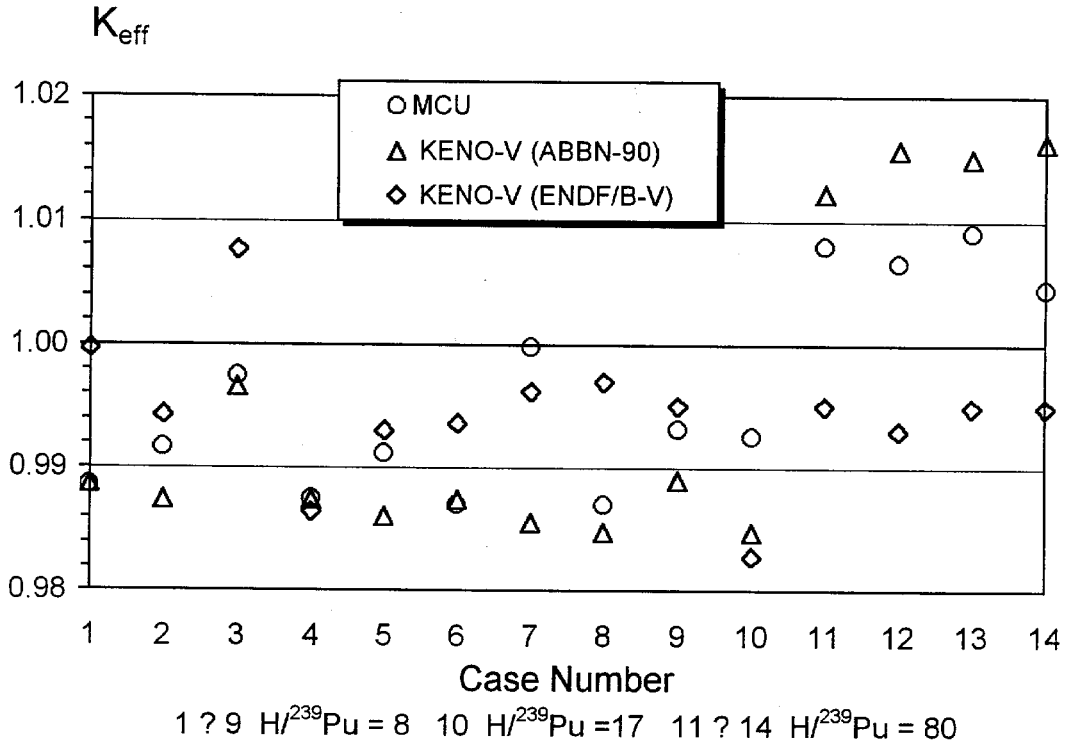

Figure 2. 2. Multiplication factors of low-moderated PuO_2-UO_2-polystyrene.

2.3. Homogeneous mixtures of polystyrene moderated plutonium and uranium oxides.

The description of these critical assemblies was taken from Ref [4, Revision 2].

The experiments determined the critical geometric dimensions of stacked compact in the form of rectangular parallelepipeds. A compact was fabricated with MOX fuel and polystyrene. In all experiments a 15-cm-thick Plexiglas was used as a reflector.

Four different homogeneous PuO_2-UO_2-polystyrene mixtures were used. Main physical parameters of the mixtures are (approximately):

Mixture 1: g(Pu+U)/liter = 843, 7.6 wt.% Pu, H/Pu = 280, H/U = 20
Mixture 2: g(Pu+U)/liter = 360, 7.89 wt.% Pu, H/Pu = 660, H/U = 55
Mixture 3: g(Pu+U)/liter = 580, 14.62 wt.% Pu, H/Pu = 210, H/U = 35
Mixture 4: g(Pu+U)/liter = 373, 30.0 wt.% Pu, H/Pu = 160, H/U = 70

The ^{240}Pu isotopic content in Pu was 23 wt.% for Mixture 1 and 8 wt.% for Mixture 2,3,4. In all cases the uranium was depleted to 0.151 wt.% ^{235}U.

The core is constructed with fuel compact length and width of 5.09 cm. Main part of the compact has height of 5.09 cm too, and the rest has height of 3.81 cm or 1.28 cm. Each fuel compact was clad with tape 0.06-cm-thick. Between them there was a small void.

Only the description of assemblies with Mixture 1 corresponds entirely to the reality.

Assemblies with Mixtures 2,3,4 are described roughly: the value of critical height of cores in absence of clad and voids are given. Redaction in critical heights is 15%, 4% and 2% for Mixtures 2, 3 and 4. It isn't clear from description if redaction in lengths and widths was made.

Note that assemblies investigated have nearly thermal neutron spectrum. And so the Chlorine ($\sigma^{th}_c \cong 33$ b) contained in the tape gives considerable contribution in a neutron capture.

Critical dimensions of the reactor cores are given in Table 2. 5.

The K_{eff} calculation results presented in Table 2. 6.

Within a section a scatter of the data is not sizeable. The averaged K_{eff} are presented in the same Table and demonstrated at Figure 2. 3.

As for MCU code, the calculations give fine results for the precisely described assembly with Mixture 1 and satisfactory results for assemblies with Mixture 3 and 4. For these assemblies the difference in the values of real and effective critical heights is not large. For assemblies with Mixture 2 the difference of calculated K_{eff} value from 1 is equal nearly 0.02. It is possible that the difference is connected with an error in effective critical value. Here the redaction of critical height is equal to 15%.

KENO-V code with ABBN-93 data and MCNP code with ENDF/B-VI data give very close results for all cases. Note they are heavily different from previous results when MCNP with ENDF/B-V data were used.

Table 2. 5. Critical dimensions and masses.

Case Number	Core dimensions, cm			Critical mass, cm	
	Length	Width	Height	Pu	U
Mixture 1					
1	61.1	66.2	11.9	3.1	37.5
2	61.1	61.1	9.1	2.2	26.5
3	66.2	66.2	10.3	2.9	35.2
4	61.1	50.9	9.5	1.9	23.0
5	61.1	56.0	10.9	2.4	29.1
6	50.9	50.1	11.5	1.9	22.8
Mixture 2					
1	40.7	45.7	32.9	1.74	20.3
2	50.9	50.8	26.4	1.94	22.6
3	61.1	61.0	22.7	2.39	27.9
4	61.1	66.0	22.1	2.53	29.5
5	61.1	55.9	23.2	2.25	26.3
6	61.1	50.8	24.4	2.15	25.1
7	40.7	40.6	36.4	1.71	20.0
Mixture 3					
1	30.5	40.7	29.8	3.1	18.4
2	40.7	40.7	23.8	3.4	19.6
3	45.8	50.9	19.8	3.9	22.9
4	50.9	50.9	18.9	4.2	24.3
5	61.1	50.9	17.7	4.7	27.3
6	61.1	61.1	16.5	5.3	30.7
Mixture 4					
1	30.5	30.5	30.9	3.2	7.5
2	35.6	35.6	24.0	3.4	7.9
3	40.7	40.7	20.2	3.8	8.8
4	50.9	45.8	17.1	4.5	10.4
5	61.1	50.9	15.5	5.4	12.7
6	61.1	56.0	15.2	5.8	13.5
7	66.2	61.1	14.4	6.5	15.2
8	50.9	50.9	16.5	4.8	11.1

Table 2. 6. Multiplication factors for PuO_2-UO_2-Polystyrene.

Case Number	K_{eff}		
	MCU	MCNP (ENDF/B-VI)	KENO-V (ABBN-90)
Mixture 1			
1	1.0013(18)	0.9821(15)	0.9855(7)
2	1.0015(18)	0.9866(13)	0.9860(7)
3	0.9999(55)	0.9853(12)	0.9842(7)
4	1.0027(27)	0.9865(14)	0.9878(7)
5	1.0000(20)	0.9886(13)	0.9886(7)
6	1.0014(16)	0.9911(13)	0.9900(7)
Averaged	1.0011± 0.0009	0.9867 ± 0.0026	0.9870 ± 0.0018
Mixture 2			
1	1.026 (1)	1.0296(14)	1.0279(7)
2	1.022 (1)	1.0232(14)	1.0223(7)
3	1.016 (1)	1.0214(12)	1.0195(7)
4	1.016 (1)	1.0210(21)	1.0193(7)
5	1.017 (1)	1.0187(12)	1.0162(7)
6	1.018(2)	1.0235(14)	1.0222(7)
7	1.020(2)	1.0294(13)	1.0295(7)
Averaged	1.0193 ± 0.0034	1.0238 ± 0.0034	1.0224 ± 0.0034
Mixture 3			
1	1.0072 (12)	1.0184(8)	1.0150(16)
2	0.9956 (12)	1.0159(8)	1.0189(13)
3	0.9916 (12)	1.0144(8)	1.0133(14)
4	0.9927 (13)	1.0132(8)	1.0111(14)
5	0.9903 (13)	1.0131(8)	1.0157(16)
6	0.9907 (13)	1.0101(7)	1.0155(14)
Averaged	0.9947 ± 0.0059	1.0142 ± 0.0026	1.0149 ± 0.0024
Mixture 4			
1	0.9965 (12)	1.0069(16)	1.0063(8)
2	0.9956 (12)	1.0082(13)	1.0071(8)
3	0.9916 (12)	1.0070(15)	1.0082(8)
4	0.9927 (13)	1.0031(15)	1.0034(8)
5	0.9903 (13)	1.0047(15)	1.0055(8)
6	0.9907 (13)	1.0024(15)	1.0057(8)
7	0.9939 (13)	1.0085(13)	1.0062(8)
8	0.9938 (13)	1.0057(14)	1.0053(8)
Averaged	0.9931 ± 0.0021	1.0058 ± 0.0021	1.0060 ± 0.0013

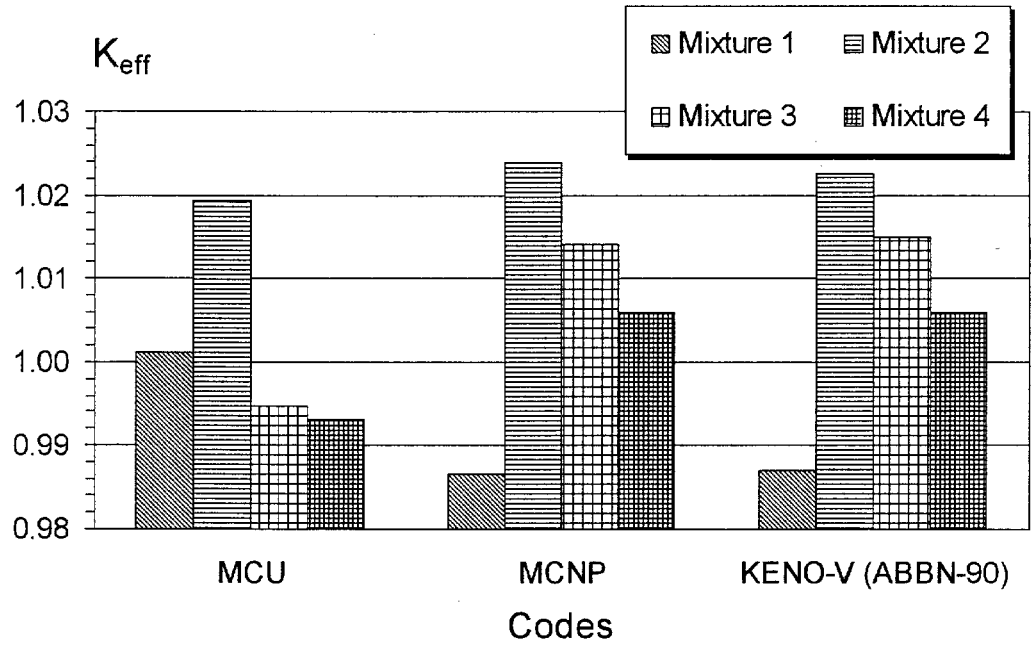

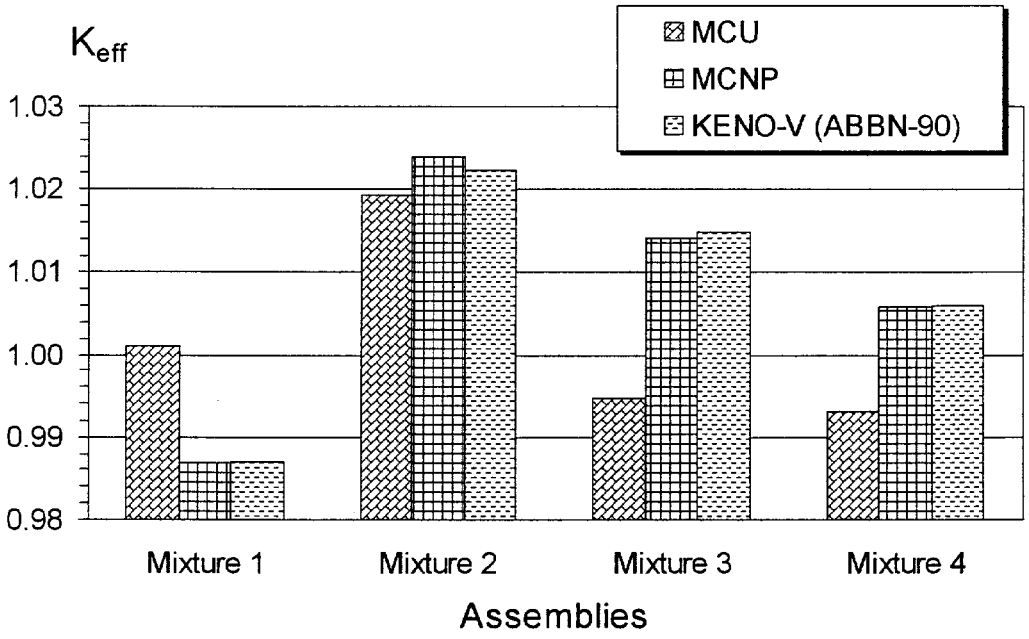

Figure 2. 3. Averaged multiplication factors for PuO_2-UO_2-Polystyrene mixtures

2.4. Neutron poison plates in $PuO_2 - UO_2$ – polystyrene mixtures.

Three compositions of the poison plate were considered: copper, aluminum and copper-cadmium (0.989 wt% Cd).

In benchmark specification the geometry of all assemblies is described without simplifications, including the compact clad and voids between compact.

Two different homogeneous $(Pu\text{-}U)O_2$ polystyrene mixtures were used. Main physical parameters of the mixtures are (approximately):

Mixture 1: g(Pu+U)/liter = 580, H/Pu = 210, H/U = 35

Mixture 2: g(Pu+U)/liter = 3450, H/Pu = 10, H/U = 4

The ^{240}Pu isotopic content in Pu was 8 wt.% for Mixture 1 and 12 wt.% for Mixture 2. In all cases the uranium was depleted to 0.151 wt.% ^{235}U.

K_{eff} calculation results are presented in Table 2. 7 and Table 2. 8.

In all cases any trend in K_{eff} dependence on poison plate thickness is not seen. Averaged values of K_{eff} calculated are shown at Figure 2. 4.

For Mixtures 1 assemblies with thermal neutron spectrum, MCU code gives K_{eff} values close to 1 and KENO-V (ABBN-93) code gives K_{eff} equal to approximately 1.01.

For Mixtures 2 assemblies with hard neutron spectrum, MCU code predicts K_{eff} values nearly to 0.99 and KENO-V (ABBN-93) code gives K_{eff} values close to 1.

For both Mixtures and for all poison plates obtained with MCU and ABBN-93 data differ in about 0.01.

Table 2. 7. Multiplication factors of assemblies with different poison plate. Mixture 1

Case Number	Poison Plate cm	K_{eff}	
		MCU	KENO-V (ABBN-93)
COPPER			
1	0.337	0.9984(14)	1.0096(8)
2	0.637	1.0009 14)	1.0089(7)
3	1.290	1.0020(14)	1.0107(7)
4	1.927	1.0020(14)	1.0089(8)
5	2.580	0.9999(13)	1.0107(7)
6	0.337	0.9999(14)	1.0066(8)
7	0.337 + 0.337	0.9981(13)	1.0112(7)
8	1.290 + 1.290	1.0010(13)	1.0103(7)
9	1.927 + 1.927	1.0032(14)	1.0098(7)
10	2.565 + 2.565	1.0044(14)	1.0093(7)
Averaged		1.0010 ± 0.0019	1.0096 ± 0.0012
ALUMINUM			
1	0.316	0.9950(13)	1.0095(8)
2	0.645	0.9951(14)	1.0105(7)
3	1.983	0.9952(14)	1.0106(7)
4	2.676	0.9968(13)	1.0105(8)
5	0.316 + 0.317	0.9977(14)	1.0120(7)
6	2.628 + 2.629	0.9950(14)	1.0099(7)
Averaged		0.9958 ± 0.0011	1.0105 ± 0.0008
COPPER-CADMIUM			
1	0.368	1.0003(13)	1.0108(7)
2	2.160	0.9988 (14)	1.0093(7)
3	0.368	1.0014 (13)	1.0120(7)
4	0.368	0.9983(13)	1.0117(8)
5	0.368 + 0.354	1.0085(14)	1.0121(8)
Averaged		1.0015 ± 0.0011	1.0112 ± 0.0011
WITHOUT PLATE			
1	–	0.9968(15)	1.0072(8)

Table 2. 8. Multiplication factors of assemblies with different poison plate. Mixture 2

Case Number	Poison Plate cm	K_{eff}	
		MCU	KENO-V (ABBN-93)
COPPER			
1	0.337	0.9911	1.0005(7)
2	0.974	0.9928	1.0024(6)
3	1.964	0.9933	1.0131(6)
Averaged		0.9924 ± 0.0009	1.0053 ± 0.0056
ALUMINUM			
1	0.316	0.9901(12)	0.9995(7)
2	0.961	0.9874(13)	1.0009(7)
3	1.971	0.9895(13)	1.0019(7)
Averaged		0.9890 ± 0.0012	1.0007 ± 0.0010
COPPER-CADMIUM			
1	0.368	0.9838(13)	0.9996(6)
2	1.085	0.9851(12)	1.0029(7)
3	2.160	0.9874(13)	1.0043(7)
Averaged		0.9854 ± 0.0015	1.0023 ± 0.0020
WITHOUT PLATE			
1	–	0.9972(14)	1.0023(6)

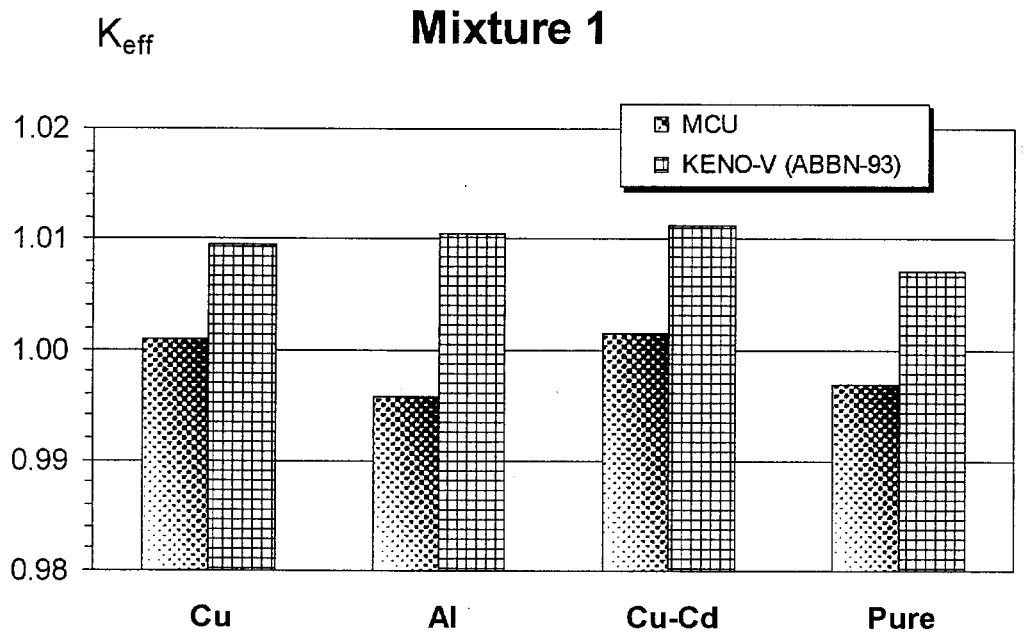

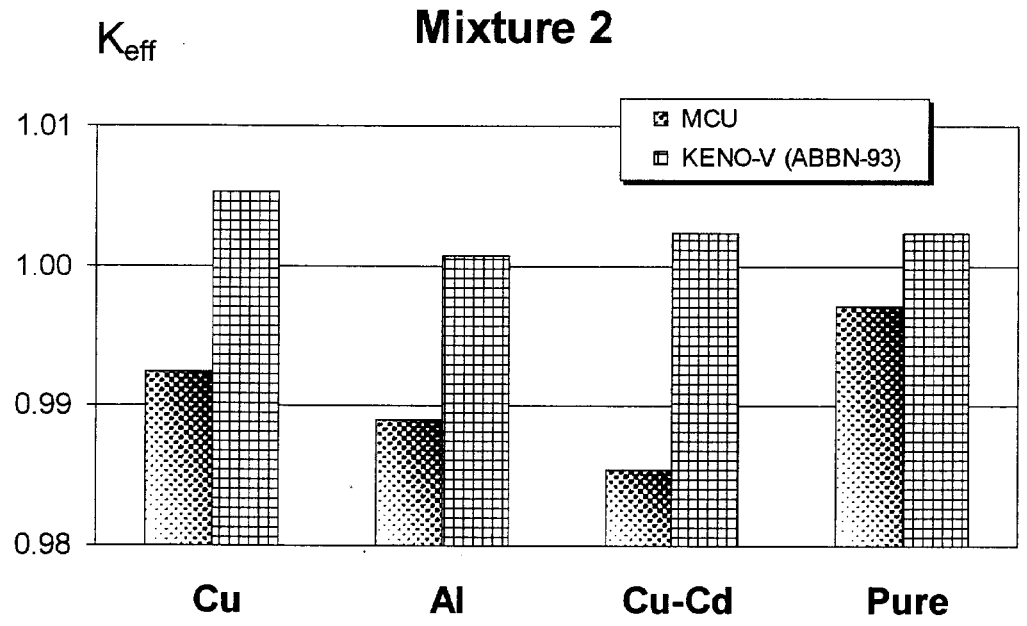

2.5. Figure 2. 4. Averaged multiplication factors for assemblies with different poison plates

2.6. Discussion

For critical assemblies with polystyrene investigated, precision of a K_{eff} calculations depends not only on plutonium neutron data but on uranium and poison materials data too. Nevertheless consider dependence of K_{eff} calculated only on H/Pu ratio.

K_{eff} calculation results by MCU code are shown in Figure 2. 5. The calculation results for the water also are given there.

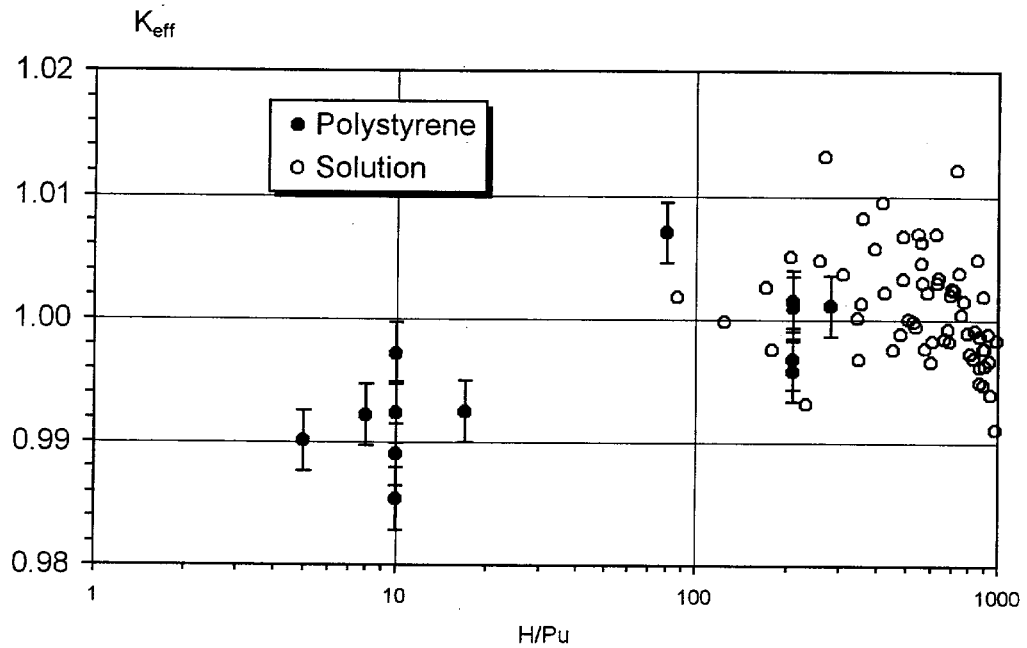

Figure 2. 5 Multiplication factors for assemblies with polystyrene and water as the moderator

For assemblies with soft neutron spectrum (high H/Pu ratios) K_{eff} values are nearly 1 for both moderators. When a H/Pu ratio decreases and neutron spectrum becames harder, a K_{eff} value tends to diminish for assemblies with polystyrene.

At the first glance it's the evidence of a problem of plutonium resonance cross sections. In the same time it's likely that K_{eff} dependence on H/Pu ratio is connected with imperfect description of neutron thermalization. Let's dwell on this subject.

As known, thermal neutron scattering law $S(\alpha,\beta)$ of an atom depends on chemical structure of the matter which contains this atom. And so $S(\alpha,\beta)$ of hydrogen combined in water, polyethylene, hydride of a metal etc is different.

$S(\alpha,\beta)$ of hydrogen in polystyrene is not known: an experimental investigation was not performed and a theoretical models was not constructed.

In the current work, all codes have used for polystyrene the polyethylene scattering law. Structures of both matters are shown at the picture bellow. It illustrates that chemical bounds of hydrogen of polyethylene and of polystyrene are heavily different so that $S(\alpha,\beta)$ should significantly differ too.

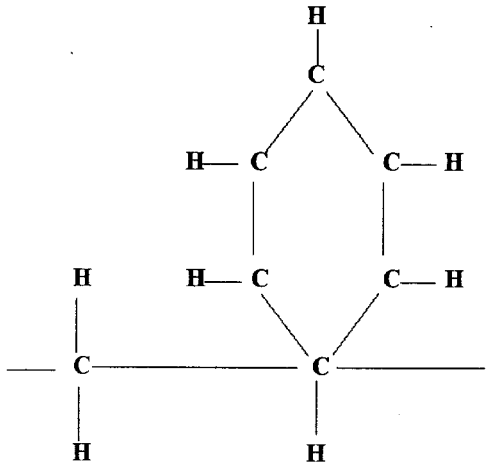

Polystyrene $(C_8H_8)_n$

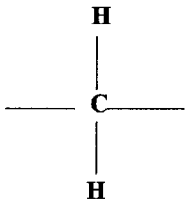

Polyethylene $(CH_2)_n$

An error of a scattering law has slight influence on spectrum of thermal neutrons if H/Pu ratio is large (for extremely high ratio neutron spectrum is close to Maxwell spectrum for any scattering law). Contrary, for low H/Pu ratio details of the scattering law affect significantly on neutron spectrum.

3. CLEAR LATTICES OF MOX RODS IN WATER.

3.1. MOX fuel with 20 wt.% Pu

The experiment is described in Ref. [1, v. VI, MIX–COMP–THERM–001].

The experimental configuration comprised an array of fuel rods within a large water tank. The fuel rods were located on a square pitch that varied within experiments. Cross section of fuel regions had rectangular shape.

In each experimental lattice assembly, the core was surrounded on all sides by at least 15 cm of a water reflector.

The rods were ~2.4 m in full length and ~91 cm fuel length. The outer diameter was equal to 0.58 cm. The fuel pin of 0.48 cm diameter was clad stainless steel.

The fuel was a mixture of PuO_2 and UO_2 with the pins comprising 19.7 wt.% plutonium. The plutonium contained 11.5 wt.% ^{240}Pu. The natural uranium was used.

Main parameters of the assemblies are given in Table 3. 1. The K_{eff} uncertainties of the benchmark models are also indicated.

Calculation results are presented in Table 3. 2 and Figure 3. 1. The KENO-V (ENDF/B-V) results are taken from Ref. [3, p.76].

In the case of ENDF/B-V data, there is trend of the K_{eff} calculated value increase with the increase of water/fuel ratio.

In the case of ABBN-93 database, the calculation results don't depend on V_M/V_F value, but K_{eff} calculated are less then 1 in ~0.01.

MCU code predicts K_{eff} values without an error.

Table 3. 1. Parameters of the lattices.

Case Number	Number of Rods	Pitch cm	V_M/V_F	$H/^{239}Pu$	δK_{eff}
1	605	0.9525	1.52	24	± 0.0025
2	279	1.2580	3.69	59	± 0.0026
3	205	1.5342	6.18	98	± 0.0032
4	162	1.9050	10.28	163	± 0.0039

Table 3. 2. Multiplication factors of the lattices of the MOX fuel rods with 20 wt.% Pu

Case Number	V_M/V_F	K_{eff}		
		MCU	KENO-V (ABBN-93)	KENO-V (ENDF/B-V)
1	1.52	1.0035(10)	0.99055(11)	0.9931(25)
2	3.69	0.9985(10)	0.99089(12)	0.9980(26)
3	6.18	0.9982(10)	0.98547(12)	0.9992(24)
4	10.28	0.9997(10)	0.98956(12)	1.0046(25)

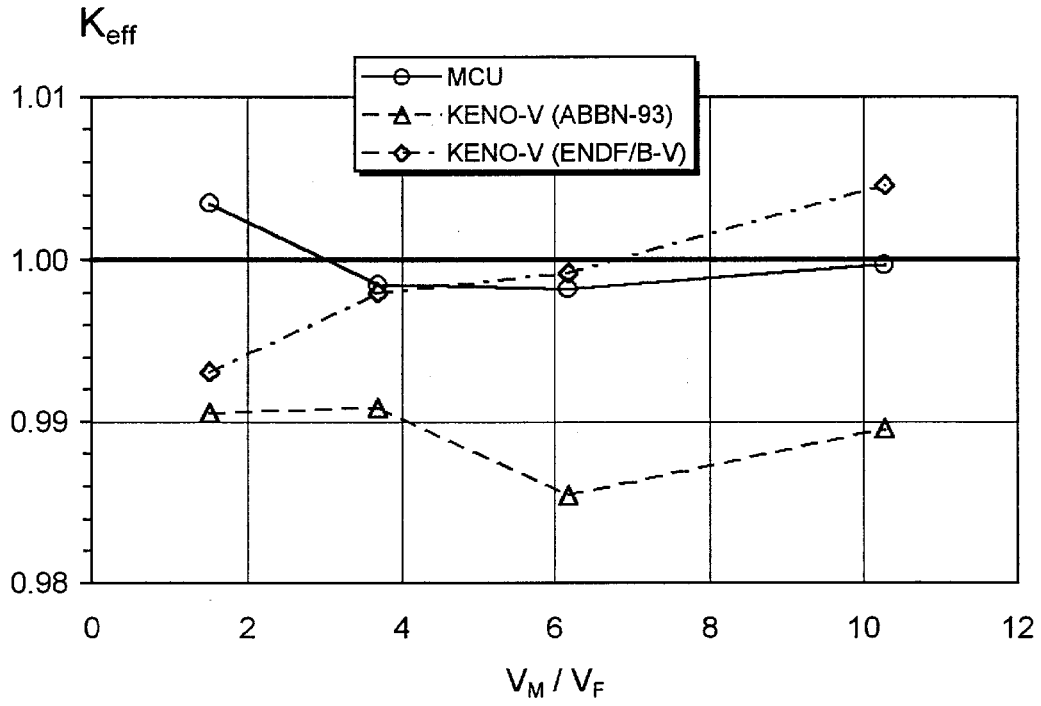

Figure 3. 1. Multiplication factors of the lattices of the MOX fuel rods with 20 wt.% Pu

3.2. MOX fuel with 2 wt.% Pu

The experiment is described in Ref. [1, v. VI, MIX–COMP–THERM–002].

In this series of experiments as in the previous one, square lattices of fuel rods inserted in a large water tank were studied. Three lattices with the different pitches were studied. The critical state was determined for each lattice in both pure and borated water.

The outer diameter of the rods and diameter of the fuel pin were equal to 1.44 and 1.28 cm, respectively.

The fuel was a mixture of natural uranium with 2 wt.% of plutonium dioxide containing 8 wt.% of ^{240}Pu.

Main parameters of the assemblies are given in Table 3. 3. together with K_{eff} of the benchmark models.

The calculation results are presented in Table 3. 4 and Figure 3. 2. The KENO-V (ENDF/B-V) results are taken from Ref. [3, p.80].

All codes give close results with a weak trend of k_{eff} value increase with the lattice pitch increase.

Table 3. 3. Parameters of the lattices.

Case Number	Number of Rods	Pitch cm	V_M/V_F	Boron $^{10}B/H$	$H/^{239}Pu$	K_{eff}
PNL-30	469	1.778	2.13		360	1.0009±0.0021
PNL-31	761	1.778	2.13	1,14E-4	360	1.0007±0.0015
PNL-32	195	2.209	7.15		1200	1.0023±0.0021
PNL-33	761	2.209	7.15	1.80E-4	1200	1.0025±0.0037
PNL-34	161	2.514	8.13		1365	1.0039±0.0035
PNL-35	689	2.514	8.13	1.27E-4	1365	1.0026±0.0052

Table 3. 4. Multiplication factors of the lattices of the MOX fuel rods with 2 wt.% Pu

Case Number	V_M/V_F	K_{eff}			
		MCU	MCNP (ENDF/B-V)	KENO-V (ABBN-93)	KENO-V (ENDF/B-V)
Pure Water					
PNL-30	2.13	1.000(2)	0.9952(8)	0.9941(10)	0.9931(16)
PNL-32	7.15	1.001(2)	1.0014(8)	1.0009(8)	0.9980(19)
PNL-34	8.13	1.002(2)	1.0050(8)	1.0021(10)	1.0024(15)
Borated Water					
PNL-31	2.13	1.000(2)	0.9982(8)	0.9992(10)	0.9994(15)
PNL-33	7.15	1.005(2)	1.0065(8)	1.0042(8)	1.0019(13)
PNL-35	8.13	1.008(2)	1.0079(8)	1.0041(10)	1.0074(13)

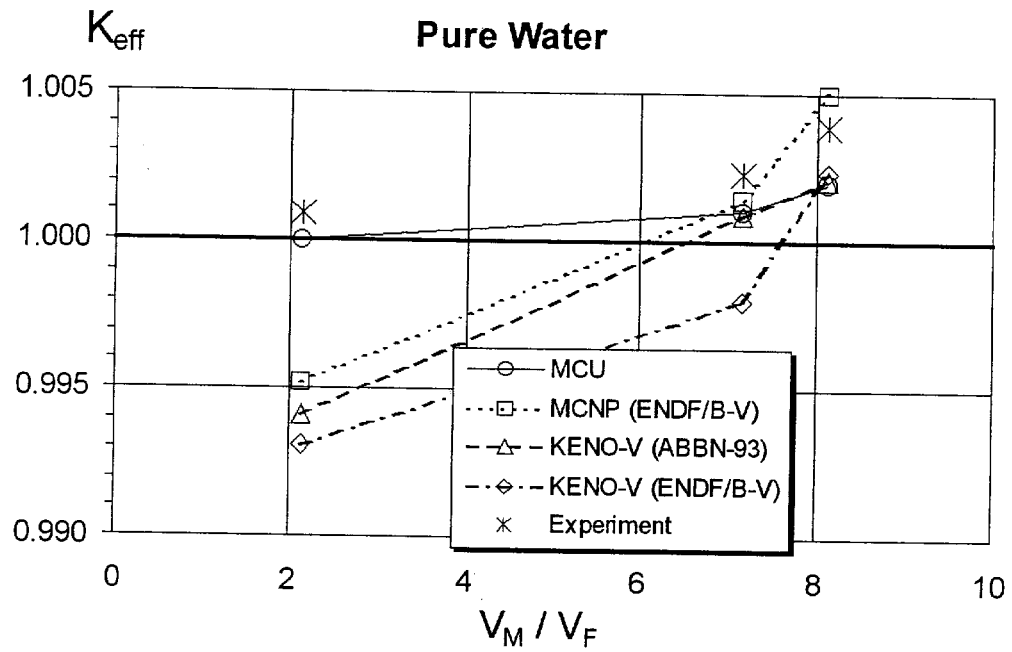

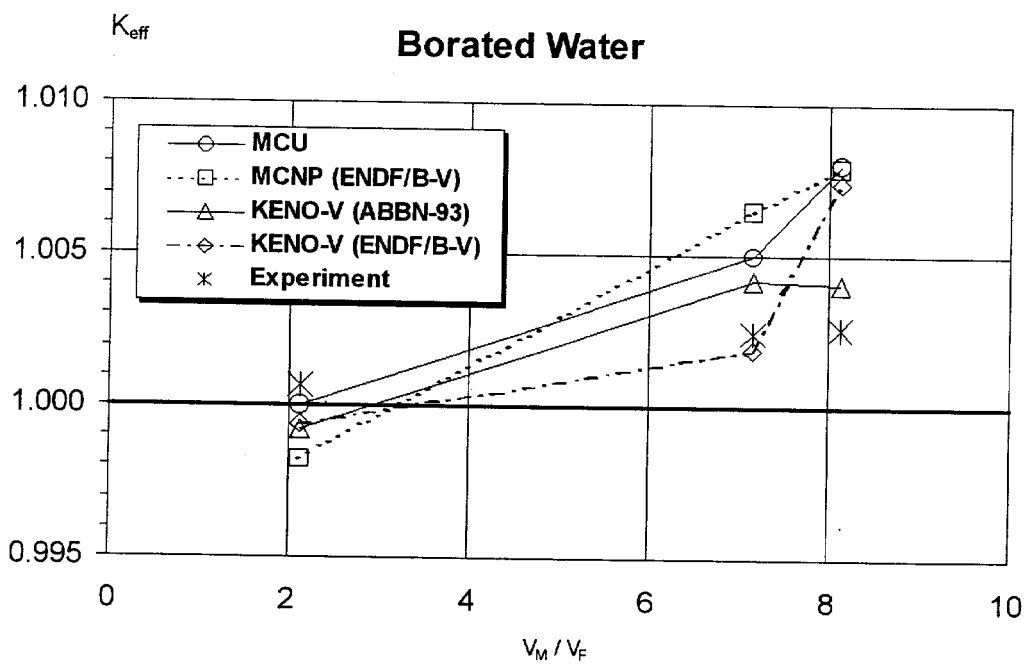

Figure 3. 2. Multiplication factors of the lattices of the MOX fuel rod with 2 wt.% Pu

4. SAXTON CRITICAL EXPERIMENTS.

Benchmark considered is based on critical experiments performed at the WREC-CRX facility SAXTON plutonium program in year 1965. Description of experimental configurations and the critical parameters are contained in Ref. [3, p.42]. Additional information and comments were provided by M.Adams Ref.[6]. Information about measurement of a pin power distribution in the cores is presented in Ref. [4].

Square array of the fuel rods was placed within a large tank that was filled with water. The level of the water could be changed in order to made the configuration critical. Side and bottom reflectors of the core had physically infinite think.

Two types of fuel rods were used.

The first type (hereinafter UO_2) contents dioxide uranium enriched with 5.81 At.% ^{235}U. Outer diameter is equal to 0.993 cm. Stainless steel cladding of 0.076 cm is used.

The second type (hereinafter MOX) contents the mixture of 6.6 Wt.% PuO_2 and UO_2. Content of isotope ^{240}Pu in plutonium is equal to 8 Wt.%. Uranium is naturally enriched with ^{235}U. Outer diameter of the rods is equal to 0.993 cm. Zircaloy 4 cladding of 0.12 cm is used.

The lattices with five different pitches were examined: 0.52 inch (1.321 cm), 0.56 inch, (1.422 cm) 0.735 inch (1.867 cm), 0.792 inch (2.012 cm), and 1.04 inch (2.642 cm). (In this context pitch is defined as the distance between centers of the nearest rods). The positions of fuel rods in the different lattice are shown at the picture below.

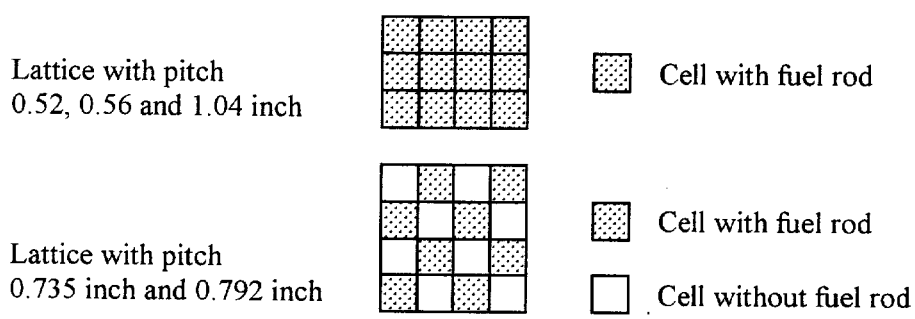

Fuel rod position in lattices.

Indicated lattices have moderator to fuel volumes relation V_M/V_F as follows: 2.0, 2.5, 3.8, 5.0, 6.0, 11.1 for MOX rods and 1.7, 2.1, 3.3, 4.4, 5.2, 9.8 for UO_2 rods. (In VVER type rector core this value is equal approximately to 2).

Core configurations differ one from another with the number and the positions of MOX and UO_2 fuel rods. In addition to it, some configurations have certain specific. The specific could be one of the following:

- Boron acid is dissolved in water;
- five fuel rods in line are moved off (water slot);
- five fuel rods in line are replaced with aluminum plate or with the control rods composed of unclad alloy of 5% Cadmium, 15% Indium and 80% Silver;

- several fuel rods are replaced with ones of the other type.
- Additional lattice of the aluminum void tubes with outer diameter 0.4725 cm is inserted in a fuel rods lattice.

Main parameters of the cores are presented in Table 4. 1. The layouts of complicated cores are shown in Fig. below (page 60).

4.1. Multiplication factors calculation results

The calculation results of neutron multiplication factors K_{eff} are collected in Table 4. 1 for all investigated cases of core parameters. This Table entirely correlates with Table 1 of Ref. [3, p. 45].

NCNP code results in Table Table 4. 1 were taken from Ref. [7, Sec.14].

The same data are duplicated in Tables below. There they are classified for some core parameter. It was done to reveal the dependence of calculation precision on core parameter.

- In Table 4. 2, K_{eff} values are presented for the clear cores with MOX fuel only and with pure water. K_{eff} depends on a value or (what is the same) on moderator to fuel volumes relation value.
- In Table 4. 3, such results are presented for UO_2 fuel.
- In Table 4. 4, K_{eff} depends on Boron content in the water. The lattice pitch is equal to 0.56 inch for all cases, only MOX fuel rods were used.
- In Table 4. 5, an influence of different voids is studied. The core investigated has the lattice pitch equals to 0.52 inch and MOX fuel rods.
- Table 4. 6 and Table 4. 7 contain the results for two-region cores where a lattice of a certain fuel is surrounded by a lattice of the other type, pure water was used in all cases.

Data of these Tables are demonstrated at the Figures.

Table 4. 1. SAXTON core parameters and multiplication factors calculation results.

Designation	Core Parameters					K_{eff}			
	Pitch (inch)	Boron (ppm)	Inner Region	Outer Region	Specifics	MCU	NCNP (ENDF/B-V)	NCNP (ENDF/B-VI)	KENO-V (ABBN-93)
SX1-1b2	0.56	0	MOX 19x19		Fig. 1	0.9943(4)	0.9995(3)	0.9936(3)	0.9908(4)
SX1-1d	0.56	0	MOX 19x19		water slot center. Fig. 4	0.9942(4)	0.9990(3)	0.9929(3)	0.9953(4)
SX1-1e	0.56	0	MOX 19x19		Al slab center. Fig. 3	0.9936(4)	0.9984(3)	0.9927(3)	0.9900(4)
SX1-1f	0.56	0	MOX 21x21		control rods center. Fig. 2	1.0052(3)	0.9990(3)	0.9927(3)	0.9920(4)
SX1-1l2	0.56	25	MOX 19x19			0.9939(12)	0.9988(3)	0.9925(5)	
SX1-1l3	0.56	50	MOX 19x19			0.9923(19)	0.9971(5)	0.9912(5)	
SX1-1m1	0.56	0	MOX 21x21			1.0003(13)	1.0005(5)	0.9941(5)	
SX1-1m2	0.56	228	MOX 21x21			0.9955(13)	0.9976(5)	0.9921(5)	
SX1-1m3	0.56	309	MOX 21x21			0.9972(13)	0.9980(5)	0.9924(5)	
SX1-1m4	0.56	337	MOX 21x21			0.9963(13)	0.9997(5)	0.9930(5)	
SX1-1n	0.56	337	MOX 21x21			0.9944(13)			

SX1-2b	0.792	0	MOX 12x12			0.9933(13)	1.0057(5)	0.9977(5)	
SX1-4b	0.735	0	MOX 13x13			0.9958(13)	1.0041(5)	0.9964(5)	
SX1-5b	1.04	0	MOX 11x11			0.9916(13)	1.0071(5)	0.9997(5)	
SX1-6b	0.56	0	UO_2 19x19			0.9934(13)	0.9967(5)	0.9931(5)	
SX1-6d	0.56	0	UO_2 19x19		water slot	0.9942(13)	0.9965(5)	0.9928(5)	
SX1-6e	0.56	0	UO_2 19x19		Al slab	0.9947(13)	0.9974(5)	0.9929(5)	
SX1-6fu	0.56	0	UO_2 21x21			0.9995(13)	1.0005(5)	0.9963(5)	
SX1-6f	0.56	0	UO_2 21x21		control rods	0.9939(10)	0.9957(5)	0.9935(5)	
SX1-6i	0.56		MOX 3x3	UO_2 19x19	15	0.9918(4)	0.9968(3)	0.9926(3)	0.9941(4)
SX1-7b	0.792	0	UO_2 13x14			0.9914	0.9986(5)	0.9941(6)	
SX1-8b	0.52	0	UO_2 449		Fig. 16	0.9945(4)			
SX1-9b	0.56	1453	MOX 11x11	UO_2 19x19	Fig. 5	0.9945(4)	0.9991(3)	0.9934(3)	0.9923(3)
SX1-10b	0.56	1425	MOX 19x19	UO_2 27x27	Fig. 6	0.9966(4)			0.9913(3)
SX1-10f	0.56	0	MOX 19x19	UO_2 27x27	3x3 UO_2 center Fig. 12	0.9960(4)	0.9998(3)	0.9940(3)	0.9941(3)

SX1-11b	0.56	1425	UO_2 11x11	MOX 19x19	Fig. 14	0.9935(4)	0.9984(3)	0.9933(3)	0.9917(4)
SX1-10e	0.56	0	MOX 19x19	UO_2 27x27	Fig. 11	0.9966(4)	0.9995(3)	0.9952(3)	0.9918(3)
SX1-9c	0.56	0	MOX 11x11	UO_2 19x19	Al plate Fig. 10	0.9932(4)	0.9981(3)	0.9933(3)	0.9916(4)
SX1-9f	0.56	1453	MOX 11x11	UO_2 21x21	control rod Fig. 7	0.9953(4)	0.9976(3)	0.9934(3)	0.9952(4)
SX1-10c	0.56	0	MOX 19x19	UO_2 27x27	water slot Fig. 9	0.9960(4)	0.9990(3)	0.9952(3)	0.9918(3)
SX1-10d	0.56	1252	MOX 19x19	UO_2 27x27	Al plate Fig. 8	0.9964(4)	1.0011(3)	0.9954(3)	0.9914(3)
SX1-12b	0.56	0	UO_2 19x19	MOX 27x27	Fig. 13	0.9936(4)	0.9994(3)	0.9950(3)	0.9920(3)
SX1-13f3	0.52	0	MOX 23x23		8x8 voids centered	0.9949(13)	0.9985(5)	0.9906(5)	
SX1-13f4	0.52	0	MOX 25x23		8x8 voids centered	0.9997(13)	1.0010(5)	0.9930(5)	
SX1-13f5	0.52	0	MOX 25x23		12x12 voids centered	0.9939(13)	0.9982(5)	0.9928(5)	
SX1-13f6	0.52	0	MOX 25x23		72 voids *) centered	0.9967(13)	0.9986(5)	0.9926(5)	
SX1-13f10	0.52	0	MOX 25x24				1.0018(5)	0.9931(5)	
	0.52	0	MOX 25x24		276 voids*) centered	0.9972(13)	0.9971(5)	0.9926(5)	
SX1-13f8	0.52	0	MOX 25x24		153 voids *) centered	0.9967(13)	0.9979(5)	0.9922(5)	

SX1-13f9	0.52	0	MOX 25x24		91 voids *) centered	0.9985(13)	0.9989(5)	0.9919(5)	
SX1-13f11	0.52	0	MOX 23x23			0.9954(13)	0.9992(5)	0.9920(5)	
SX1-13f12	0.52	0	MOX 23x23		4x4 voids centered	0.9935(13)	0.9975(5)	0.9919(5)	
SX1-13f13	0.52	0	MOX 23x23		4x4 voids *) out center	0.9956(13)	0.9975(5)	0.9917(5)	
SX1-13f14	0.52	0	MOX 23x23		4x4 voids *) out center	0.9947(13)	0.9975(5)	0.9918(5)	
SX1-13f15	0.52	0	MOX 23x23		4x4 voids *) out center	0.9978(13)	0.9977(5)	0.9920(5)	
SX1-13f16	0.52	0	MOX 23x23	UO_2 29x29	4x4 voids centered	1.0057(13)			
SX1-13f17	0.52	0	MOX 23x23	UO_2 29x29	8x8 voids centered	1.006(13)			

Table 4. 2. Multiplication factors depended on lattice pitch. MOX fuel rods

Designation	Core Parameters		K_{eff}			
	V_M/V_F	Fuel	MCU	NCNP (ENDF/B-V)	NCNP (ENDF/B-VI)	KENO-V (ABBN-93)
SX1-13f11	2.0	MOX 25x24		1.0018(5)	0.9931(5)	
SX1-13f11	2.0	MOX 23x23	0.9954(13)	0.9992(5)	0.9920(5)	
SX1-1b2	2.5	MOX 19x19	0.9943(4)	0.9995(3)	0.9936(3)	0.9908(4)
SX1-1m1	2.5	MOX 21x21	1.0003(13)	1.0005(5)	0.9941(5)	
SX1-4b	5.0	MOX 13x13	0.9958(13)	1.0041(5)	0.9964(5)	
SX1-2b	6.0	MOX 12x12	0.9933(13)	1.0057(5)	0.9977(5)	
SX1-5b	11.1	MOX 11x11	0.9916(13)	1.0071(5)	0.9997(5)	

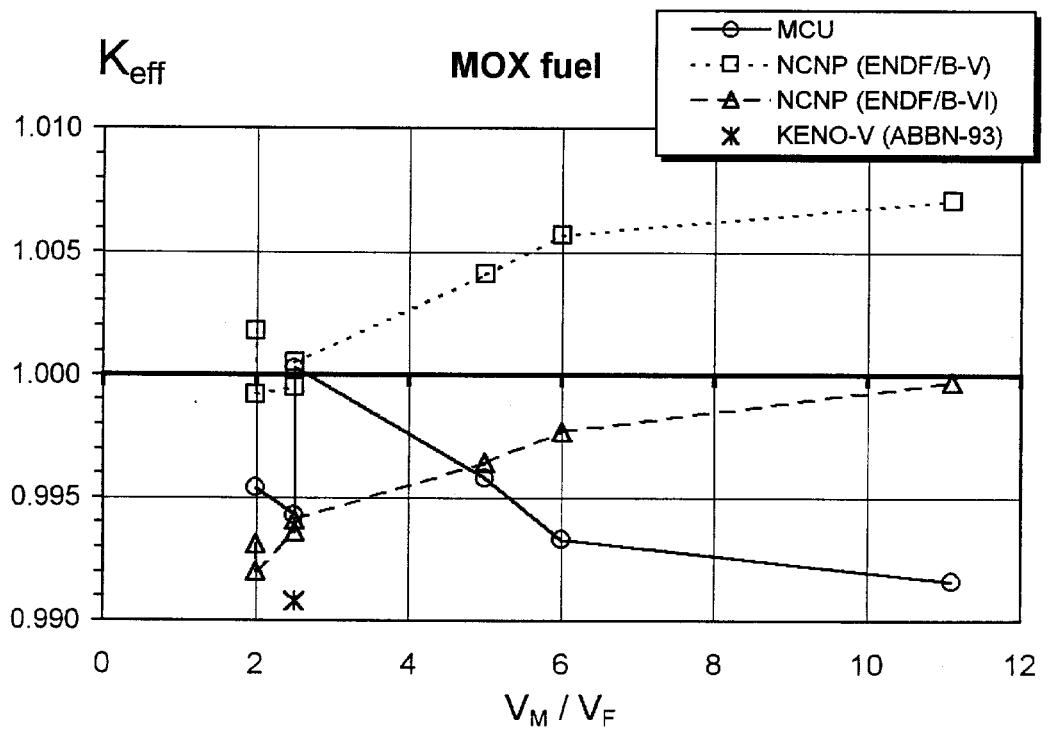

Figure 4. 1. Multiplication factors depended on lattice pitch.

Table 4. 3. K_{eff} calculation results depended on lattice pitch. UO_2 fuel rods

Designation	Core Parameters		K_{eff}		
	V_M/V_F	Fuel	MCU	NCNP (ENDF/B-V)	NCNP (ENDF/B-VI)
SX1-8b	1.7	UO_2 449	0.9945(4)		
SX1-6b	2.1	UO_2 19x19	0.9942(13)	0.9965(5)	0.9928(5)
SX1-6fu	2.1	UO_2 21x21	0.9995(13)	1.0005(5)	0.9963(5)
SX1-7b	5.2	UO_2 13x14	0.9914(13)	0/9986(5)	0.9942(5)

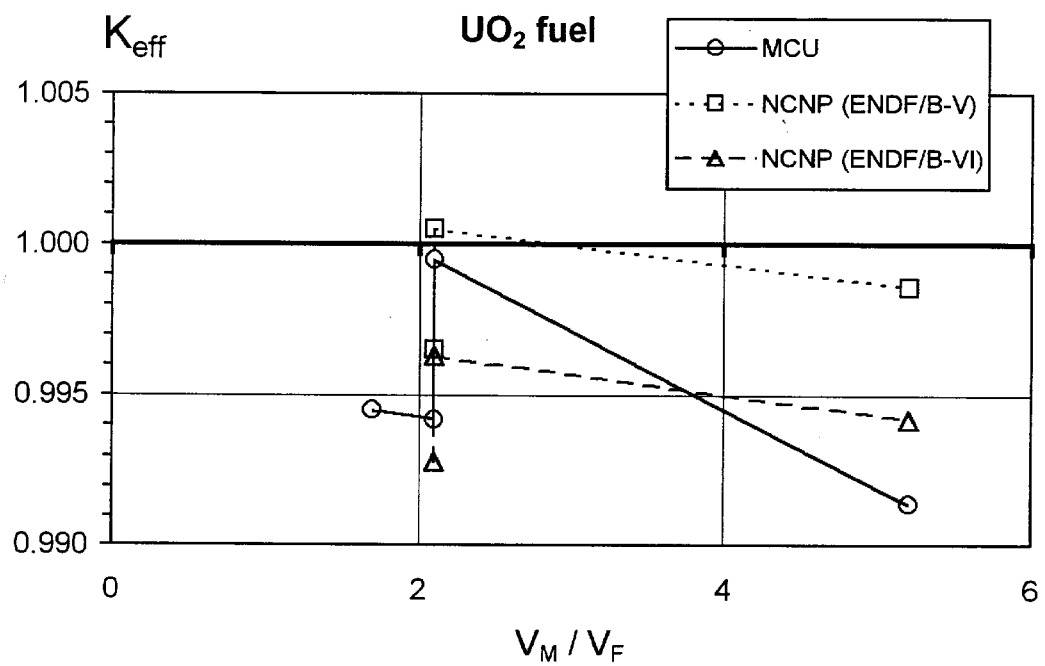

Figure 4. 2. Multiplication factors depended on lattice pitch.

Table 4. 4. K_{eff} calculation results depended on Boron content. MOX fuel rods, 0.56 inch lattice pitch.

Designation	Core Parameters		K_{eff}		
	Boron (ppm)	Fuel	MCU	NCNP (ENDF/B-V)	NCNP (ENDF/B-VI)
SX1-1b2	0	MOX 19x19	0.9943(4)	0.9995(3)	0.9936(3)
SX1-1m1	0	MOX 21x21	1.0003(13)	1.0005(5)	0.9941(5)
SX1-1l2	25	MOX 19x19	0.9939(12)	0.9988(3)	0.9925(5)
SX1-1l3	50	MOX 19x19	0.9923(19)	0.9971(5)	0.9912(5)
SX1-1m2	228	MOX 21x21	0.9955(13)	0.9976(5)	0.9921(5)
SX1-1m3	309	MOX 21x21	0.9972(13)	0.9980(5)	0.9924(5)
SX1-1m4	337	MOX 21x21	0.9963(13)	0.9997(5)	0.9930(5)
SX1-1n	337	MOX 21x21	0.9944(13)		

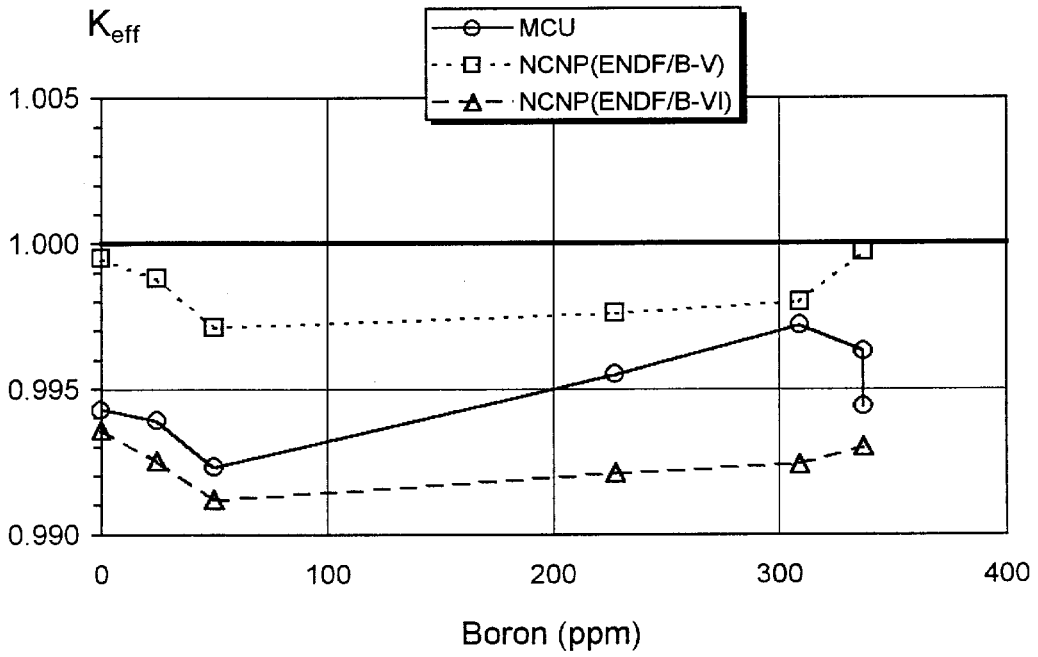

Figure 4. 3. Multiplication factors depended on Boron content.

Table 4. 5. K_{eff} calculation results depended on voids.
MOX fuel rods, 0.52 inch lattice pitch.

Designation	Core Parameters		K_{eff}		
	Fuel	Voids	MCU	NCNP (ENDF/B-V)	NCNP (ENDF/B-VI)
SX1-1b2	MOX 19x19	no	0.9943(4)	0.9995(3)	0.9936(3)
SX1-1m1	MOX 21x21	no	1.0003(13)	1.0005(5)	0.9941(5)
SX1-13f12	MOX 23x23	4x4 centered	0.9935(13)	0.9975(5)	0.9919(5)
SX1-13f13	MOX 23x23	4x4 3 cells west	0.9956(13)	0.9975(5)	0.9917(5)
SX1-13f14	MOX 23x23	4x4 6 cells west	0.9947(13)	0.9975(5)	0.9918(5)
SX1-13f15	MOX 23x23	4x4 9 cells west	0.9978(13)	0.9977(5)	0.9920(5)
SX1-13f3	MOX 23x23	8x8 centered	0.9949(13)	0.9985(5)	0.9906(5)
SX1-13f5	MOX 25x23	12x12 centered	0.9939(13)	0.9982(5)	0.9928(5)
SX1-13f6	MOX 25x23	72 [1] centered	0.9967(13)	0.9986(5)	0.9926(5)
SX1-13f9	MOX 25x24	91 [2] centered	0.9985(13)	0.9989(5)	0.9919(5)
SX1-13f8	MOX 25x24	153 [3] centered	0.9967(13)	0.9979(5)	0.9922(5)
SX1-13f7	MOX 25x24	276 [4] centered	0.9972(13)	0.9971(5)	0.9926(5)

[1] 12x12 lattice, one of two in line
[2] 13x15 lattice, one of two in line
[3] 17x18 lattice, one of two in line
[4] 23x24 lattice, one of two in line

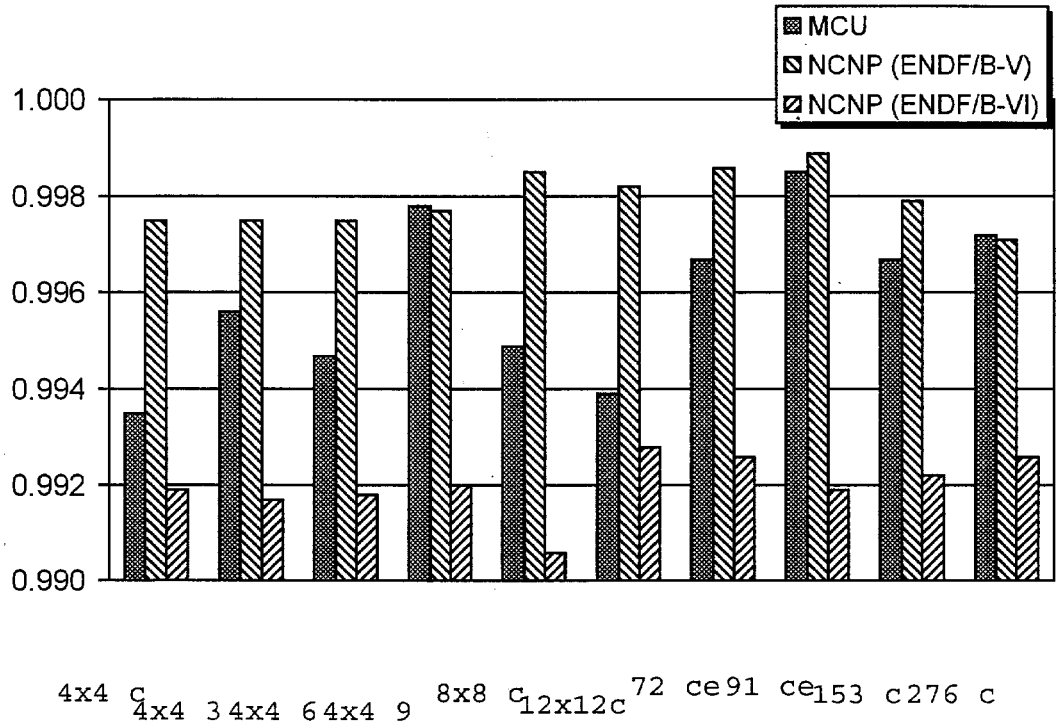

Figure 4. 4. Multiplication factors of the lattice with voids.

Table 4. 6. K_{eff} calculation results for two region cores. MOX inner region.

Designation	Core Parameters				K_{eff}			
	Pitch (inch)	Inner Region	Outer Region	Specifics	MCU	NCNP (ENDF/B-V)	NCNP (ENDF/B-VI)	KENO-V (ABBN-93)
SX1-6i	0.56	MOX 3x3	UO_2 19x19		0.9918(4)	0.9968(3)	0.9926(3)	0.9941(4)
SX1-9b	0.56	MOX 11x11	UO_2 19x19	Fig.	0.9945(4)	0.9991(3)	0.9934(3)	0.9923(3)
SX1-10b	0.56	MOX 19x19	UO_2 27x27	Fig.	0.9966(4)			0.9913(3)
SX1-10f	0.56	MOX 19x19	UO_2 27x27	3x3 UO_2 center Fig.	0.9935(4)	0.9984(3)	0.9933(3)	0.9917(4)
SX1-10e	0.56	MOX 19x19	UO_2 27x27	Fig.	0.9966(4)	0.9995(3)	0.9952(3)	0.9918(3)
SX1-9c	0.56	MOX 11x11	UO_2 19x19	Al plate Fig.	0.9932(4)	0.9981(3)	0.9933(3)	0.9916(4)
SX1-9f	0.56	MOX 11x11	UO_2 21x21	control rod Fig.	0.9953(4)	0.9976(3)	0.9934(3)	0.9952(4)
SX1-10c	0.56	MOX 19x19	UO_2 27x27	water slot Fig.	0.9960(4)	0.9990(3)	0.9952(3)	0.9918(3)
SX1-10d	0.56	MOX 19x19	UO_2 27x27	Al plate Fig.	0.9964(4)	1.0011(3)	0.9954(3)	0.9914(3)
SX1-13f16	0.52	MOX 23x23	UO_2 29x29	4x4 voids centered	1.0057(13)			
SX1-13f17	0.52	MOX 23x23	UO_2 29x29	8x8 voids centered	1.006(13)			

Table 4. 7. K_{eff} calculation results for two region cores. UO_2 inner region.

Designation	Core Parameters				K_{eff}			
	Pitch (inch)	Inner Region	Outer Region	Specifics	MCU	NCNP (ENDF/B-V)	NCNP (ENDF/B-VI)	KENO-V (ABBN-93)
SX1-11b	0.56	UO_2 11x11	MOX 19x19	Fig.	0.9935(4)	0.9984(3)	0.9933(3)	0.9917(4)
SX1-12b	0.56	UO_2 19x19	MOX 27x27	Fig.	0.9936(4)	0.9994(3)	0.9950(3)	0.9920(3)

The analysis of the results obtained didn't reveal the significant correlation of K_{eff} and parameters of active core. The values of K_{eff} averaged by assemblies of the same type are presented below.

	MCU	NCNP (ENDF/B-V)	NCNP (ENDF/B-VI)	KENO-V (ABBN-93)
MOX	0.9960 ± 0.0027	0.9991 ± 0.0020	0.9928 ± 0.0015	0.9920 ± 0.0020
UO_2	0.9941 ± 0.0023	0.9989 ± 0.0036	0.9946 ± 0.0023	
MOX + UO_2	0.9970 ± 0.0042	0.9991 ± 0.0010	0.9942 ± 0.0009	0.9923 ± 0.0012

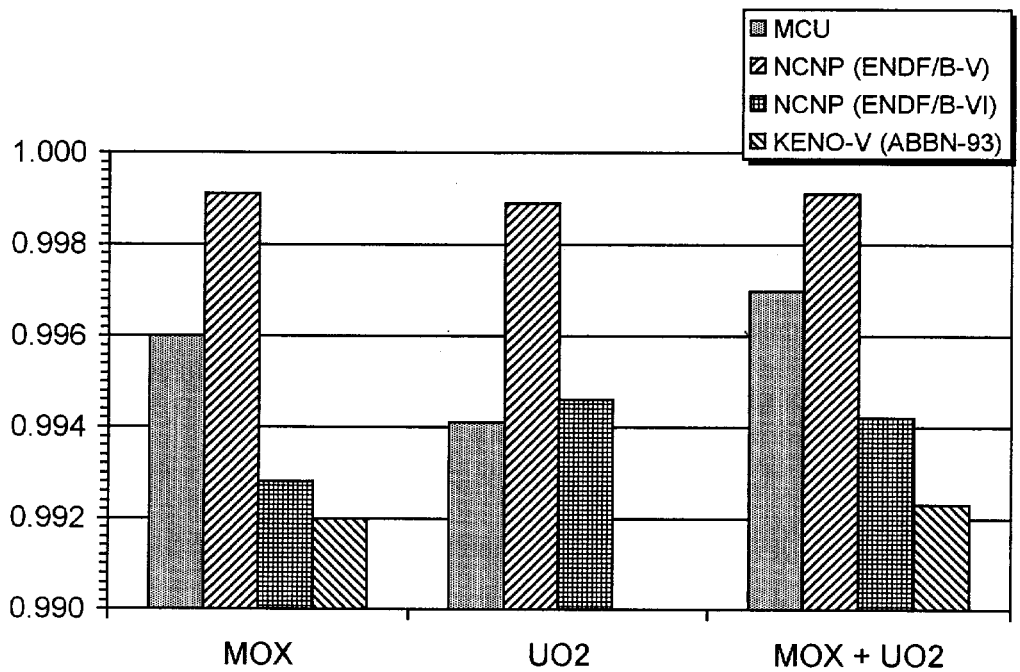

All neutron data used underestimate the multiplication factors. At that the precision of calculations satisfies the practical requirements for all codes.

Earlier in Kurchatov Institute the MCU code was applied to calculation analysis of ZR-6 critical assemblies which have modeled the reactor of VVER type. These assemblies were recognized as benchmark and included in International Handbook Ref. [1]. There is no doubt in the reliability of their description. The average calculated value of K_{eff} for all assemblies coincides with 1 and the dispersion of results is small (compare with $K_{eff} = 0.994$ for UO_2 assemblies). It's not excepted that the error in Saxton calculation is determined by benchmark model but not by neutron data.

4.2. Pin power distribution.

In critical assemblies with 0.52-inch lattice pitch experimental investigation of relative power distribution in the cores was performed. Local power peaking was measured for MOX single region cores near the following perturbations: control rods, water slot and aluminum plate. Power sharing measurements were performed for multi-region cores of MOX and UO_2 fuel rods in different pattern.

The method employed in the measurements and evaluated results for 15 cores is presented in Ref.[4]. The layouts of the cores and rod-detector location are given in figures below together with the experimental and calculation results.

The reported accuracy (2 Standard Deviations) of relative power data for single regions configuration is ± 1.4%. For multi-regions cores the accuracy of relative power data in the region that contains the reference rod is ± 2% and in the other region is ± 7%.

The calculation results by MCU and ABBN-93 are given in the two following sections. The MCNP results one can find in Ref. [7, Sec.14].

4.2.1. MCU Code Results

MCU code was used to calculate pin dependence of fission reactor rate in the cores. For this purpose 6.10^6 neutron histories were modeled in each case. It provides approximately 2% statistical accuracy (1 Standard Deviations).

To be compared with experimental data, results of the calculation must be normalized. One can use several ways of normalization. In this work normalization factor A was obtained from following equation:

$$\sum_K EXP_K = A \sum_K CALC_K \ ,$$

where EXP_K and $CALC_K$ is results of measurements and calculations for the rod number k.

Comparisons of a calculation results with experimental data are presented in Fig. 1÷15. The Fig. numbers is in correlation with ones in the Table 4. 1.

As one can see calculation and experimental results are coincide if take into account experimental errors and statistical accuracy of calculation.

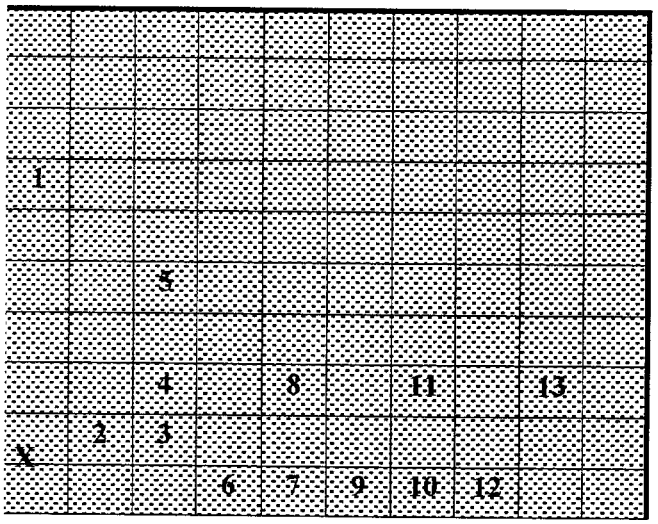

Rod-detector positions

Pin power distribution

Pin	EXP	CALC	C/E-1 %
1	1.000	1.014	1.4
2	1.041	1.259	1.7
3	1.077	1.237	0.1
4	1.000	1.212	0.2
5	0.886	1.124	0.2
6	0.928	1.196	-0.4
7	0.951	1.155	0.3
8	1.077	1.123	0.3
9	1.079	1.092	-0.8
10	1.040	1.009	3.1
11	1.045	0.988	-3.4
12	1.082	0.938	-0.1
13	0.849	0.928	-2.8

Fig. 1. Relative pin power distribution
SX1-1b2 : 19x19 MOX, 1.4224-cm pitch.

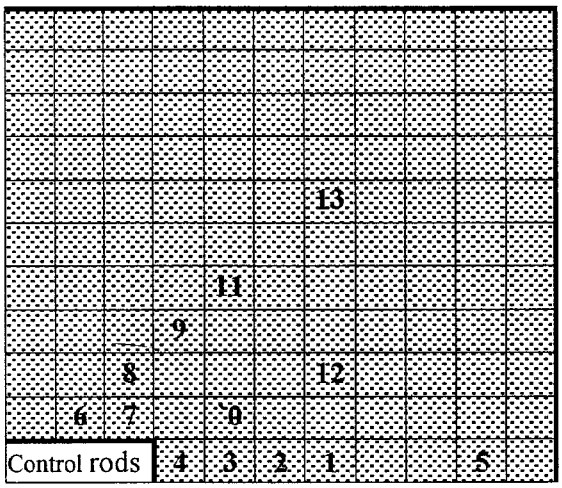

Rod-detector positions

Pin power distribution

Pin	EXP	CALC	C/E-1 %
1	1.000	0.985	-1.5
2	1.041	1.038	-0.3
3	1.077	1.077	0.0
4	1.000	0.997	-0.3
5	0.886	0.878	-0.9
6	0.928	0.953	2.7
7	0.951	0.986	3.8
8	1.077	1.079	0.1
9	1.079	1.071	-0.8
10	1.040	1.057	1.6
11	1.045	1.059	1.3
12	1.082	1.045	-3.4
13	0.849	0.830	-2.2

Fig. 2. Relative pin power distribution.
SX1-1f : 21x21 MOX, 1.4224 pitch,
5 MOX center rods replace with Ag-In-Cd control rods.

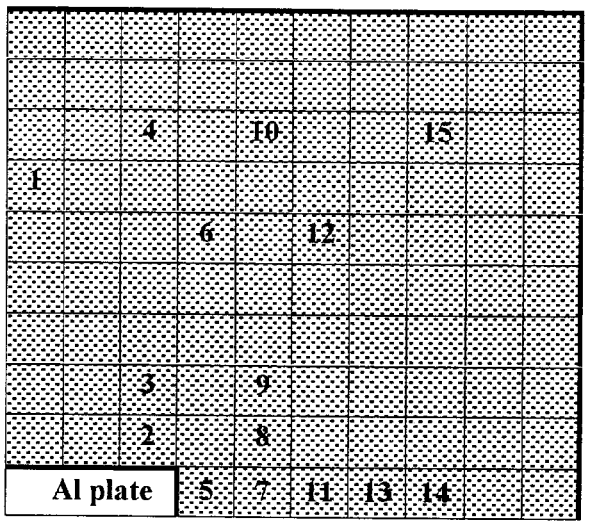

Rod-detector positions

Pin power distribution

Pin	EXP	CALC	C/E-1 %
1	1.0000	1.010	1.0
2	1.4552	1.494	2.7
3	1.2484	1.245	-0.3
4	0.9308	0.912	-2.0
5	1.3972	1.416	1.4
6	1.0283	1.020	-0.8
7	1.1739	1.172	-0.1
8	1.1570	1.155	-0.2
9	1.1245	1.126	0.2
10	0.8700	0.841	-3.3
11	1.0816	1.089	0.6
12	0.9256	0.928	0.2
13	1.0002	1.020	2.0
14	0.9401	0.935	-0.6
15	0.7168	0.688	-4.0

Fig. 3. Relative pin power distribution
SX1-1e: 19x19 MOX, 1.4224-cm pitch,
5 MOX center rods replace with Al plate.

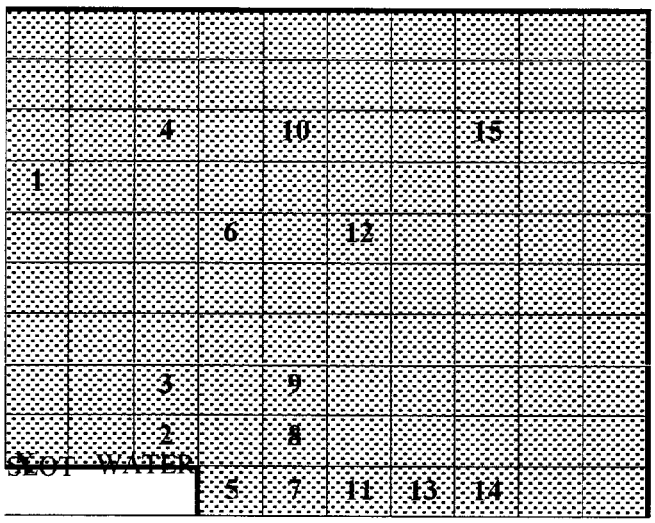

Rod-detector positions

Pin power distribution

Pin	EXP[1]	CALC	C/E-1 %
1	1.000	0.976	-2.4
2	2.000	2.031	1.5
3	1.792	1.814	1.2
4	1.362	1.363	0.1
5	1.095	1.113	1.7
6	1.615	1.630	0.9
7	1.424	1.422	-0.1
8	1.253	1.254	0.1
9	1.155	1.140	-1.3
10	0.97	0.976	0.6
11	1.066	1.067	0.1
12	1.114	1.090	-2.2
13	0.939	0.925	-1.5
14	0.737	0.720	-2.3

Fig 4. Relative pin power distribution
SX1-1d: 19x19 MOX, 1.4224-cm pitch,
5 MOX center rods replace with water slot.

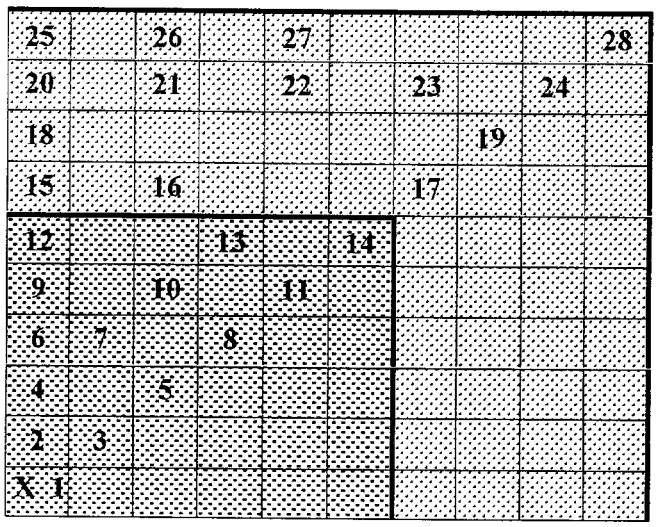

Rod-detector positions

Pin power distribution

Pin	EXP	CALC	C/E-1 %
1	1.0000	1.005	0.5
2	0.9930	0.985	-0.8
3	0.9881	0.965	-2.3
4	0.9735	0.964	-0.9
5	0.9433	0.945	0.2
6	0.9657	0.932	-3.5
7	0.9570	0.939	-1.9
8	0.9126	0.890	-2.5
9	0.925	0.909	-1.7
10	0.9038	0.898	-0.6
11	0.85940	0.844	-1.8
12	0.9592	0.940	-2.0
13	0.9239	0.894	-3.3
14	0.894	0.875	-2.1
15	0.7701	0.795	3.2
16	0.7589	0.777	2.3
17	0.6697	0.683	2.0
18	0.8045	0.814	1.1
19	0.6073	0.627	3.3
20	0.8395	0.849	1.1
21	0.8092	0.823	1.7
22	0.7512	0.769	2.4
23	0.6607	0.676	2.3
24	0.6207	0.634	2.2
25	1.1703	1.181	0.9
26	1.1236	1.131	0.7
27	0.9993	1.019	2.0
28	0.996	1.017	2.1

Fig. 5. Relative pin power distribution
SX1-9b: 19x19 core, 11x11 MOX inner region, 1.4224-cm pitch.

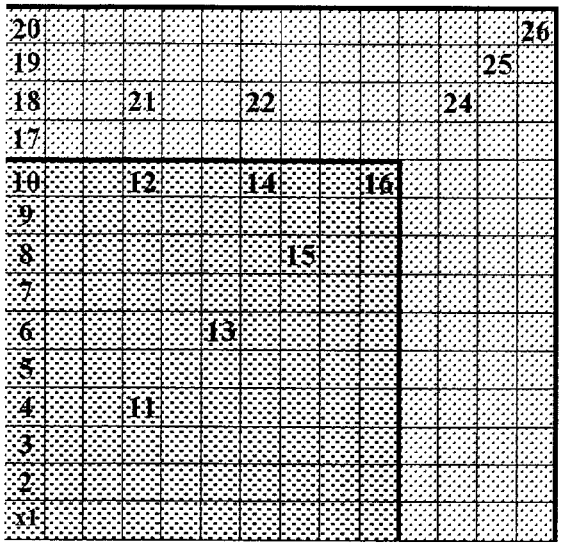

Rod-detector positions

Pin power distribution

Pin	EXP	CALC	C/E-1 %
1	1.000	0.980	-2.0
2	0.985	0.993	0.8
3	0.989	0.985	-0.4
4	0.968	0.962	-0.6
5	0.947	0.948	0.1
6	0.904	0.899	-0.5
7	0.86	0.863	0.4
8	0.801	0.816	1.9
9	0.754	0.753	-0.1
10	0.759	0.753	-0.7
11	0.942	0.926	-1.7
12	0.723	0.722	-0.2
13	0.805	0.804	-0.1
14	0.644	0.632	-1.9
15	0.648	0.647	-0.1
16	0.56	0.549	-2.0
17	0.572	0.587	2.6
18	0.559	0.572	2.3
19	0.526	0.530	0.7
20	0.575	0.601	4.5
21	0.537	0.527	-1.8
22	0.474	0.471	-0.6
23	0.383	0.393	2.6
24	0.315	0.324	3.0
25	0.276	0.270	-2.1
26	0.297	0.297	0.0

Fig 6. Relative pin power distribution
SX1-10b: 7x27 core, 19x19 MOX center region, UO_2 outer region, 1.4224-cm pitch, 1.453 ppm Boron.

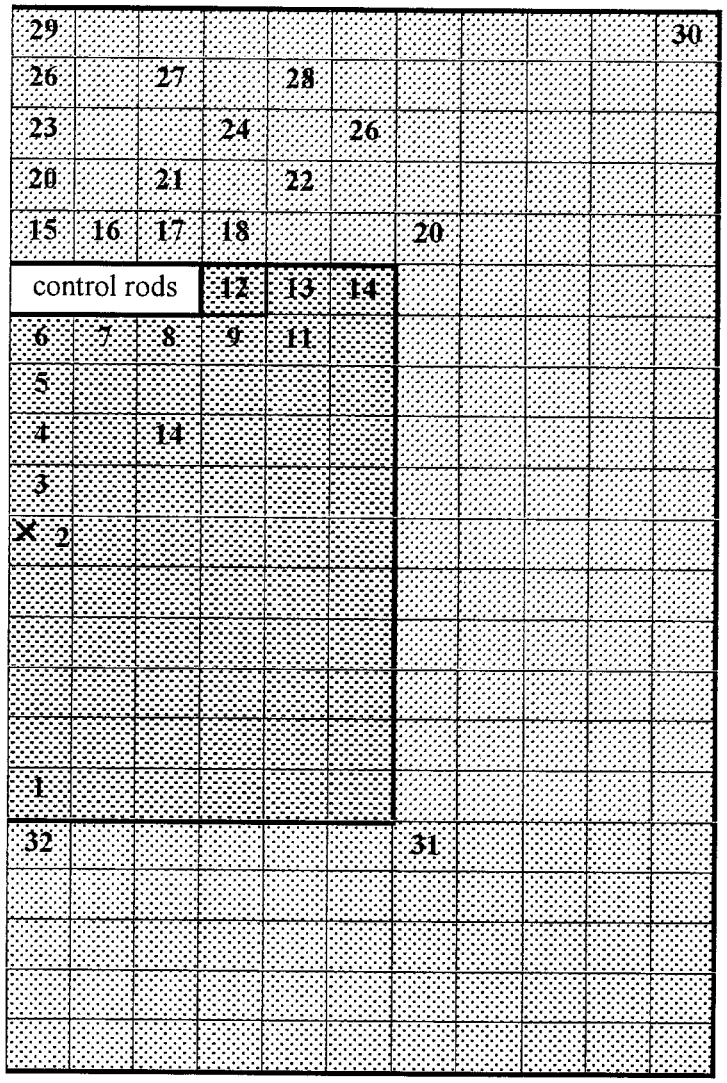

Rod-detector positions

Pin power distribution

Pin	EXP	CALC	C/E-1 %
1	1.0000	0.949	-5.1
2	0.9534	0.890	-6.6
3	0.8697	0.882	1.4
4	0.8519	0.843	-1.0
5	0.7773	0.764	-1.7
6	0.6263	0.653	4.2
7	0.6264	0.665	6.2
8	0.6619	0.684	3.3
9	0.7323	0.726	-0.9
10	0.7755	0.762	-1.7
11	0.7197	0.718	-0.3
12	0.7815	0.770	-1.4
13	0.8255	0.802	-2.8
14	0.9472	0.840	-11.3
15	0.5309	0.570	7.4
16	0.5495	0.570	3.7
17	0.5548	0.588	6.0
18	0.600	0.617	2.8
19	0.6427	0.637	-0.8
20	0.6105	0.640	4.9
21	0.6169	0.649	5.1
22	0.6408	0.646	0.9
23	0.6196	0.647	4.5
24	0.6467	0.637	-1.5
25	0.5948	0.606	1.9
26	0.6552	0.671	2.4
27	0.654	0.669	2.3
28	0.6237	0.627	0.5
29	0.9467	0.966	2.1
30	0.8167	0.798	-2.3
31	0.7335	0.720	-1.8
32	0.8183	0.796	-2.7

Fig.7 Relative pin power distribution.
SX1-9f.: 21x21 core, 11x11 MOX center region, UO_2 outer region, 1.4224,
5 MOX rods replaced with Ag-In-Cd rods.

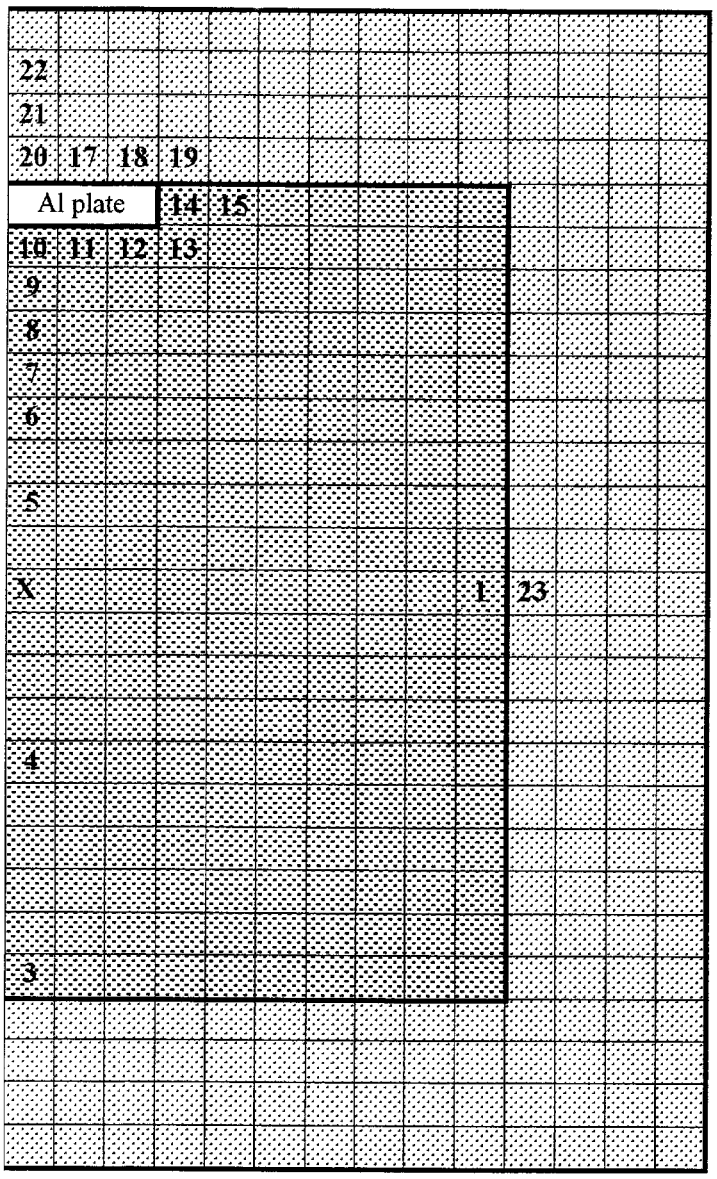

Rod-detector positions

Pin power distribution

Pin	EXP	CALC	C/E-1 %
1	1.0000	0.987	-1.3
2	1.3065	1.295	-0.9
3	1.0052	0.997	-0.8
4	1.2449	1.232	-1.0
5	1.3012	1.284	-1.3
6	1.2329	1.225	-0.6
7	1.1806	1.185	0.4
8	1.1251	1.129	0.3
9	1.1051	1.093	-1.1
10	1.2049	1.234	2.5
11	1.2273	1.196	-2.5
12	1.1549	1.137	-1.6
13	1.0204	1.000	-2.0
14	1.0961	1.093	-0.3
15	0.9558	0.924	-3.3
16	0.9751	0.992	1.7
17	0.9366	0.987	5.4
18	0.8943	0.914	2.2
19	0.7867	0.805	2.3
20	0.7861	0.807	2.7
21	0.7037	0.717	1.9
22	0.7768	0.778	0.1
23	0.7654	0.773	1.0

Fig.8 Pin power distribution.
SX1-10d: 27x27 core,19x19 MOX center region, UO_2 outer region, 1.4224-cm pitch, 5 MOX rods replaced with Al plate, 1453 ppm Boron

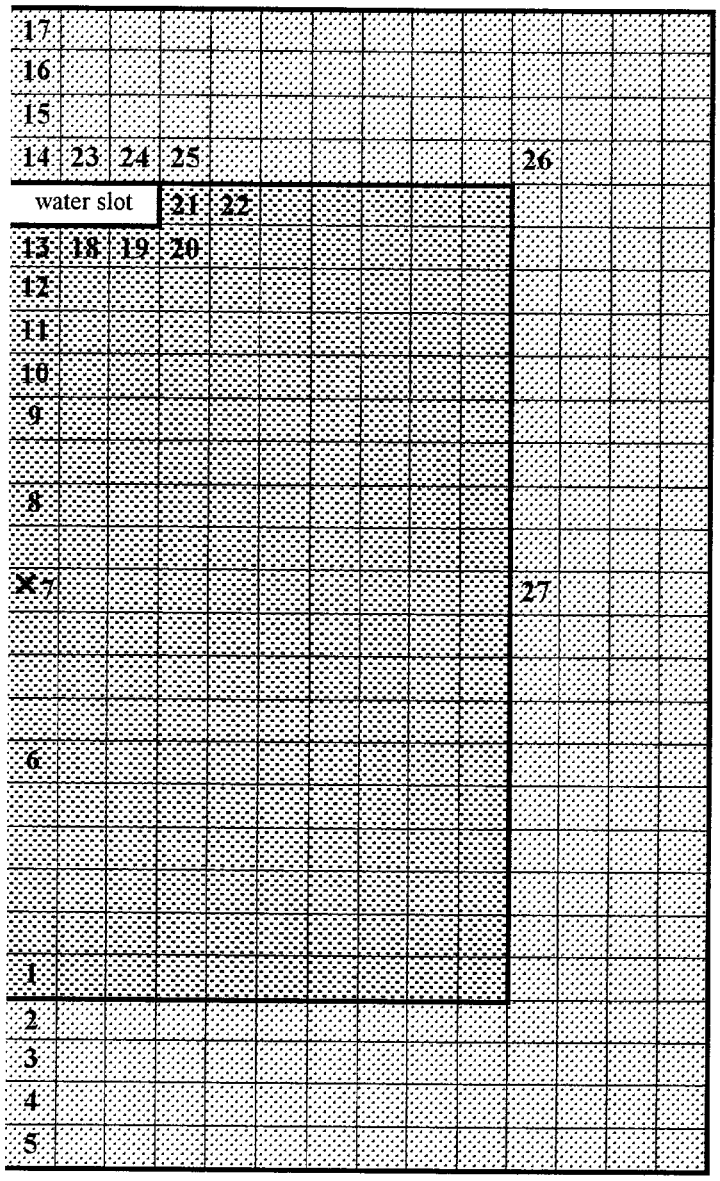

Pin power distribution

Pin	EXP	CALC	C/E-1 %
1	1.0000	0.966	-3.4
2	0.7598	0.783	3.1
3	0.7452	0.772	3.6
4	0.6994	0.701	0.2
5	0.7811	0.784	0.4
6	1.2404	1.229	-1.0
7	1.3046	1.297	-0.6
8	1.2988	1.281	-1.4
9	1.2257	1.226	0.0
10	1.1664	1.174	0.6
11	1.1314	1.134	0.2
12	1.1121	1.118	0.5
13	1.3713	1.374	0.2
14	1.1168	1.117	0.0
15	0.8233	0.812	-1.3
16	0.7064	0.697	-1.3
17	0.7621	0.761	-0.1
18	1.3375	1.351	1.0
19	1.2508	1.248	-0.2
20	1.0516	1.024	-2.7
21	1.141	1.151	0.8
22	0.9478	0.936	-1.3
23	1.0921	1.108	1.5
24	0.9883	1.005	1.7
25	0.8145	0.817	0.4
26	0.5067	0.500	-1.4
27	0.7701	0.779	1.1

Fig. 9. Relative pin power distribution.
SX1-10c.: 27x27 core, 19x10 MOX center region, UO_2 outer region, 1.4224-cm pitch, 5 MOX rods replaced with water slot.

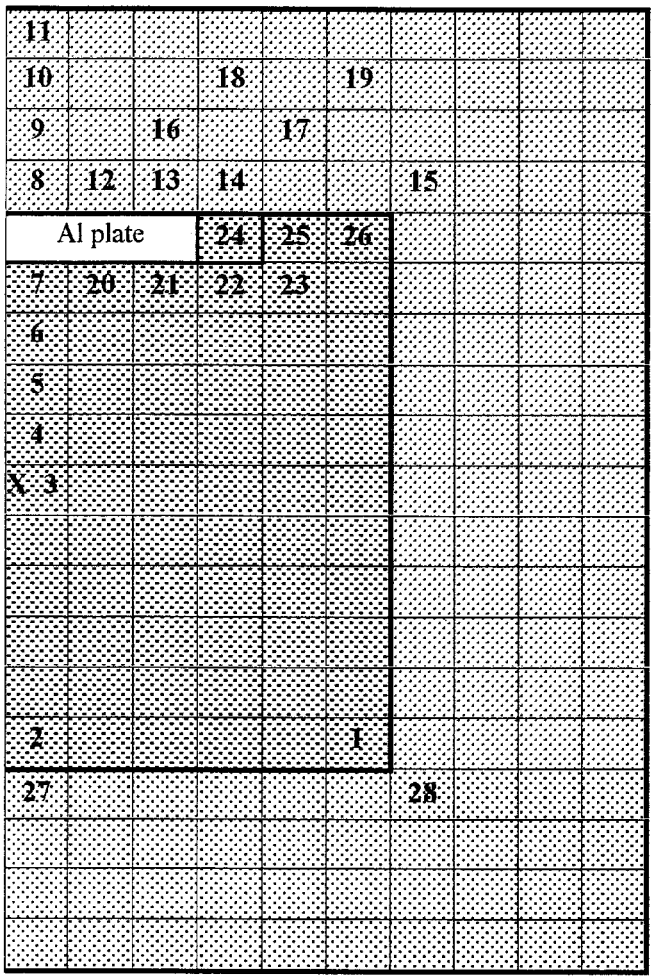

Rod-detector positions

Pin power distribution

Pin	EXP	CALC	C/E-1 %
1	1.000	0.983	-1.7
2	1.075	1.057	-1.7
3	1.111	1.110	-0.1
4	1.097	1.094	-0.2
5	1.097	1.087	-0.9
6	1.141	1.109	-2.8
7	1.358	1.340	-1.3
8	1.117	1.146	2.6
9	0.957	0.970	1.4
10	0.930	0.968	4.0
11	1.294	1.338	3.4
12	1.095	1.140	4.1
13	1.028	1.055	2.6
14	0.884	0.915	3.5
15	0.749	0.765	2.1
16	0.903	0.930	3.0
17	0.811	0.830	2.4
18	0.879	0.892	1.5
19	0.780	0.798	2.4
20	1.344	1.291	-4.0
21	1.289	1.221	-5.3
22	1.070	1.046	-2.2
23	0.976	0.960	-1.6
24	1.204	1.172	-2.7
25	1.027	0.989	-3.7
26	0.997	0.981	-1.6
27	0.863	0.878	1.8
28	0.750	0.761	1.5

Fig.10 Relative pin power distribution.
SX1-9c: 19x19 core,11x11 MOX center region, UO_2 outer region, 1.4224-cm pitch,
5 MOX rods replaced with Al slab.

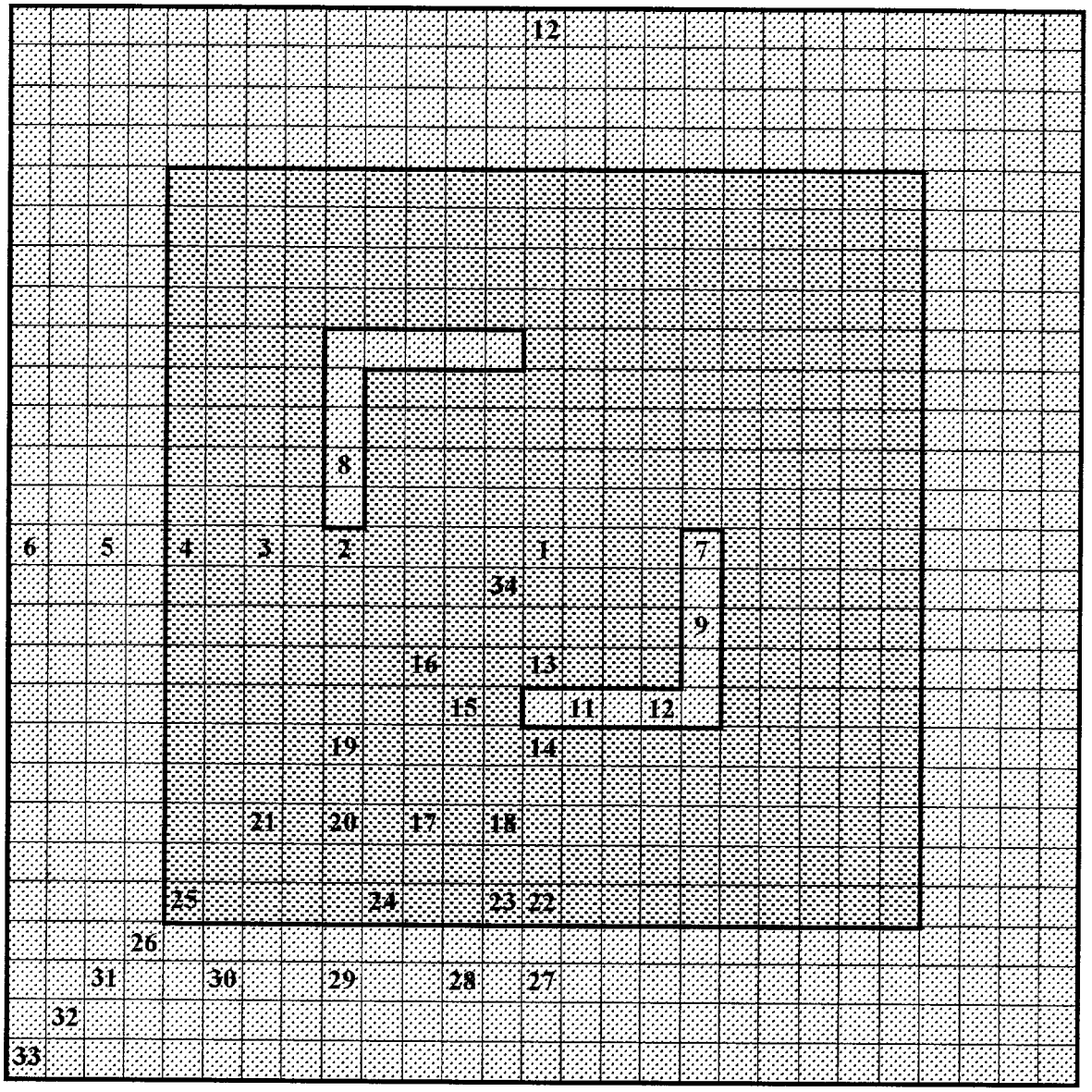

Fig. 11.1. Core layout and positions of rod-detectors.
SX1-10e: 27x27 core, 19x19 MOX inner region, 1.422-cm pitch.

Pin power distribution

Pin	EXP [a)]	CALC [b)]	C/E-1 %
1	1.0000	1.006	0.6
2	1.0490	0.946	-9.8
3	0.8263	0.818	-1.0
4	0.7629	0.768	0.6
5	0.5671	0.586	3.3
6	0.5906	0.609	3.1
7	0.7800	0.797	2.2
8	0.7551	0.770	2.0
9	0.7960	0.826	3.8
10	0.7920	0.822	3.8
11	0.8098	0.835	3.1
12	0.8565		
13	1.0519	1.033	-1.8
14	1.0605	0.970	-8.6
15	0.9740	0.941	-3.4
16	0.9507	0.942	-0.9
17	0.7920	0.765	-3.4
18	0.8363	0.823	-1.6
19	0.8071	0.820	1.5
20	0.7197	0.725	0.7
21	0.6425	0.664	3.4
22	0.7624	0.756	-0.8
23	0.7556	0.750	-0.7
24	0.7056	0.712	0.9
25	0.5517	0.559	1.4
26	0.3809	0.407	6.8
27	0.5930	0.597	0.7
28	0.5726	0.578	1.0
29	0.5218	0.527	0.9
30	0.4210	0.424	0.8
31	0.3230	0.321	-0.7
32	0.2767	0.282	1.8
33	0.3022	0.307	1.5
34	0.9984	1.013	1.4

Fig. 11.2. Relative pin power distribution
SX1-10e: 27x27 core, 19x19 MOX inner region, 1.422-cm pitch.

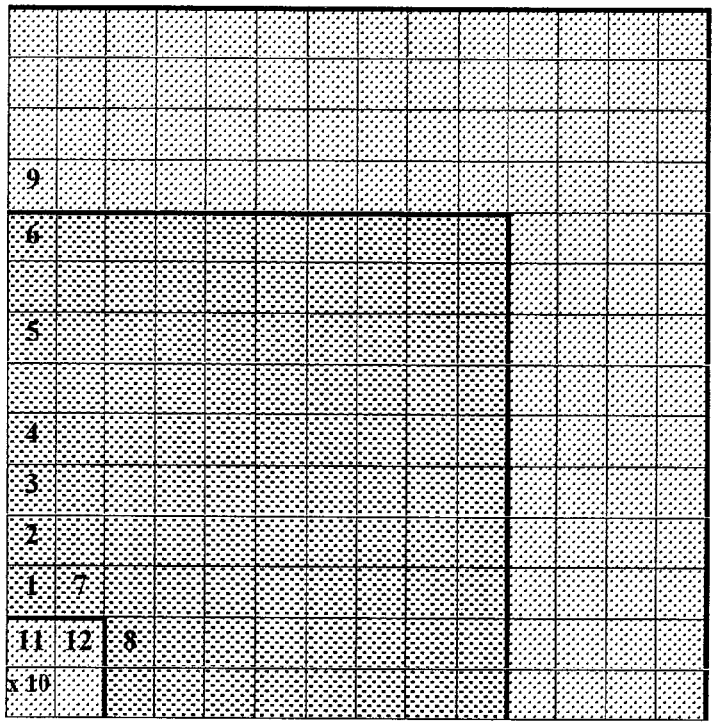

Rod-detector positions

Pin power distribution

Pin	EXP	CALC	C/E-1 %
1	1.000	1.016	1.6
2	0.917	0.916	-0.1
3	0.883	0.873	-1.2
4	0.869	0.841	-3.2
5	0.756	0.767	1.5
6	0.706	0.727	3.0
7	0.989	0.959	-3.0
8	1.014	1.004	-1.1
9	0.548	0.556	1.5
10	0.905	0.872	-3.6
11	0.853	0.877	2.8
12	0.815	0.845	3.8

Fig.12. Relative pin power distribution
SX1-9b: 27x27 core, 19x19 MOX inner region, 1.4224-cm pitch.
3x3 MOX replaced with UO_2 in center, 1425 ppm Boron.

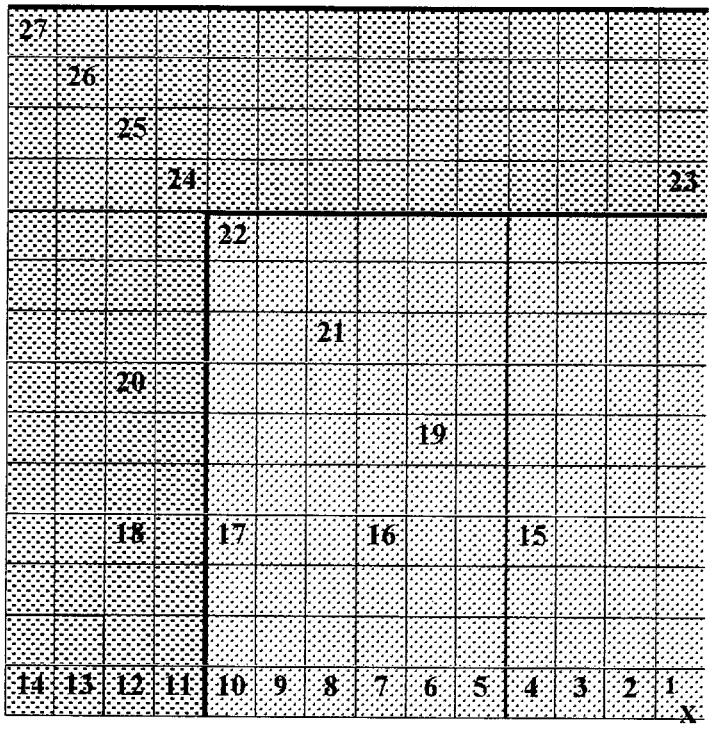

Rod-detector positions

Pin power distribution

Pin	EXP	CALC	C/E-1 %
1	1.0000	0.974	-2.6
2	0.9479	0.967	2.0
3	0.9250	0.939	1.5
4	0.9047	0.931	2.9
5	0.8886	0.911	2.6
6	0.8406	0.868	3.2
7	0.8157	0.844	3.4
8	0.7640	0.781	2.2
9	0.6970	0.715	2.6
10	0.6110	0.607	-0.7
11	0.6558	0.622	-5.2
12	0.5260	0.500	-5.0
13	0.4771	0.459	-3.8
14	0.5959	0.564	-5.4
15	0.8814	0.892	1.2
16	0.7842	0.800	2.0
17	0.5652	0.587	3.9
18	0.5054	0.484	-4.3
19	0.7647	0.788	3.1
20	0.4531	0.437	-3.6
21	0.6053	0.629	3.8
22	0.3833	0.395	3.2
23	0.6590	0.625	-5.1
24	0.3789	0.359	-5.1
25	0.2896	0.275	-4.9
26	0.2537	0.238	-6.1
27	0.3432	0.325	-5.3

Fig 13. Relative pin power distribution
SX1-12b: 27x27 core, 19x19 UO_2 inner region, 1.4224-cm pitch,
1252 ppm Boron.

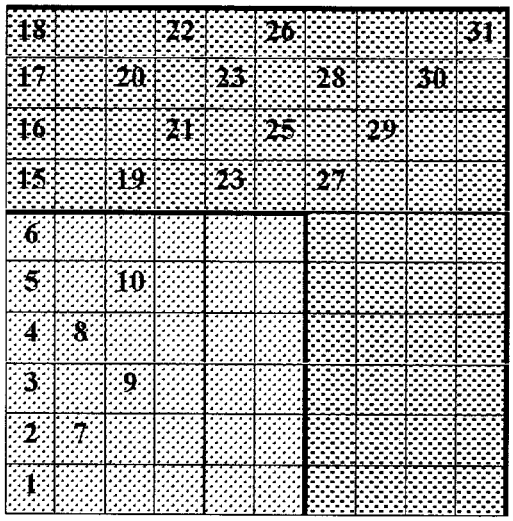

Rod-detector positions

Pin power distribution

Pin	EXP	CALC	C/E-1 %
1	1.0000	1.038	3.8
2	0.9916	1.037	4.6
3	0.9849	1.025	4.0
4	0.9433	0.972	3.0
5	0.8758	0.915	4.5
6	0.7752	0.805	3.9
7	0.9807	1.018	3.8
8	0.9307	0.973	4.5
9	0.9517	0.995	4.6
10	0.8516	0.894	5.0
11	0.8871	0.912	2.8
12	0.7213	0.752	4.2
13	0.7797	0.813	4.3
14	0.6027	0.619	2.8
15	0.8798	0.830	-5.7
16	0.7189	0.679	-5.6
17	0.707	0.682	-3.5
18	1.0949	1.084	-1.0
19	0.8547	0.806	-5.7
20	0.7060	0.664	-5.9
21	0.6810	0.656	-3.7
22	1.0419	1.025	-1.6
23	0.7744	0.739	-4.6
24	0.6543	0.642	-1.8
25	0.6113	0.580	-5.1
26	0.9591	0.928	-3.2
27	0.6173	0.589	-4.6
28	0.558	0.538	-3.5
29	0.5176	0.488	-5.8
30	0.5326	0.505	-5.2
31	1.0092	0.991	-1.8
32	0.8183	0.796	-2.7
25	0.2896	0.275	-4.9
26	0.2537	0.238	-6.1
27	0.3432	0.325	-5.3

Fig 14. Relative pin power distribution
SX1-11b: 19x19 core, 11x11 UO_2 inner region, 1.4224-cm pitch,

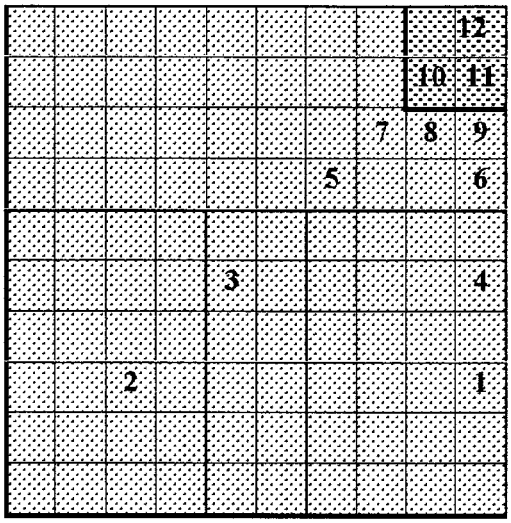

Rod-detector positions

Pin power distribution

Pin	EXP	CALC	C/E-1 %
1	1.0000	1.006	0.6
2	0.7400	0.739	-0.1
3	0.9608	0.984	2.4
4	1.144	1.155	1.0
5	1.1877	1.212	2.0
6	1.2288	1.250	1.8
7	1.2234	1.258	2.8
8	1.1792	1.240	5.1
9	1.1985	1.211	1.1
10	1.4772	1.417	-4.1
11	1.4036	1.364	-2.8
12	1.3182	1.225	-7.1

Fig 15. Relative pin power distribution
SX1-6i: 19x19 core, 3x3 MOX in center region, UO_2 inner region, 1.4224-cm pitch,

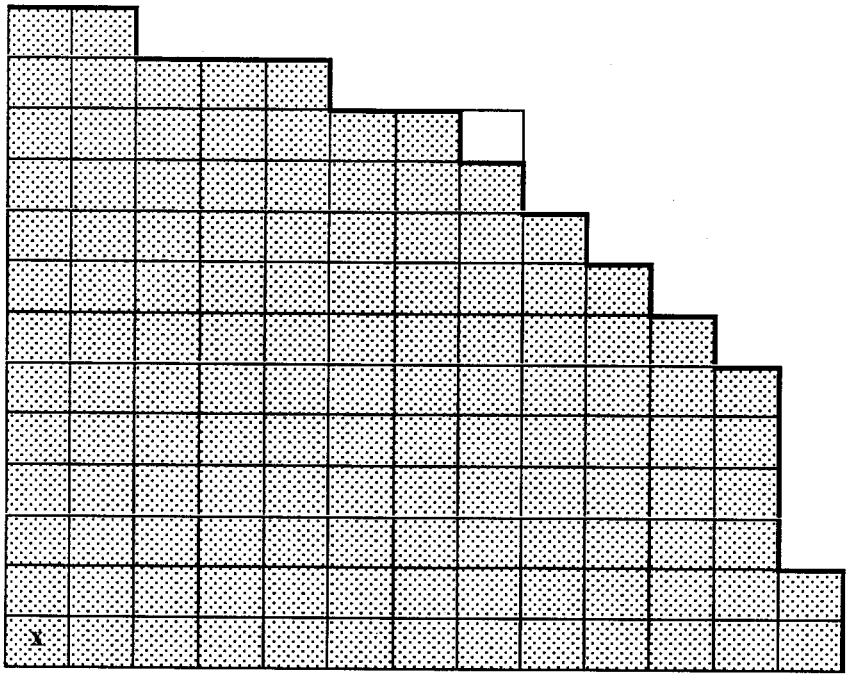

Fig. 16. SX1-8b: 449 MOX, 1.3208-cm pitch.

4.2.3. KENO-V (ABBN-93) calculation results.

Fifteen configurations of evaluated critical experiments with relative pin power distribution were calculated using the Monte-Carlo code KENO-Va and CONSYST2/ABBN-93 constant's system. In all cases the KENO-Va calculations used 5000 generations at 1000 neutrons per generation. Ten generations were skipped before averaging. Relative pin power distributions were obtained with accurate treatment of energy releases in each nuclide using ABBN-93 data set.

Relative power distribution calculated results presented in Tables 4.8 to 4.22.

In this Tables Δ = (Calc.-Meas.)/Meas. in %

Table 4. 8. Measured and Calculated Relative Pin Power Distribution for Case SX1-1b2

pin #	Measured Relative Pin Power	Calculated Relative Pin Power	Δ, %
1	1.0000	1.0000	0.00
2	1.1220	1.0925	-2.63
3	1.2101	1.1933	-1.39
4	1.1190	1.1188	-0.01
5	0.9791	0.9649	-1.45
6	0.9552	0.9206	-3.62
7	1.2385	1.2151	-1.89
8	1.2357	1.2218	-1.13
9	1.2013	1.1891	-1.01
10	1.1520	1.1272	-2.15
11	1.1007	1.0488	-4.72
12	1.0232	0.9970	-2.56
13	0.9390	0.9359	-0.34

Table 4. 9. Measured and Calculated Relative Pin Power Distribution for Case SX1-1f

pin #	Measured Relative Pin Power	Calculated Relative Pin Power	Δ, %
1	0.8492	0.8566	0.87
2	1.0449	1.0268	-1.73
3	1.0788	1.0652	-1.26
4	1.0774	1.0742	-0.30
5	1.0816	0.9907	-8.40
6	0.9283	0.9234	-0.53
7	0.9507	0.9632	1.31
8	1.0399	1.0476	0.74
9	1.0003	0.9895	-1.08
10	1.0768	1.0577	-1.77
11	1.0413	1.0245	-1.62
12	1.0000	1.0000	0.00
13	0.8863	0.9128	2.99

Table 4. 10. Measured and Calculated Relative Pin Power Distribution for Case SX1-1e

pin #	Measured Relative Pin Power	Calculated Relative Pin Power	Δ, %
1	0.9308	0.9027	-3.02
2	0.8700	0.8198	-5.77
3	0.7168	0.6711	-6.38
4	1.0000	1.0000	0.00
5	1.0283	0.9871	-4.01
6	0.9256	0.9021	-2.54
7	1.2484	1.2465	-0.15
8	1.1245	1.1050	-1.73
9	1.4552	1.4574	0.15
10	1.1570	1.1311	-2.24
11	1.3973	1.3877	-0.69
12	1.1734	1.1316	-3.56
13	1.0816	1.0700	-1.07
14	1.0002	0.9836	-1.66
15	0.9401	0.9137	-2.81

Table 4. 11. Measured and Calculated Relative Pin Power Distribution for Case SX1-1d

pin #	Measured Relative Pin Power	Calculated Relative Pin Power	Δ, %
1	1.0000	1.0000	0.00
2	0.7367	0.7224	-1.94
3	1.0954	1.1181	2.07
4	0.9703	0.9802	1.02
5	1.3620	1.3752	0.97
6	1.1135	1.0264	-7.82
7	2.0005	2.0559	2.77
8	1.7921	1.8109	1.05
9	1.4236	1.4329	0.65
10	1.6152	1.6283	0.81
11	1.2527	1.2639	0.90
12	1.1550	1.1392	-1.37
13	1.0662	1.0801	1.30
14	0.9840	0.9845	0.05

Table 4. 12. Measured and Calculated Relative Pin Power Distribution for Case SX1-9b

pin #	Measured Relative Pin Power	Calculated Relative Pin Power	Δ, %
1	1.0000	1.0000	0.00
2	0.9927	1.0050	1.24
3	0.9881	1.0082	2.04
4	0.9735	0.9985	2.56
5	0.9433	0.9636	2.15
6	0.9657	0.9533	-1.28
7	0.9570	0.9584	0.14
8	0.9126	0.9034	-1.01
9	0.9250	0.9448	2.14
10	0.9038	0.9177	1.54
11	0.8594	0.8663	0.80
12	0.9592	0.9792	2.09
13	0.9239	0.9180	-0.64
14	0.8940	0.8859	-0.91
15	0.7701	0.7744	0.56
16	0.7589	0.7669	1.06
17	0.6697	0.6769	1.07
18	0.8045	0.7947	-1.21
19	0.6073	0.6150	1.26
20	0.8395	0.8303	-1.09
21	0.8092	0.8210	1.45
22	0.7512	0.7557	0.60
23	0.6607	0.6739	1.99
24	0.6207	0.6234	0.44
25	1.1703	1.1961	2.20
26	1.1236	1.1104	-1.18
27	0.9993	1.0346	3.53
28	0.9960	1.0108	1.48

Table 4. 13. Measured and Calculated Relative Pin Power Distribution for Case SX1-10b

pin #	Measured Relative Pin Power	Calculated Relative Pin Power	Δ, %
1	1.0000	1.0000	0.00
2	0.9845	1.0210	3.71
3	0.9893	1.0000	1.09
4	0.9679	1.0092	4.27
5	0.9424	0.9515	0.97
6	0.9467	0.9693	2.39
7	0.9038	0.9334	3.28
8	0.8053	0.8387	4.15
9	0.8603	0.8740	1.60
10	0.8010	0.8130	1.49
11	0.6480	0.6652	2.66
12	0.7535	0.7660	1.65
13	0.7594	0.7610	0.21
14	0.7231	0.7376	2.01
15	0.6441	0.6590	2.31
16	0.5604	0.5635	0.55
17	0.5718	0.5817	1.74
18	0.3830	0.3909	2.05
19	0.5586	0.5609	0.41
20	0.5370	0.5433	1.17
21	0.4741	0.4897	3.29
22	0.3146	0.3117	-0.91
23	0.5258	0.5231	-0.51
24	0.2763	0.2704	-2.12
25	0.5753	0.6060	5.34
26	0.2969	0.3000	1.05

Table 4. 14. Measured and Calculated Relative Pin Power Distribution for Case SX1-9f

pin #	Measured Relative Pin Power	Calculated Relative Pin Power	Δ, %
1	1.0000	1.0000	0.00
2	0.9354	0.9653	3.19
3	0.8697	0.9296	6.89
4	0.8519	0.8760	2.83
5	0.7773	0.8072	3.85
6	0.6263	0.6464	3.20
7	0.6264	0.6326	0.99
8	0.9472	0.8651	-8.66
9	0.6616	0.6711	1.43
10	0.7323	0.7419	1.31
11	0.7197	0.7171	-0.36
12	0.7755	0.7797	0.55
13	0.7815	0.7836	0.27
14	0.8255	0.8354	1.20
15	0.8183	0.8292	1.33
16	0.5309	0.5137	-3.23
17	0.6105	0.6147	0.69
18	0.6196	0.6350	2.49
19	0.6552	0.6658	1.61
20	0.9467	0.9546	0.84
21	0.5495	0.5255	-4.37
22	0.5548	0.5430	-2.14
23	0.6169	0.6332	2.64
24	0.6540	0.6776	3.61
25	0.6000	0.6051	0.85
26	0.6167	0.6265	1.58
27	0.6408	0.6567	2.49
28	0.6237	0.6461	3.59
29	0.5948	0.6141	3.24
30	0.7335	0.7305	-0.40
31	0.6427	0.6425	-0.04
32	0.8167	0.8130	-0.45

Table 4. 15. Measured and Calculated Relative Pin Power Distribution for Case SX1-10d

pin #	Measured Relative Pin Power	Calculated Relative Pin Power	Δ, %
1	1.0052	1.0106	0.54
2	1.2449	1.2429	-0.17
3	1.3065	1.3019	-0.36
4	1.3012	1.2737	-2.12
5	1.2329	1.2022	-2.49
6	1.1806	1.1821	0.13
7	1.1251	1.0909	-3.04
8	1.1051	1.1097	0.41
9	1.2049	1.2117	0.56
10	1.2273	1.2074	-1.62
11	1.1549	1.1488	-0.53
12	1.0204	1.0371	1.63
13	1.0961	1.0727	-2.13
14	0.9558	0.9263	-3.09
15	1.0000	1.0000	0.00
16	0.7654	0.7588	-0.87
17	0.9751	0.9470	-2.88
18	0.7861	0.7785	-0.96
19	0.7037	0.6925	-1.60
20	0.7768	0.7419	-4.49
21	0.9366	0.9321	-0.48
22	0.8943	0.8731	-2.37
23	0.7837	0.7723	-1.46

Table 4. 16. Measured and Calculated Relative Pin Power Distribution for Case SX1-10c

pin #	Measured Relative Pin Power	Calculated Relative Pin Power	Δ, %
1	1.0000	1.0000	0.00
2	1.2404	1.2423	0.15
3	1.3046	1.3115	0.53
4	1.2988	1.2999	0.08
5	1.2257	1.2129	-1.04
6	1.1664	1.1776	0.96
7	1.1314	1.1182	-1.17
8	1.1121	1.1261	1.26
9	1.3713	1.3820	0.78
10	1.3375	1.3689	2.35
11	1.2508	1.2623	0.92
12	1.0516	1.0419	-0.92
13	1.1410	1.1392	-0.15
14	0.9478	0.9479	0.01
15	0.7811	0.7833	0.29
16	0.6994	0.6987	-0.10
17	0.7452	0.7551	1.33
18	0.7597	0.7671	0.98
19	1.1168	1.0701	-4.18
20	0.8233	0.8101	-1.61
21	0.7064	0.6927	-1.94
22	0.7621	0.7680	0.78
23	1.0921	1.0522	-3.65
24	0.9883	0.9681	-2.05
25	0.8145	0.7869	-3.39
26	0.7701	0.7432	-3.49
27	0.5067	0.4980	-1.71

Table 4. 17. Measured and Calculated Relative Pin Power Distribution for Case SX1-9c

pin #	Measured Relative Pin Power	Calculated Relative Pin Power	Δ, %
1	1.0749	1.0821	0.67
2	1.1108	1.1510	3.62
3	1.0970	1.1387	3.80
4	1.0971	1.1235	2.40
5	1.1405	1.1488	0.73
6	1.3579	1.3818	1.76
7	1.3437	1.3421	-0.12
8	1.2893	1.2853	-0.31
9	1.0697	1.0974	2.59
10	1.2036	1.2400	3.03
11	0.9763	0.9852	0.91
12	1.0265	1.0324	0.57
13	1.0000	1.0000	0.00
14	0.9966	1.0292	3.27
15	0.8630	0.8748	1.37
16	1.1173	1.1796	5.58
17	0.9567	0.9875	3.22
18	0.9300	0.9659	3.86
19	1.2944	1.3456	3.96
20	1.0954	1.1599	5.89
21	1.0277	1.0780	4.90
22	0.9028	0.9362	3.70
23	0.8831	0.9421	6.69
24	0.8790	0.9040	2.85
25	0.8101	0.8403	3.73
26	0.7801	0.8195	5.06
27	0.7504	0.7654	2.00
28	0.7489	0.7800	4.15

Table 4. 18. Measured and Calculated Relative Pin Power Distribution for Case SX1-10e

pin #	Relative Pin Power (calculated)	Relative Pin Power (measured)	Δ, %
1	0.5647	0.5517	2.35
2	0.7726	0.7629	1.27
3	0.6357	0.6425	-1.06
4	0.8255	0.8263	-0.09
5	0.7165	0.7197	-0.45
6	0.8131	0.8071	0.74
7	0.9444	1.0490	-9.98
8	0.7011	0.7056	-0.64
9	0.7825	0.7920	-1.19
10	0.9502	0.9507	-0.06
11	0.9536	0.9740	-2.09
12	0.7675	0.7556	1.57
13	0.8277	0.8363	-1.03
14	1.0210	0.9984	2.26
15	0.7668	0.7624	0.58
16	0.9836	1.0605	-7.25
17	1.0220	1.0519	-2.84
18	1.0000	1.0000	0.00
19	0.7607	0.8565	-11.18
20	0.7539	0.7551	-0.15
21	0.7861	0.8098	-2.93
22	0.7713	0.7920	-2.61
23	0.7774	0.7960	-2.34
24	0.7591	0.7800	-2.68
25	0.3089	0.3022	2.21
26	0.5977	0.5906	1.20
27	0.2717	0.2767	-1.82
28	0.3175	0.3230	-1.71
29	0.5585	0.5671	-1.52
30	0.3885	0.3809	1.98
31	0.4157	0.4210	-1.25
32	0.5079	0.5218	-2.67
33	0.5591	0.5726	-2.36
34	0.5633	0.5930	-5.01

Table 4. 19. Measured and Calculated Relative Pin Power Distribution for Case SX1-10f

pin #	Calculated Relative Pin Power	Measured Relative Pin Power	Δ, %
1	1.0000	1.0000	0.00
2	0.8913	0.9166	-2.76
3	0.8557	0.8832	-3.11
4	0.8090	0.8387	-3.54
5	0.7285	0.7560	-3.64
6	0.6700	0.7055	-5.03
7	0.9495	0.9887	-3.97
8	0.9509	1.0143	-6.25
9	0.8627	0.9050	-4.67
10	0.8299	0.8533	-2.74
11	0.7905	0.8146	-2.96
12	0.5174	0.5476	-5.51

Table 4. 20. Measured and Calculated Relative Pin Power Distribution for Case SX1-6i

pin #	Measured Relative Pin Power	Calculated Relative Pin Power	Δ, %
1	1.3182	1.3398	1.64
2	1.4772	1.5002	1.56
3	1.4036	1.4214	1.26
4	1.2234	1.2456	1.81
5	1.1792	1.2005	1.80
6	1.1985	1.1966	-0.16
7	1.1877	1.2107	1.94
8	1.2288	1.2564	2.25
9	0.9608	0.9903	3.07
10	1.1440	1.1606	1.45
11	0.7400	0.7509	1.47
12	1.0000	1.0000	0.00

Table 4. 21. Measured and Calculated Relative Pin Power Distribution for Case SX1-12b

pin #	Measured Relative Pin Power	Calculated Relative Pin Power	Δ, %
1	0.5959	0.6182	3.73
2	0.3432	0.3456	0.71
3	0.4771	0.4839	1.42
4	0.2537	0.2604	2.63
5	0.5260	0.5373	2.14
6	0.5054	0.5145	1.81
7	0.4531	0.4593	1.37
8	0.2896	0.2958	2.16
9	0.6558	0.6545	-0.20
10	0.3789	0.3822	0.87
11	0.6590	0.6658	1.04
12	0.6110	0.6206	1.57
13	0.5652	0.6103	7.98
14	0.3833	0.4091	6.74
15	0.6970	0.7296	4.68
16	0.7640	0.8010	4.85
17	0.6053	0.6410	5.90
18	0.8157	0.8604	5.49
19	0.7842	0.8317	6.06
20	0.8406	0.9028	7.40
21	0.7647	0.8147	6.54
22	0.8886	0.9429	6.11
23	0.9047	0.9805	8.38
24	0.8814	0.9388	6.51
25	0.9250	0.9843	6.41
26	0.9479	0.9958	5.05
27	1.0000	1.0000	0.00

Table 4. 22. Calculated and Measured Relative Pin Power Distribution for Case SX1-11b

pin #	Measured Relative Pin Power	Calculated Relative Pin Power	Δ, %
1	1.0949	1.0645	-2.77
2	1.0419	1.0200	-2.10
3	0.9591	0.9262	-3.43
4	1.0092	0.9638	-4.50
5	0.7070	0.6839	-3.26
6	0.7060	0.6696	-5.16
7	0.6543	0.6067	-7.28
8	0.5580	0.5322	-4.63
9	0.5326	0.5012	-5.90
10	0.7189	0.6917	-3.79
11	0.6810	0.6652	-2.31
12	0.6133	0.5785	-5.68
13	0.5176	0.5092	-1.62
14	0.8798	0.8439	-4.08
15	0.8547	0.8057	-5.73
16	0.7744	0.7408	-4.34
17	0.6173	0.5972	-3.26
18	0.7752	0.7701	-0.66
19	0.7213	0.7239	0.36
20	0.6027	0.6043	0.27
21	0.8758	0.8902	1.65
22	0.8516	0.8650	1.58
23	0.7797	0.7816	0.25
24	0.9433	0.9403	-0.31
25	0.9307	0.9411	1.11
26	0.8871	0.8823	-0.55
27	0.9849	0.9812	-0.38
28	0.9517	0.9577	0.63
29	0.9916	1.0066	1.51
30	0.9807	0.9824	0.18
31	1.0000	1.0000	0.00

5. ESADA CRITICAL EXPERIMENTS.

Benchmark considered is based on the critical experiments conducted at the Westinghouse Reactor Evaluation Center in year 1967. These series of the experiments have name ESADA.

Descriptions of experimental configuration and benchmark specification were taken from Ref. [4]. Information about measurement of a power distribution in core is presented in the same report.

5.1. Description of Experimental Configuration and multiplication factors calculation results.

The square array of the fuel rods was placed within a ~112 cm diameter tank that was filled with water. The height of the water could be changed in order to made the configuration critical. The water level was under the top of a fuel in all cases.

Fuel rods were rested on 3 cm or 5 cm aluminum plates and were supported by layers of thin aluminum plates at the top, middle and bottom parts of fuel rods.

Three different types of fuel rods were used during experimental program: two types of MOX fuel and the third type a low enriched UO_2. MOX fuel was distinguished by the isotopes content of plutonium. Content of ^{240}Pu is equal to 8 wt.% or 24 wt.% .

MOX fuel contents the mixture of 2 wt.% PuO_2 and UO_2. Uranium is naturally enriched. MOX fuel rods outer diameter equals to 1.443 cm. Zircaloy 2 cladding is used.

UO_2 fuel contents dioxide uranium enriched with 2.72 wt.% ^{235}U. Outer diameter equals to 1.03 cm. Zircaloy 4 cladding is used.

Two lattice plates were available with lattice pitch equal to 1.7526 cm (0.69 in) and 1.9050 cm (0.75 in). With these plates, five different fuel rods lattice were investigated. Lattice pitch indicated in Table below together with moderator to fuel volume relations V_M / V_F. (Note, in VVER type rector core this value is equals approximately to 2).

Pitch, cm	V_M / V_F	
	MOX	UO_2
1.7526	1.11	2.42
1.9050	1.54	4.48
2.4785	3.49	7.58
2.6942	4.35	8.95
3.5052	8.24	15.15

The positions of fuel rods in the different lattice are shown at the following picture

Lattice with pitch
1.7526, 1.9050, 3.5052 cm

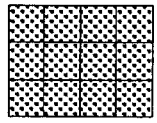

Cell with fuel rod

Lattice with pitch
2.4785, 2.6942 cm

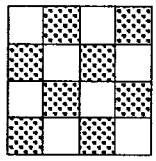

Cell with fuel rod

Cell without fuel rod

Core configurations differ one from another with the number and the positions of MOX and UO_2 fuel rods. Authors of description divided all configurations in four groups:

Single region cores contained fuel rods of the same type. Pure and borate water was used. In some cores one or five rods in center were moved off to obtain water hole.

Concentric region cores were constructed by using two different fuel rods types in the inner and outer regions of the core. Moderator to fuel volume ratios was different in the inner and outer regions because of MOX and UO2 fuel rods have different diameter.

Salt and pepper region cores were constructed by loading two different fuel rods types in checkerboard pattern.

Slab cores consisted of two UO_2 slabs sandwiched a center plutonium fueled slab. A water gap of 1,608 cm was placed between the slab regions. Lattice pitch for UO_2 slab was 1.4605 cm and 1.7526 cm for MOX region and so moderator to fuel volume ratios was the same for both regions.

Layouts of all core configurations are given in Ref.[4].

Main parameters of cores investigated in this report are presented in Tables below together with K_{eff} calculation results.

Multiplication factors calculated are provided in Tables and demonstrated at Figures that follow.

All used codes underestimate multiplication factors in 0.005 ÷ 0.01. It concerns the critical assemblies of all types including the assemblies with uranium fuel only. The same picture takes place for SAXTON assemblies too but for them the calculation error is slightly smaller.

Table 5. 1. Multiplication factors of single region core configurations.

Case Num.	Diagram Num. [b)]	Core parameters [a)]				K_{eff}			
		Fuel Type	Pitch (cm)	Number of Rods	Boron (ppm)	MCU	MCNP (ENDF/B-VI)	MCNP (ENDF/B-V)	KENO-V (ABBN-93)
1	6	8% ^{240}Pu	1.7526	514	0	0.9873(4)	0.9853(7)	0.9919(7)	0.987
2	7	8% ^{240}Pu	1.7526	552	0	0.9849(6)	0.9840(7)	0.9908(7)	0.985
8	13	8% ^{240}Pu	1.7526	631	261	0.9875(9)	0.9850(7)	0.9919(7)	0.985
10	15	8% ^{240}Pu	1.7526	749	526	0.9876(9)	0.9850(7)	0.9917(7)	0.992
3	8	8% ^{240}Pu	1.9050	321	0	0.9891(9)	0.9866(7)	0.9956(7)	0.989
4	9	8% ^{240}Pu	2.4785	160	0	0.9926(7)	0.9955(7)	1.0030(7)	0.993
5	10	8% ^{240}Pu	2.4785	169	0	0.9924(9)	0.9950(6)	1.0025(7)	0.992
9	14	8% ^{240}Pu	2.4785	243	261	0.9926(9)	0.9971(7)	1.0030(7)	0.994
6	11	8% ^{240}Pu	2.6942	152	0	0.9935(8)	0.9964(7)	1.0046(7)	0.995
7	12	8% ^{240}Pu	3.5052	249	0	0.9945(8)	0.9998(7)	1.0069(7)	0.994
46	29	24% ^{240}Pu	2.4785	247	0	1.0007(9)	0.9991(7)	1.0064(6)	1.000
47	30	24% ^{240}Pu	2.6942	243	0	0.9998(8)	1.0026(7)	1.0075(6)	0.999
52	33	UO_2	1.7526	317	0	0.9953(8)	0.9894(6)	0.9939(6)	0.995
53	34	UO_2	2.4785	293	0	0.9960(8)	0.9923(6)	0.9967(6)	0.995

[a)] Tables 1 and 2 of description [1]
[b)] Figures of description [1]

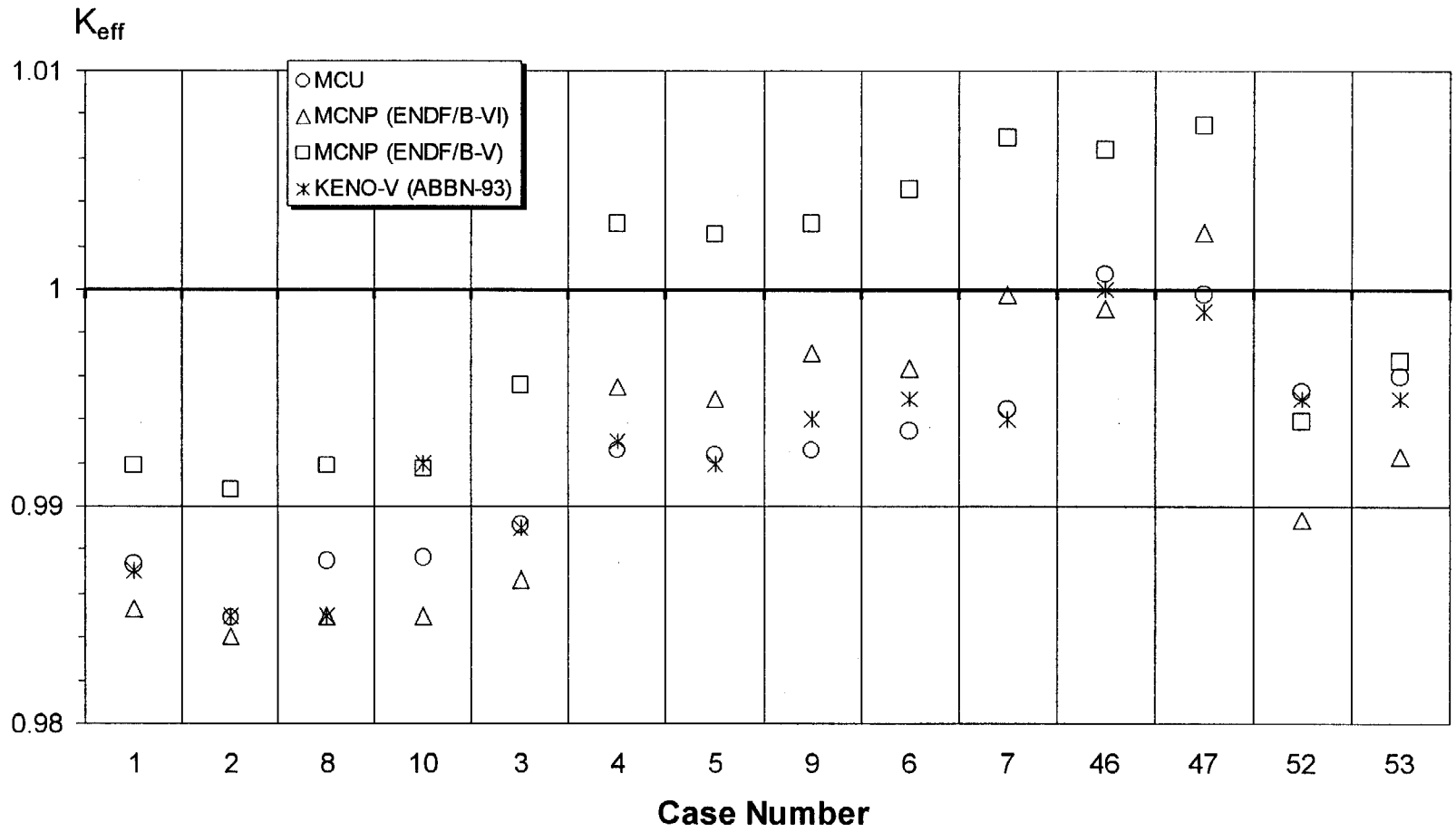

Figure 5. 1. Multiplication factors of single region core configurations.

Table 5. 2. Multiplication factors of salt and pepper core configurations.

Case Num.	Diagram Num [b)]	Core parameters a)		K_{eff}			
		Number and Type of Fuel Rods	Specific	MCU	MCNP (ENDF/B-VI)	MCNP (ENDF/B-V)	KENO-V (ABBN-93)
1	-	(365 - 8%^{240}Pu) (364 - UO_2)		0.9868(8)*	0.9917(7)	0.9957(7)	0.986
2	4	(356 - 8%240Pu) (364 - UO2)	9 water holes	0.9846(8)	0.9914(7)	0.9977(7)	0.985
3	4	(356 - 8%^{240}Pu) (364 - UO_2)	9 control rods	0.9952(8)	0.9902(7)	0.9958(7)	0.992
4	5	(365 - 8%^{240}Pu) (364 – 24%^{240}Pu)		0.9925(8)	0.9900(6)	0.9962(7)	0.990
5	6	(265 - 8%^{240}Pu) (264 - UO_2)		0.9913(9)	0.9876(6)	0.9927(7)	0.990
6	7	(265 -24%^{240}Pu) (264 - UO_2)		0.9992(8)	0.9923(7)	0.9977(7)	0.995
7	8	(288 -24%^{240}Pu) (288 - UO_2)		0.9992(8)	0.9920(6)	0.9977(7)	0.995
8	9	(313 -24%^{240}Pu) (312 - UO_2)		0.9974(8)	0.9914(7)	0.9961(6)	0.993
9	10	(249 -24%^{240}Pu) (256 - UO_2)		0.9961(9)	0.9927(6)	0.9966(6)	0.996

a) Table 1 of description [2], 1.7526 lattice pitch at all cases, pure water at all cases.
b) Figure of description [2]

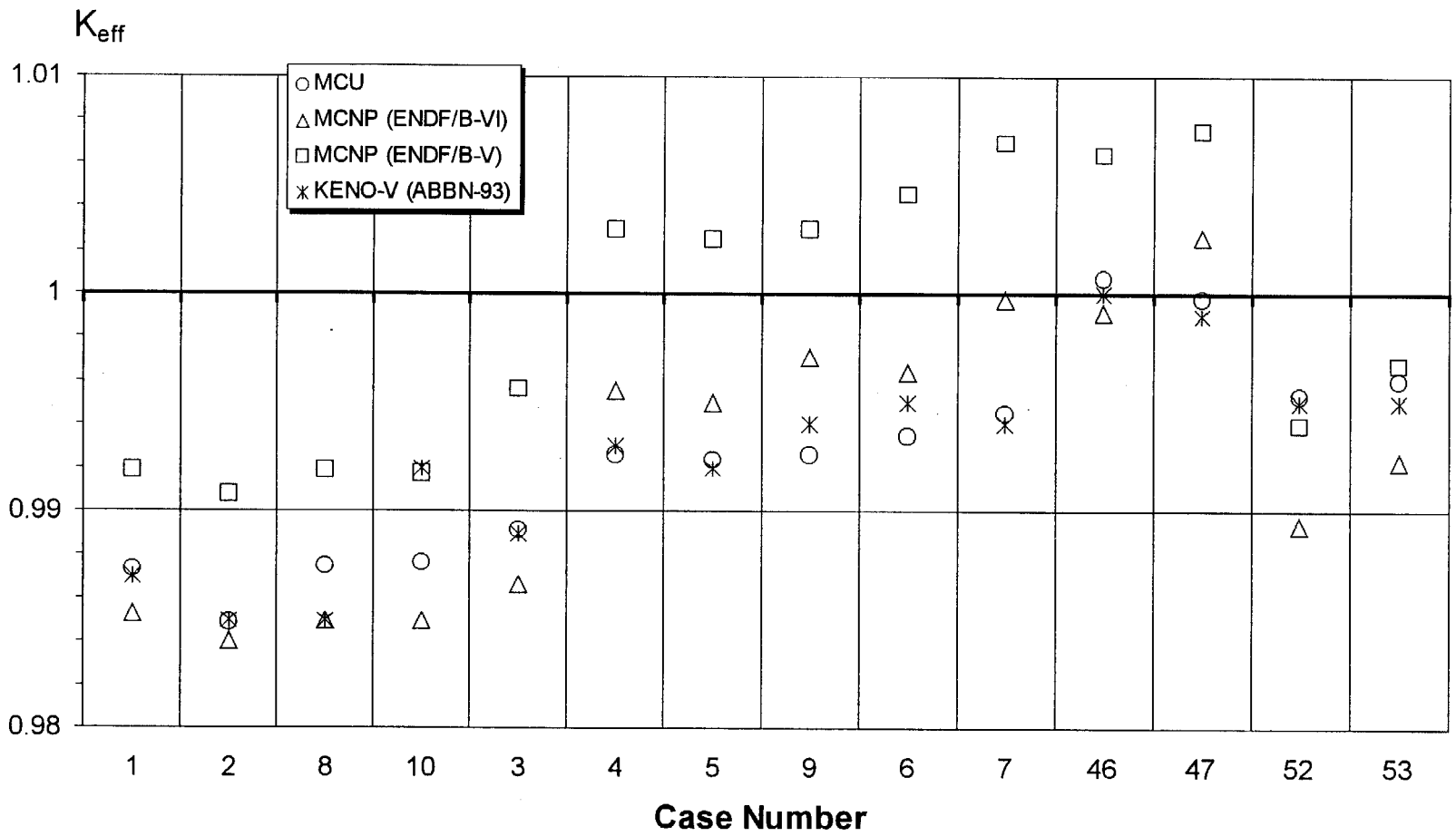

Figure 5. 2. Multiplication factors of single region core configurations.

Table 5. 3. Multiplication factors of multi-region concentric core configurations.

	Core Parameters						K_{eff}			
	Inner Region			Outer Region			MCU	MCNP (ENDF/B-VI)	MCNP (ENDF/B-V)	KENO-V (ABBN-93)
Case Number	Fuel	Fuel Rods	Lattice Pitch (cm)	Fuel	Fuel Rods	Lattice Pitch (cm)				
1	UO_2	225	1.7526	24% ^{240}Pu	400	1.7526	0.9931(8)	0.9919(7)	0.9952(7)	0.988
2	8% ^{240}Pu	225	1.7526	UO_2	400	1.7526	0.9880(8)			
3	24% ^{240}Pu	225	1.7526	UO_2	400	1.7526	0.9936(8)	0.9903(7)	0.9959(7)	0.992
4	24% ^{240}Pu	121	1.7526	UO_2	408	1.7526		0.9903(7)	0.9948(7)	0.995
5	24% ^{240}Pu	225	1.7526	8% ^{240}Pu	492	1.7526		0.9882(7)	0.9830(7)	0.994
6	24% ^{240}Pu	221	1.7526	8% ^{240}Pu	468	1.7526		0.9980(7)	0.9928(7)	0.989
7	24% ^{240}Pu	157	1.9050	8% ^{240}Pu	264	1.9050		0.9927(7)	0.9968(7)	0.990
8	24% ^{240}Pu	89	1.9059	8% ^{240}Pu	143	2.6942		0.9957(7)	1.0016(7)	0.993
										0.995

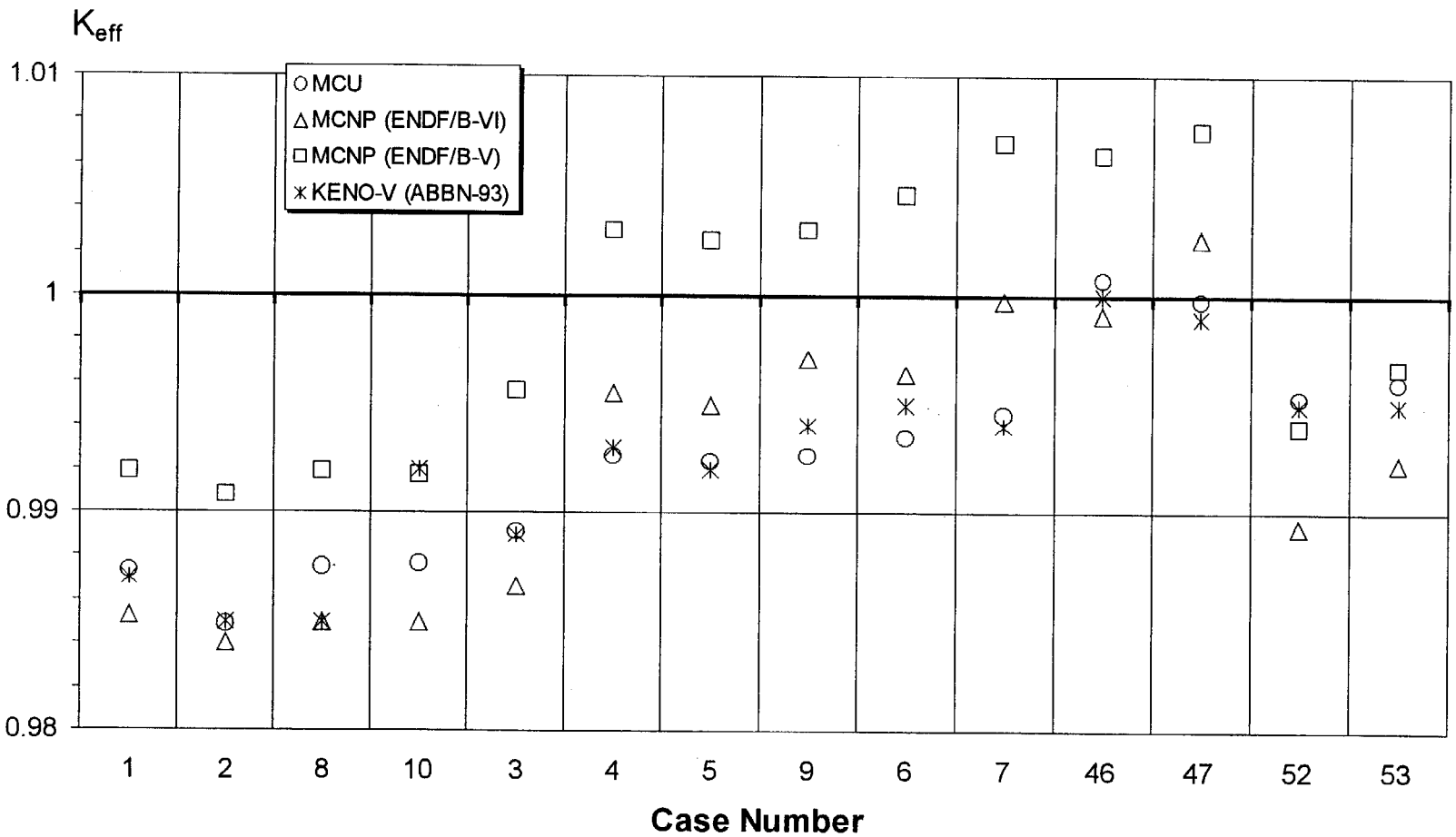

Figure 5. 3. Multiplication factors of single region core configurations.

Table 5. 4. K_{eff} calculation results of multi-region slab core configurations.

Case No	Diagram No [b)]	Core Parameters [a)]				K_{eff}	
		Number of UO_2 Rods	Number of MOX Rods	Boron (ppm)	Specifics of inner region	MCU	KENO-V (ABBN-93)
19	19	460	361 (8% ^{240}Pu)	0		0.9943(31)	0.981
20	20	460	361 (8% ^{240}Pu)	0	4×4 Al void tubes	0.9964(30)	
21	21	460	361 (8% ^{240}Pu)	0	10×10 Al void tubes	1.0065(3)	
22	22	810	437 (8% ^{240}Pu)	526		0.9860(30)	0.967

[a)] Table 1 of description [2]
[b)] Figure of description [2]

5.2. Pin Power Distribution

Power distribution measurements in X-Y cross-section of core were performed both in single-region and multi- region core configurations.

The method employed and results obtained are presented in Ref.[4].

For single-region cores, the measurement of gamma activity of irradiated fuel rods is sufficient. The activity of each rod was related to activity of the reference rod.

For multi-region cores, calorimetric measurements were realized additionally.

An experimental accuracy no indicated in Ref.[4].

In current report the calculation results by MCU code are presented.

MCNP results one can find in Ref.[7].

MCU code was used to calculate pin by pin distribution of fission reaction rate in the cores. For this purpose 10^7 neutron histories were modeled in each case. It provides approximately 1.5% statistical accuracy (1 Standard Deviation).

To be compared with experimental data, the results of the calculation must be normalized. One can use several ways of normalization. In this work two ways were used:

At first, the calculation results were equated with experimental one for some arbitrary fuel rod.

At second, normalization factor A was obtained from following equation:

$$\sum_K EXP_K = A \sum_K CALC_K \ ,$$

where EXP_K and $CALC_K$ are results of measurements and calculations.

We believe the second way is more reasonable.

For multi region core configurations the comparison was carried out for each region separately.

Comparison of calculation results with experimental data is presented in Tables below. Layout of cores is shown in Fig. Reference on a core description and the experimental data is indicated in the comments to the Fig.

Results obtained aren't display problems with pin power distribution.

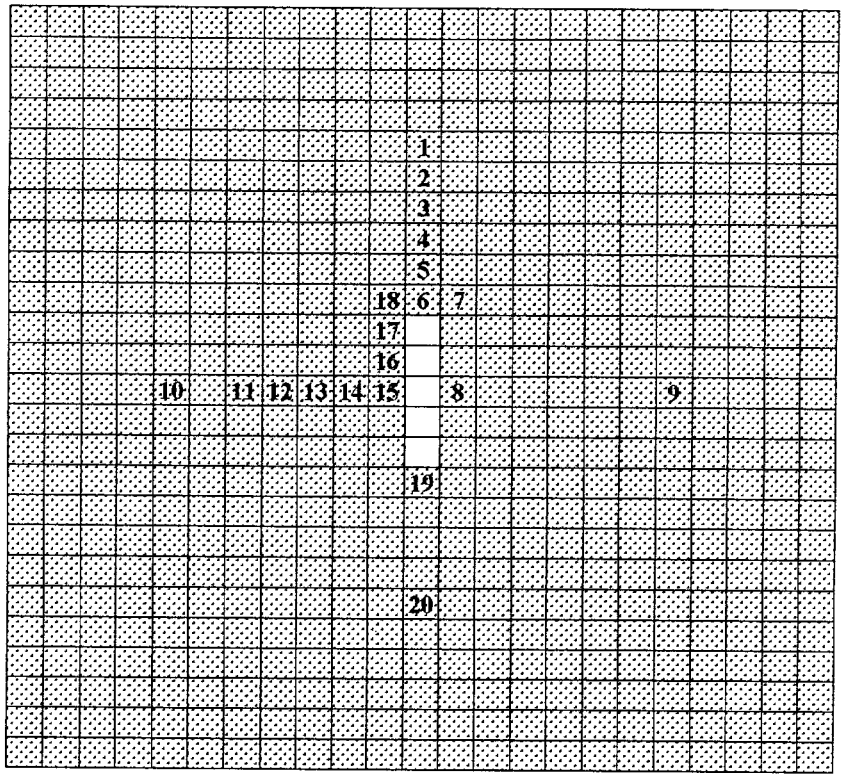

Fig.1. Fuel rods layout and detector positions.
Single region, 1.7526 pitch, 8% ^{240}Pu, 570 rods, 5 cells water slot.
(Tab. 1, Case 2)

Pin power distribution for Fig. 1.

Pin	EXP [a)]	CALC [a)]	(C/E-1) %	CALC [b)]	(C/E-1)
1	0.434	0.427	-1.5	0.425	-1.9
2	0.475	0.472	-0.5	0.470	-0.9
3	0.504	0.501	-0.7	0.499	-1.1
4	0.541	0.536	-1.0	0.534	-1.4
5	0.592	0.594	0.4	0.592	0.0
6	0.760	0.758	-0.3	0.755	-0.7
7	0.656	0.663	1.1	0.660	0.7
8	1.000	0.992	-0.8	0.988	-1.2
9	0.450	0.449	-0.2	0.447	-0.6
10	0.459	0.459	0.1	0.457	-0.3
11	0.521	0.524	0.6	0.522	0.2
12	0.557	0.559	0.3	0.557	0.0
13	0.596	0.605	1.5	0.603	1.1
14	0.691	0.685	-0.9	0.682	-1.3
15	**1.000**	**1.000**	0.0	0.996	-0.4
16	0.910	0.966	6.1	0.962	5.7
17	0.837	0.850	1.6	0.847	1.2
18	0.671	0.658	-1.9	0.655	-2.3
19	0.752	0.765	1.7	0.762	1.3
20	0.473	0.466	-1.6	0.464	-1.9

[a)] Normalized to Pin 15

[b)] Sums of measurement and calculated values are equal.

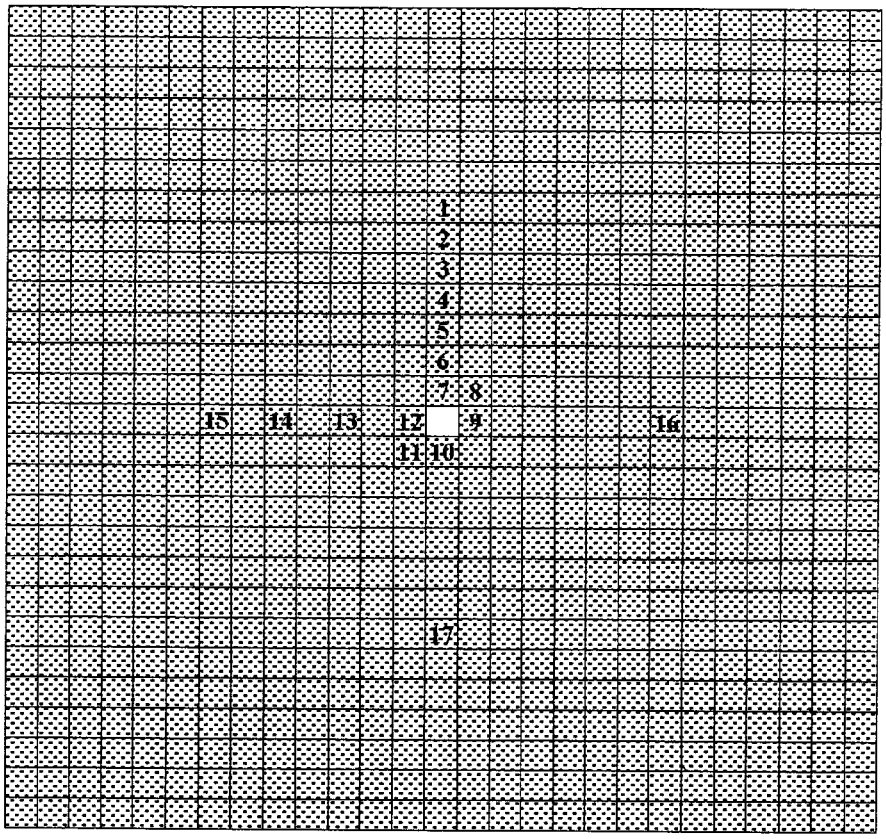

Fig.2. Fuel rods layout and detector positions.
Single region, 1.7526 pitch, 8% ^{240}Pu, 728 rods, center water hole.
(Tab. 1, Case 3)

Pin power distribution for Fig. 2.

Pin	EXP [a)]	CALC [a)]	(C/E-1) %	CALC [b)]	(C/E-1)
1	0.646	0.651	0.8	0.654	1.4
2	0.681	0.678	-0.5	0.681	0.0
3	0.724	0.725	0.2	0.729	0.7
4	0.759	0.749	-1.3	0.753	-0.8
5	0.777	0.779	0.2	0.783	0.7
6	0.833	0.828	-0.5	0.832	0.0
7	0.987	0.989	0.2	0.994	0.7
8	0.887	0.876	-1.2	0.880	-0.7
9	0.972	0.987	1.5	0.992	2.0
10	0.985	0.985	0.0	0.990	0.6
11	0.928	0.880	-5.2	0.884	-4.7
12	**1.000**	**1.000**	0.0	1.005	0.5
13	0.776	0.788	1.5	0.792	2.0
14	0.732	0.717	-2.0	0.721	-1.5
15	0.655	0.648	-1.1	0.651	-0.6
16	0.655	0.650	-0.8	0.653	-0.3
17	0.655	0.653	-0.3	0.656	0.2

[a)] Normalized to Pin 12

[b)] Sums of measurement and calculated values are equal.

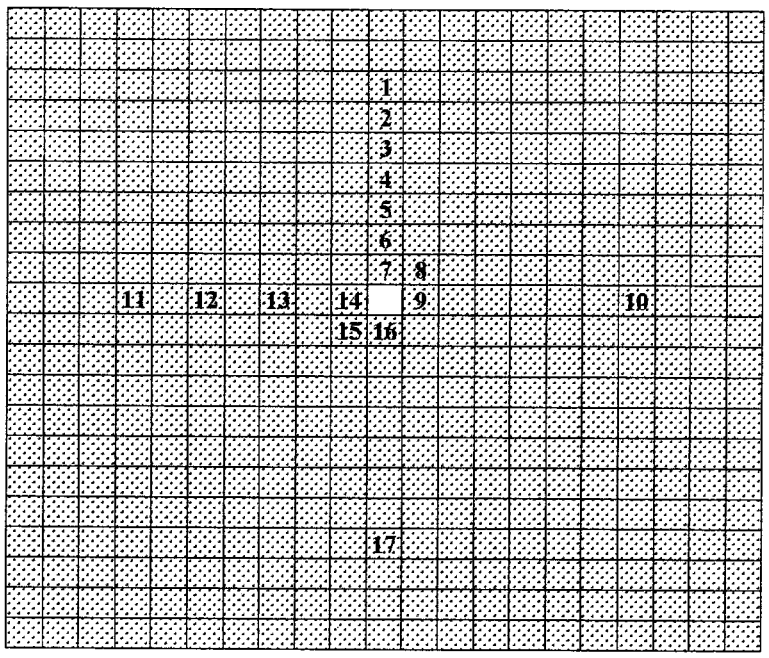

Fig.3. Fuel rods layout and detector positions.
Single region, 1.905 pitch, 24% ^{240}Pu, 440 rods, center water hole.
(Tab. 1, Case 5)

Pin power distribution for Fig. 3.

Pin	EXP [a)]	CALC [a)]	(C/E-1) %	CALC [b)]	(C/E-1)
1	0.599	0.591	-1.4	0.596	-0.6
2	0.665	0.662	-0.4	0.668	0.4
3	0.706	0.705	-0.1	0.711	0.7
4	0.764	0.743	-2.8	0.749	-2.0
5	0.794	0.796	0.3	0.803	1.1
6	0.851	0.833	-2.1	0.840	-1.3
7	0.994	0.995	0.1	1.003	1.0
8	0.898	0.892	-0.6	0.899	0.2
9	0.997	0.994	-0.3	1.002	0.5
10	0.600	0.612	1.9	0.617	2.8
11	0.596	0.599	0.5	0.604	1.3
12	0.710	0.711	0.2	0.717	1.0
13	0.827	0.793	-4.2	0.800	-3.4
14	**1.000**	**1.000**	0.0	1.008	0.8
15	0.904	0.890	-1.5	0.897	-0.7
16	1.003	0.992	-1.1	1.000	-0.3
17	0.605	0.593	-2.0	0.598	-1.2

[a)] Normalized to Pin 14

[b)] Sums of measurement and calculated values are equal.

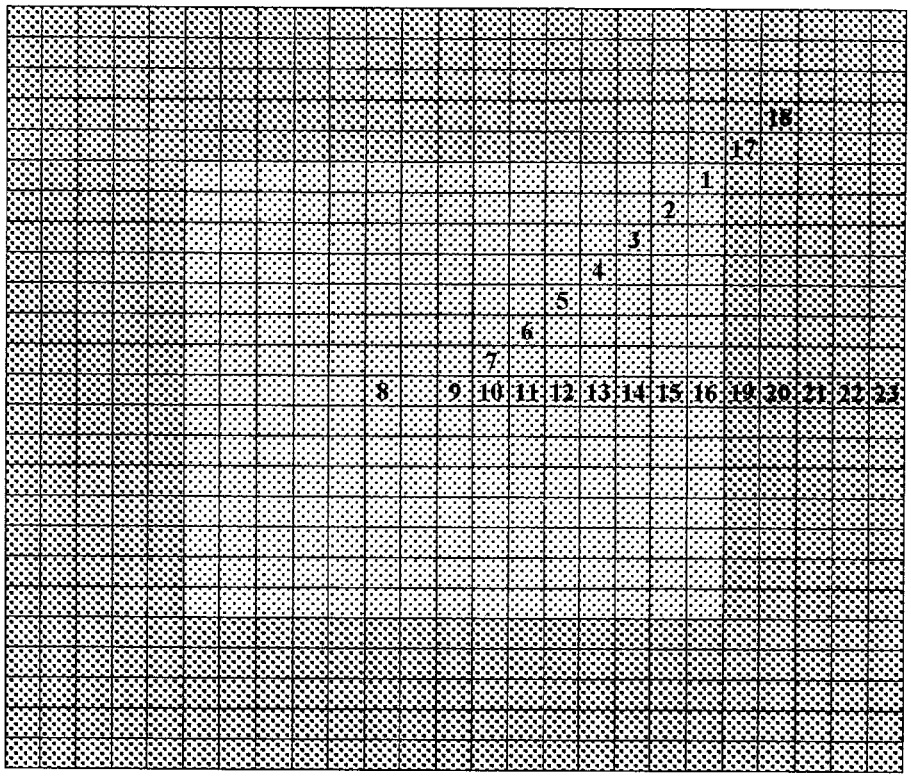

Fig.4. Fuel rods layout and detector positions.
25x25 Concentric region, 1.7526 pitch,
15x15 8%^{240}Pu inner region, UO_2 outer region.
(Tab. 8, Case 7)

Pin power distribution for Fig. 4.

Pin	EXP [a)]	CALC [a)]	(C/E-1) %	CALC [b)]	(C/E-1)
8% ^{240}Pu inner region					
1	0.965	0.957	-0.9	0.958	-0.8
2	0.796	0.786	-1.3	0.786	-1.2
3	0.776	0.785	1.1	0.785	1.2
4	0.819	0.826	0.9	0.826	1.0
5	0.862	0.856	-0.6	0.856	-0.6
6	0.888	0.901	1.5	0.902	1.6
7	0.917	0.902	-1.6	0.903	-1.6
8	0.904	0.905	0.1	0.906	0.2
9	0.909	0.905	-0.5	0.906	-0.4
10	0.920	0.915	-0.5	0.916	-0.4
11	0.923	0.906	-1.9	0.907	-1.8
12	0.906	0.894	-1.3	0.895	-1.2
13	0.863	0.873	1.1	0.873	1.2
14	0.845	0.859	1.7	0.859	1.7
15	0.853	0.867	1.6	0.867	1.7
16	**1.000**	**1.000**	0.0	1.000	0.0
UO_2 outer region					
17	0.754	0.728	-3.5	0.745	-1.2
18	0.672	0.652	-3.0	0.668	-0.7
19	0.845	0.817	-3.3	0.837	-1.0
20	0.930	0.902	-3.0	0.924	-0.7
21	0.901	0.887	-1.5	0.908	0.8
22	0.883	0.859	-2.7	0.880	-0.4
23	**1.000**	**1.000**	0.0	1.024	2.4

[a)] Normalized to Pin 16 in inner region, to Pin 23 in outer region
[b)] Sums of measurement and calculated values are equal.

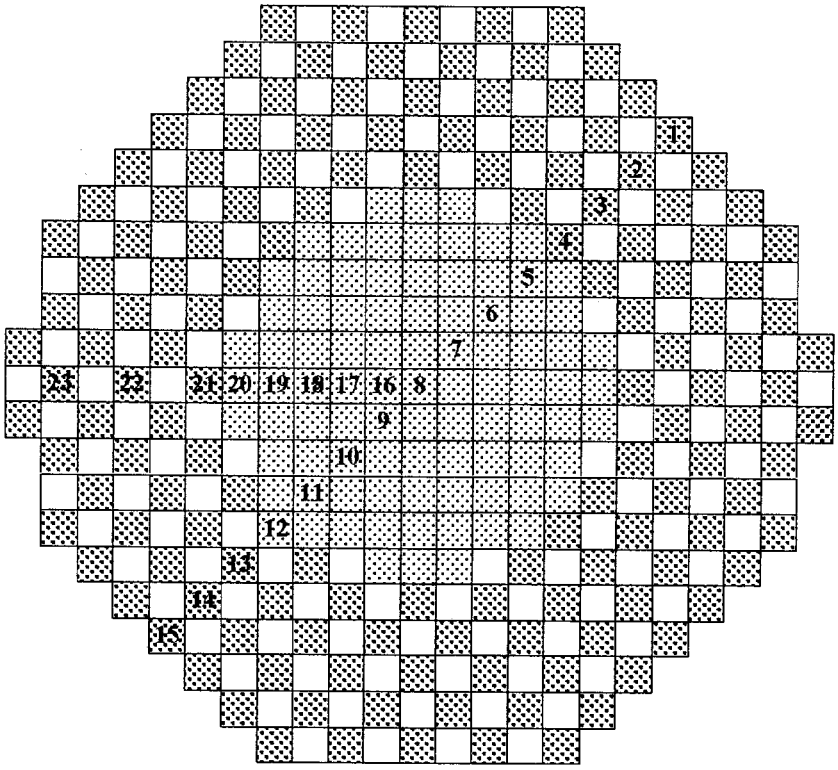

Fig.5. Fuel rods layout and detector positions.
25x25 concentric region,
1.7526 pitch, 89 24% ^{240}Pu inner region,
2.6942 pitch, 143 8% ^{240}Pu outer region.
(Tab. 8, Case 13)

Pin power distribution for Fig. 5.

Pin	EXP [a)]	CALC [a)]	(C/E-1) %	CALC [b)]	(C/E-1)
1	0.832	0.835	0.3	0.834	0.2
2	0.882	0.886	0.5	0.885	0.4
3	0.994	0.996	0.2	0.995	0.1
4	0.825	0.834	1.0	0.833	0.9
5	0.559	0.572	2.3	0.571	2.2
6	0.550	0.557	1.2	0.556	1.1
7	0.551	0.559	1.5	0.558	1.4
8	0.562	0.570	1.5	0.569	1.4
9	0.557	0.591	6.0	0.590	5.9
10	0.553	0.556	0.6	0.555	0.5
11	0.572	0.561	-2.0	0.560	-2.1
12	0.837	0.830	-0.9	0.829	-1.0
13	**1.000**	**1.000**	0.0	0.999	-0.1
14	0.892	0.882	-1.1	0.881	-1.2
15	0.837	0.847	1.2	0.846	1.1
16	0.562	0.561	-0.2	0.560	-0.3
17	0.547	0.555	1.5	0.554	1.4
18	0.549	0.556	1.2	0.555	1.1
19	0.573	0.583	1.7	0.582	1.6
20	0.644	0.660	2.4	0.659	2.3
21	0.962	0.877	-8.8	0.876	-8.9
22	0.950	0.944	-0.6	0.943	-0.7
23	0.751	0.748	-0.4	0.747	-0.5

[a)] Normalized to Pin 13

[b)] Sums of measurement and calculated values are equal.

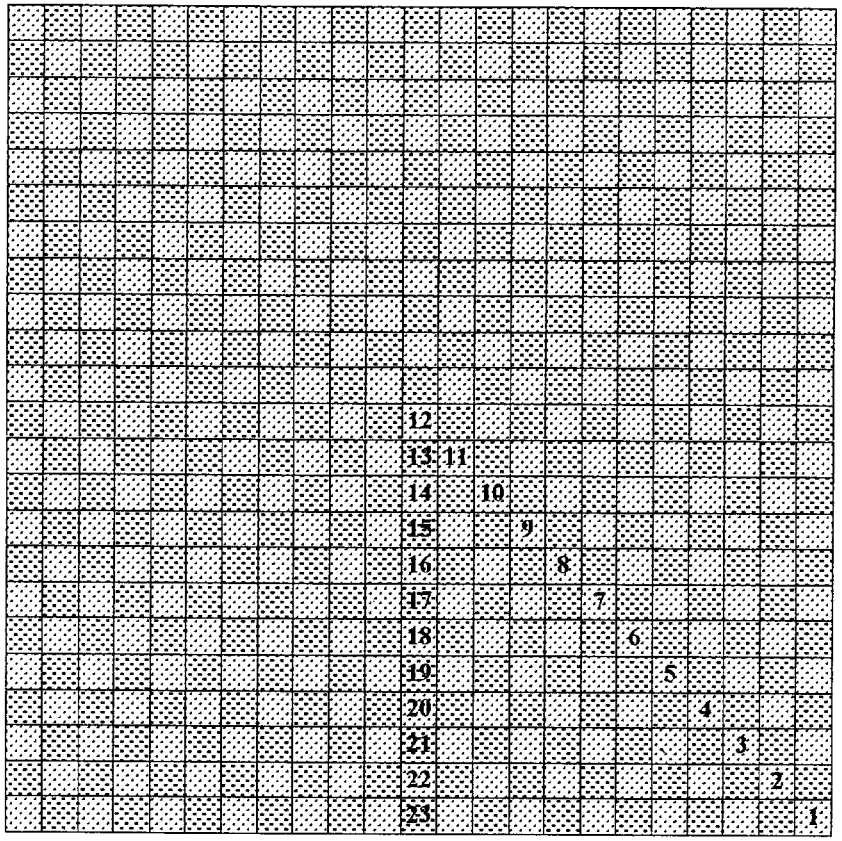

Fig.6. Fuel rods layout and detector positions.
Salt and pepper core configuration.
1.7526 pitch, 23x23 rods, 8% ^{240}Pu and UO_2.
(Tab. 16, Case 15)

Pin power distribution for Fig. 6.

Pin	EXP [a)]	CALC [a)]	(C/E-1) %	CALC [b)]	(C/E-1)
24% ^{240}Pu MOX					
1	0.500	0.521	4.1	0.517	3.2
2	0.384	0.380	-0.9	0.377	-1.8
3	0.415	0.405	-2.5	0.401	-3.3
4	0.492	0.494	0.3	0.490	-0.6
5	0.585	0.585	-0.1	0.580	-1.0
6	0.669	0.676	1.1	0.670	0.2
7	0.766	0.774	1.1	0.767	0.2
8	0.861	0.872	1.2	0.864	0.3
9	0.930	0.933	0.3	0.925	-0.5
10	0.966	0.964	-0.3	0.955	-1.1
11	0.980	1.010	3.1	1.001	2.2
12	**1.000**	**1.000**	0.0	0.991	-0.9
14	0.986	0.983	-0.3	0.975	-1.2
16	0.927	0.940	1.4	0.932	0.5
18	0.813	0.828	1.9	0.821	1.0
20	0.705	0.703	-0.3	0.697	-1.1
22	0.619	0.641	3.5	0.636	2.7
UO_2					
13	**1.000**	**1.000**	0.0	0.999	-0.1
15	0.980	0.963	-1.7	0.963	-1.7
17	0.880	0.893	1.5	0.892	1.4
19	0.770	0.752	-2.3	0.752	-2.3
21	0.642	0.661	2.9	0.661	2.9
23	0.845	0.851	0.7	0.850	0.6

[a)] Normalized to Pin 12 in inner region, to Pin 13 in outer region
[b)] Sums of measurement and calculated values are equal.

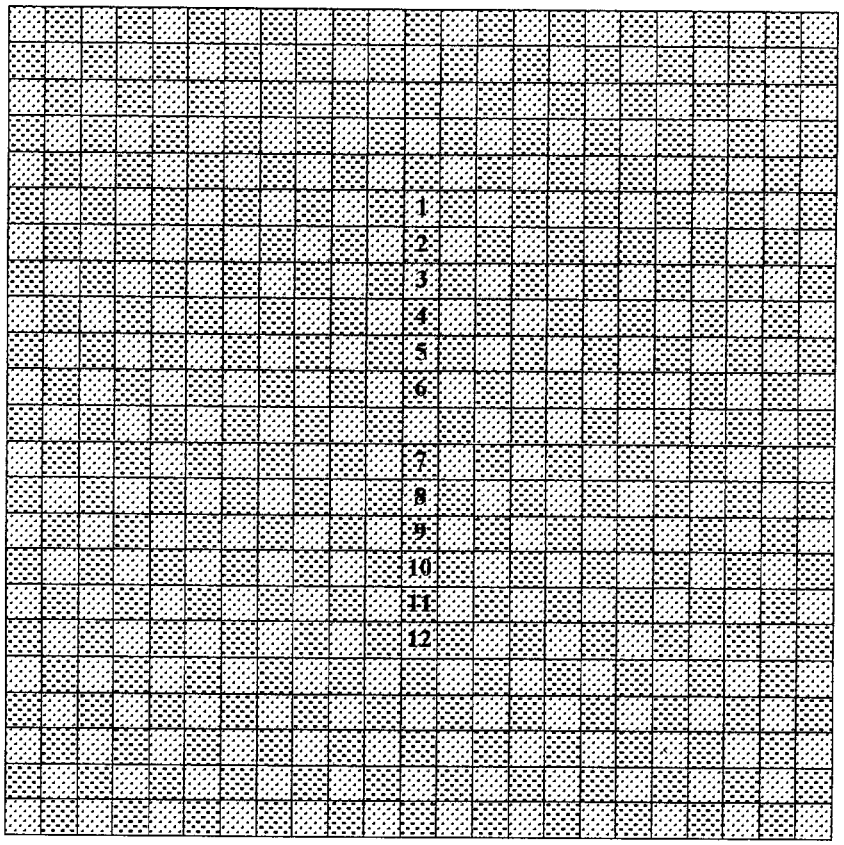

Fig.7. Fuel rods layout and detector positions.
Salt and pepper core configuration.
1.7526 pitch, 23x23 rods, 24%^{240}Pu and UO_2.
(Tab. 16, Case 16)

Pin power distribution for Fig. 7.

Pin	EXP [a)]	CALC [a)]	(C/E-1) %	CALC [b)]	(C/E-1)
24% ^{240}Pu MOX					
1	1.024	1.000	-2.3	1.001	-2.3
3	1.131	1.145	1.2	1.146	1.3
5	1.208	1.219	1.0	1.220	1.0
8	1.226	1.219	-0.5	1.220	-0.5
10	1.145	1.145	0.1	1.146	0.1
12	**1.000**	**1.000**	0.0	1.001	0.1
UO_2					
2	1.024	1.000	-2.3	1.001	-2.3
4	1.131	1.145	1.2	1.146	1.3
6	1.208	1.219	1.0	1.220	1.0
7	1.226	1.219	-0.5	1.220	-0.5
9	1.145	1.145	0.1	1.146	0.1
11	**1.000**	**1.000**	0.0	1.001	0.1

[a)] Normalized to Pin 12 in inner region, to Pin 11 in outer region
[b)] Sums of measurement and calculated values are equal.

CONCLUSION

SAXTON and ESADA have the direct relationship to water moderated reactor with MOX fuel. All used codes underestimate multiplication factors right up till 0.01. To link certainly this deviation with neutron data it's desirable to specify the experiment descriptions. In particular, K_{eff} of the benchmark models should be estimated.

For the critical assemblies with core of plutonium nitrate solution, MCU and ABBN-93 neutron data allow to forecast the criticality with the error not greater than the experiment error.

The use of ENDF/B-V neutron data cause the overestimation in approximately 0.01.

For the reactors of VVER type with MOX fuel, it makes sense to use the same cross-sections of plutonium isotopes in Russian and U.S. codes.

To secure it one should compare the actual used neutron data and to provide the joint evaluation of cross-sections. In this evaluation, the results presented in current report should be also taken into account.

REFERENCE

1. NEA Nuclear Science Committee, International Handbook of Evaluated Criticality Safety Benchmark Experiments. NEA/NSC/DOC(95), 1995.
2. Neutronics Benchmarks for the Utilization of Mixed Oxide Fuel – Updated Progress Report for Fiscal Year 1997. Volume III – Experimental Benchmarks. ORNL. May 2,1997.
3. Neutronics Benchmarks for the Utilization of Mixed Oxide Fuel – Updated Progress Report for Fiscal Year 1997. Volume VI – Evaluations of Critical Experiments. ORNL. May 7,1997.
4. Neutronics Benchmarks for the Utilization of Mixed Oxide Fuel: Joint U.S./Russian Progress Report for Fiscal Year 1997. ORNL. 1998.
5. Cross Section Evaluation Working Group, Thermal Reactor Benchmark Compilation, BNL-19302 (ENDF-202), 1974.
6. Marvin L. Adams. Texas A&M University. Private information to M. Yudkevich, 1998.
7. Fourth U.S./Russian Technical Specialist's Meeting Water Reactors 1 and 6 Fissile Materials Disposition Program, June 17-19, 1998, St. Petersburg, Russia.
8. Neutronics Benchmarks for the Utilization of Mixed Oxide Fuel – Updated Progress Report for Fiscal Year 1997. Volume 3 – Calculations Performed in the Russian Federation. ORNL. June 1998.
9. L. M. Petrie, N. F. Landers, "KENO V.a: An Improved Monte Carlo Criticality Program with Supergrouping," NUREG/CR-0200, Revision 5, Volume
10. G.N. Manturov, M.N. Nikolaev, A.M. Tsiboulia. ABBN-93 Group Data Library. Part 1: Nuclear Data for Calculation of Neutron and Photon Radiation Fields. IAEA, INDC (CCP) 409/L, August 1997, p.65-110.
11. ABBN-93 - Modified "ABBN-90 Package of Multigroup Constants for Calculation of Neutron and Photon Radiation Fields and their Functional", RSICC Peripheral Routine Collection DLC-182/ABBN-90, ORNL.

Comments by ORNL staff on ORNL/SUB/99-B99398V-5

1. Page 2. The last sentence states that "(delta) A is the mean-square error." This is also known as the standard deviation of the values about the mean. It states that "the statistical dispersion of the particular variant wasn't taken into account. It's valid as the scattering of the values to be averaged is much greater than the statistical dispersion." This is generally true and acceptable for the statistical uncertainty in the calculated values. However, the reader should note that the uncertainties in some of the measured critical states translate into rather large uncertainties in k-effective (on the order of 0.5%). We have assumed that the statement is not interpreted to be that the scattering of calculated k-effectives was different from the Gaussian distribution defined by the standard error of the mean from any one of the calculations. If that were the case, then one must question if the problem was converged.

2. Pages 4 and 7; Tables 1.1 and 1.2. "D (inch)" is interpreted to mean the diameter of the cylindrical vessel.

3. Page 9. There is no uncertainty value for the KENO-V (ENDF/B-V) result in Table 1.4. It is our interpretation that the last two paragraphs on this page should be combined into one. Otherwise, it seems that the comment stating that the experiments are unacceptable applies to the experiments presented in Table 1.3 as well as Table 1.4. We believe that the author's intent is to indicate that only the experiment with the 17.9-in. diameter is unacceptable.

4. Page 11. Regarding the first bullet at the bottom of the page, it is assumed that "Delta Keff = –1" should be replaced by "Delta K-eff = (calculated K) –1." Regarding the third bullet, the reader should note that the averages in Table 1.5 are the subject of discussion. The range for the MCU-calculated k-effective is from 0.995 (p. 7, case 14-8) to 1.024 (p. 4, case 9-1). The "Delta K-eff" should just be "Keff." Likewise, for the fourth bullet, the statement refers to the averages in Table 1.5. The upper value in the range of MCNP Keff values is 1.024 (p. 4, case 9-1). The "Delta Keff" should just be "Keff." Regarding the fifth bullet, the values given don't appear to be averages over all of the cases presented in the previous tables, but individual values taken from Table 1.5. For example, the values that we compute for the ABBN-93 and ENDF/B-V group results Tables 1.1 through 1.4 are

   ABBN-93: Delta Keff = 0.003 ± 0.005.
   ENDF/B-V: Delta Keff = 0.011 ± 0.006.

   Likewise, the "Group approach" values do not appear to be averages over the values reported in Tables 1.1 through 1.4.

5. Page 15. The comment at the end of the second paragraph "Calculation results with ENDF/B data are not known to us" appears to be in error because Table 1.7 contains results with KENO using ENDF/B-V data.

6. Page 17. In the third paragraph from the bottom, 0.025 should be 1.025. It is not clear that ^{241}Pu is the cause of the trend in k-effective because the fraction of ^{241}Pu absorption is unchanged as the H/Pu ratio changes.

7. Page 24. The 8 cm probably should be 80 cm.

8. Page 27. Table 2.2 indicates ABBN-90 (not ABBN-93). We assume that the library was actually ABBN-93. Similar notations are used in Figs. 2.1, 2.2, and 2.3, and Tables 2.4 and 2.6. On p. 32, the last paragraph states that ABBN-93 was used, while Table 2.6 indicates that ABBN-90 was used.

9. Pages 47 and 52. “NCNP:” should be “MCNP:”.

10. Page 60. The normalization factor, A, is consistent with the ESADA methodology, yet we felt that pin powers should be computed relative to the standard rod. This was done by IPPE for KENO/ABBN calculations (see page 78).

11. Pages 61–77. The figure numbers should be consistent with the other figures in this chapter. For example, Fig. 1 on page 61 should be Fig. 4.5. Also, it would be helpful to the reader if these figure numbers could be added to Table 4.6.

12. Page 100. The meaning of the last sentence on this page is not clear.

INTERNAL DISTRIBUTION

1–5. B. B. Bevard
6. M. D. DeHart
7. F. C. Difilippo
8. R. J. Ellis
9–13. J. C. Gehin
14. S. R. Greene
15. R. Holdaway
16. D. T. Ingersoll
17. S. B. Ludwig
18. D. L. Moses
19. M. A. Kuliasha
20. G. E. Michaels
21. M. G. McGinnis
22–26. R. T. Primm III
27. C. C. Southmayd
28. ORNL Central Research Library
29. ORNL Laboratory Records–RC

EXTERNAL DISTRIBUTION

30. M. L. Adams, Department of Nuclear Engineering, Texas A&M University, Zachry 129, College Station, TX 77843-3133
31. H. Akkurt, 2919 Cooley Building, 2355 Bonisteel Boulevard, Ann Arbor, MI 48109-2104
32. D. Alberstein, Los Alamos National Laboratory, P.O. Box 1663, MS-K551, Los Alamos, NM 87545
33. J. Baker, Office of Fissile Materials Disposition, U.S. Department of Energy, NN-63, 1000 Independence Avenue SW, Washington, DC 20585
34. J. B. Briggs, Idaho National Environmental and Engineering Laboratory, P.O. Box 1625-3855, Idaho Falls, ID 83415-3855
35. A. K. Caponiti, Office of Fissile Materials Disposition, U.S. Department of Energy, NN-63, 1000 Independence Avenue SW, Washington, DC 20585
36. N. Fletcher, Office of Fissile Materials Disposition, U.S. Department of Energy, NN-63, 1000 Independence Avenue SW, Washington, DC 20585
37. K. Chidester, Los Alamos National Laboratory, P.O. Box 1663, MS-E502, Los Alamos, NM 87545
38. W. Danker, U.S. Department of Energy, NN-62, 1000 Independence Avenue SW, Washington, DC 20585
39. T. Gould, Lawrence Livermore National Laboratory, P.O. Box 808, MS-L186, Livermore, CA 94551
40. L. Holgate, Office of Fissile Materials Disposition, U.S. Department of Energy, NN-60, 1000 Independence Avenue SW, Washington, DC 20585
41. L. Jardine, Lawrence Livermore National Laboratory, P.O. Box 808, MS-L166, Livermore, CA 94551
42. Dr. Alexander Kalashnikov, Institute of Physics and Power Engineering, 1 Bondarenko Square, Obninsk, Kaluga Region, Russia 249020

43–47. D. E. Klein, Associate Vice Chancellor for Special Engineering Programs, The University of Texas System, 210 West Sixth Street, Austin, TX 78701

48. J. O. Nulton, Office of Fissile Materials Disposition, U.S. Department of Energy, NN-61, 1000 Independence Avenue SW, Washington, DC 20585
49. Dr. Stephen L. Passman, Booz-Allen & Hamilton, 555 13th Street, NW, No. 480E, Washington, DC 20004

50–54. Dr. Alexander Pavlovitchev, Russian Research Center "Kurchatov Institute," Institute of Nuclear Reactors, VVER Division, VVER Physics Department, 123182, Kurchatov Square, 1, Moscow, Russia

55. K. L. Peddicord, Associate Vice Chancellor, Texas A&M University, Zachry 120, College Station, TX 77843-3133
56. G. Radulescu, Framatome Cogema Fuels, 1261 Town Center Drive, MS-423, Las Vegas, Nevada 89143
57. W. D. Reece, Texas A&M University, Department of Nuclear Engineering, Zachry 129, College Station, TX 77843-3133
58. P. T. Rhoads, Office of Fissile Materials Disposition, U.S. Department of Energy, NN-61, 1000 Independence Avenue SW, Washington, DC 20585
59. J. Thompson, Office of Fissile Materials Disposition, U.S. Department of Energy, NN-61, 1000 Independence Avenue SW, Washington, DC 20585
60. F. Trumble, Westinghouse Savannah River Company, Building 730R, Room 3402, Aiken, SC 29808
61. Mr. Richard H. Clark, Duke/Cogema/Stone & Webster, 400 South Tryon Street, WC-32G, P.O. Box 1004, Charlotte, NC 28202
62. Mr. Steve Nesbit, Duke/Cogema/Stone & Webster, 400 South Tryon Street, WC-32G, P.O. Box 1004, Charlotte, NC 28202
63. M. S. Chatterton, Office of Nuclear Reactor Regulation, MS O10B3, U.S. Nuclear Regulatory Commission, Washington, DC 20555-0001
64. R. W. Lee, Office of Nuclear Reactor Regulation, MS O10B3, U.S. Nuclear Regulatory Commission, Washington, DC 20555-0001
65. U. Shoop, Office of Nuclear Reactor Regulation, MS O10B3, U.S. Nuclear Regulatory Commission, Washington, DC 20555-0001
66. Nagao Ogawa; Director and General Manager; Plant Engineering Department; Nuclear Power Engineering Corporation; Shuwa-Kamiyacho Building, 2F; 3-13, 4-Chome Toranomon; Minato-Ku, Tokyo 105-0001, Japan
67. Dr. Kiyonori Aratani; Surplus Weapons Plutonium Disposition Group; International Cooperation and Nuclear Material Control Division; Japan Nuclear Cycle Development Institute; 4-49 Muramatsu, Tokai-mura, Naka-gun, Ibaraki-ken, Japan
68. E. Siskin, Office of Fissile Materials Disposition, U.S. Department of Energy, NN-60, 1000 Independence Avenue SW, Washington, DC 20585
69. Boris E. Volkov; Head of Division; EDO Gidropress; 21 Ordzhonikidze Street; Podolsk, Moscow District, Russia 142103